



University of Kentucky
UKnowledge

Theses and Dissertations--Pharmacology and
Nutritional Sciences

Pharmacology and Nutritional Sciences

2016

Novel Role of CD47 in Obesity-Associated Metabolic Dysfunctions

Heather L. Norman-Burgdorf

University of Kentucky, hlnorman11@gmail.com

Author ORCID Identifier:

 <http://orcid.org/0000-0002-2444-6491>

Digital Object Identifier: <https://doi.org/10.13023/ETD.2016.491>

[Right click to open a feedback form in a new tab to let us know how this document benefits you.](#)

Recommended Citation

Norman-Burgdorf, Heather L., "Novel Role of CD47 in Obesity-Associated Metabolic Dysfunctions" (2016).
Theses and Dissertations--Pharmacology and Nutritional Sciences. 17.
https://uknowledge.uky.edu/pharmacol_etds/17

This Doctoral Dissertation is brought to you for free and open access by the Pharmacology and Nutritional Sciences at UKnowledge. It has been accepted for inclusion in Theses and Dissertations--Pharmacology and Nutritional Sciences by an authorized administrator of UKnowledge. For more information, please contact UKnowledge@lsv.uky.edu.

STUDENT AGREEMENT:

I represent that my thesis or dissertation and abstract are my original work. Proper attribution has been given to all outside sources. I understand that I am solely responsible for obtaining any needed copyright permissions. I have obtained needed written permission statement(s) from the owner(s) of each third-party copyrighted matter to be included in my work, allowing electronic distribution (if such use is not permitted by the fair use doctrine) which will be submitted to UKnowledge as Additional File.

I hereby grant to The University of Kentucky and its agents the irrevocable, non-exclusive, and royalty-free license to archive and make accessible my work in whole or in part in all forms of media, now or hereafter known. I agree that the document mentioned above may be made available immediately for worldwide access unless an embargo applies.

I retain all other ownership rights to the copyright of my work. I also retain the right to use in future works (such as articles or books) all or part of my work. I understand that I am free to register the copyright to my work.

REVIEW, APPROVAL AND ACCEPTANCE

The document mentioned above has been reviewed and accepted by the student's advisor, on behalf of the advisory committee, and by the Director of Graduate Studies (DGS), on behalf of the program; we verify that this is the final, approved version of the student's thesis including all changes required by the advisory committee. The undersigned agree to abide by the statements above.

Heather L. Norman-Burgdolf, Student

Dr. Shuxia Wang, Major Professor

Dr. Howard Glauert, Director of Graduate Studies

NOVEL ROLE OF CD47 IN OBESITY-ASSOCIATED METABOLIC
DYSFUNCTIONS

DISSERTATION

A dissertation submitted in partial fulfillment of the
requirements for the degree of Doctor of Philosophy in the
College of Medicine
at the University of Kentucky

By

Heather L. Norman-Burgdolf

Lexington, Kentucky

Director: Dr. Shuxia Wang, Professor of Pharmacology and Nutritional Sciences

Lexington, Kentucky

2016

Copyright © Heather L. Norman-Burgdolf 2016

ABSTRACT OF DISSERTATION

NOVEL ROLE OF CD47 IN OBESITY-ASSOCIATED METABOLIC DYSFUNCTIONS

Obesity and its associated comorbidities are of global concern. These complications are largely driven by perturbations in energy homeostasis, inflammation, and oxidative stress within metabolic tissues. Although these underlying pathways have been established, molecular mechanisms augmenting metabolic dysfunction have not been fully defined. CD47, a ubiquitously expressed cell membrane receptor, has been previously implicated in the development of inflammation and oxidative stress in a number of disease conditions. Previous work from our lab and others has confirmed that the most potent ligand of CD47, TSP1, plays a critical role in facilitating inflammation and metabolic dysfunction in diet-induced obesity. Whether these effects of TSP1 are mediated by CD47 has never been explored. Specifically, the functions of CD47 in white and brown adipose tissue, skeletal muscle, and the liver have never been characterized under obese conditions. Within our studies, we clearly defined distinct regulatory functions of CD47 in different metabolic tissues of a diet-induced obesity rodent model. We found that CD47 deficiency was associated with reduced adiposity and systemic inflammatory markers which preserved glucose homeostasis. In white adipose tissue, CD47 deficiency was associated with suppressed inflammation and macrophage recruitment which may be attributed to smaller adipocyte size driven by enhanced lipid mobilization. Further, whole body CD47 deficiency stimulated brown adipose tissue energy expenditure through increased FFA-mediated uncoupling and enhanced fatty acid oxidation. Interestingly, no significant changes were observed in skeletal muscle-dependent energy expenditure. In the liver, both TSP1 and CD47 deficiency protected mice from diet-induced fatty liver disease. *In vitro* studies demonstrated that TSP1 induces liver oxidative stress comparable to free fatty acids and that CD47 blockade partially attenuates this effect. From these studies, we concluded that increased lipid turnover fueled the enhanced energy requirements of activated brown adipose tissue resulting in a leaner phenotype despite high fat diet challenge. In addition, the increased TSP1-CD47 protein expression in the liver may augment ROS in fatty liver disease. Together, these studies provide evidence to suggest CD47 may contribute to metabolic

dysfunction in a tissue-specific manner and that the pathological roles of CD47 function should expand to include obesity and its associated comorbidities.

KEYWORDS: diet-induced obesity, non-alcoholic fatty liver disease, oxidative stress, CD47, thrombospondin1

Heather L. Norman-Burgdolf

November 22, 2016

NOVEL ROLE OF CD47 IN OBESITY-ASSOCIATED METABOLIC
DYSFUNCTIONS

By

Heather L. Norman-Burgdolf

Dr. Shuxia Wang

Director of Dissertation

Dr. Howard Glauert

Director of Graduate Studies

November 22, 2016

ACKNOWLEDGEMENTS

Over the past five years I have had the privilege of developing relationships with several individuals who have been instrumental in my efforts of pursuing a PhD. First, I would like to thank my mentor Dr. Shuxia Wang for seeing my true potential and pushing me to be the best version of myself as a trainee. Dr. Wang allowed me to craft my doctoral training in a manner that prepared me for a career in college teaching and learning. For that, I am incredibly grateful. In addition, I want to thank all members of the Wang lab, past and present, for their help and support. And above all, I must thank Hasiyet Meimeitiymin for teaching me so many technical “bench” skills that I know today and for being such a good friend during my doctoral training. I am incredibly grateful for the wisdom she has shared with me over the years.

It has been such a pleasure to pursue my PhD at the University of Kentucky where so many faculty are committed to student success. I would like to thank the members of my committee, Drs. Lisa Cassis, Nancy Webb, and Olivier Thibault for continuously supporting me with time, support, and expertise. I believe that my committee members are exemplary in their service to student training and mentorship. In addition, I would like to thank Dr. David Randall for his time and efforts as my outside examiner.

Many times I have told people that the best parts of graduate school are the friendships that develop between peers and colleagues. I believe the camaraderie and support the students and staff within our department show each other is truly special and sets our program apart from others. To my friends,

thank you for the friendships and for the many trips to the Kentucky Clinic Starbucks.

Finally, I want to thank my family. To my parents, Gary and Pam Norman, and my brother, Landon Norman, I must thank them for their tremendous support and constant prayers. Even in my childhood, my parents understood the power of education and never once let me doubt there was something I could not accomplish. Last, my best friend and husband, Adam Burgdolf, has been a constant source of inspiration and comfort. He has been committed to my endeavor of obtaining a PhD from the very beginning and has never shown anything short of support, patience, and encouragement. For everything, I am incredibly grateful.

TABLE OF CONTENTS

ACKNOWLEDGEMENTS.....	iii
TABLE OF CONTENTS	v
LIST OF TABLES	x
LIST OF FIGURES	xi
LIST OF ABBREVIATIONS	xiii
Section 1: BACKGROUND.....	1
1.1 Defining Obesity.....	1
1.1.1 Prevalence of Obesity.....	1
1.1.2 Characteristics of Adipose Tissue.....	3
1.1.2.1 White Adipose Tissue (WAT)	5
1.1.2.2 Brown Adipose Tissue (BAT)	6
1.1.2.3 Beige Adipose Tissue	8
1.2 Pathophysiology of Obesity.....	8
1.2.1 Obesity-associated Inflammation.....	9
1.2.2 Dyslipidemia	10
1.2.3 Insulin Resistance	11
1.2.4 Obesity-associated Brown Adipose Tissue Dysfunction.....	12
1.2.5 Obesity-associated Comorbidities	12
1.2.5.1 Type II Diabetes Mellitus (T2DM)	13
1.2.5.2 Cardiovascular Disease (CVD).....	13
1.2.5.3 Non-Alcoholic Fatty Liver Disease (NAFLD).....	14
1.2.5.4 Metabolic Syndrome	14
1.3 NAFLD: Impacts on Metabolic Health	15
1.3.1 Hepatic Lipid Metabolism.....	16
1.3.2 Pathophysiology of NAFLD.....	18
1.3.3 Contribution of Other Cell Types to NAFLD Development	21
1.4 The Canonical NO/cGMP Signaling Pathway.....	22
1.4.1 Impacts of NO/cGMP Signaling on Metabolic Health	23
1.5 Thrombospondins: Multi-functional Signaling Molecules	25
1.5.1 Links Between Thrombospondin 1 (TSP1) and Metabolic Dysfunction	26
1.6 CD47: Potent Receptor to TSP1	30
1.6.1 Structure and Functions of CD47.....	30

1.6.2 Downstream Signaling Effects of TSP1-CD47 Interaction.....	32
1.6.3 Other Characterized Interactions of CD47	33
1.6.3.1 Integrins	33
1.6.3.2 Signal Regulatory Proteins (SIRPs)	34
1.7 Statement of the Problem	35
1.7.1 Impact	39
Section 2: METHODS.....	46
2.1 Breeding and Genotyping.....	46
2.2 Animal Experimental Protocols	46
2.2.1 Aim 1	47
2.2.2 Aim 2	47
2.3 Indirect Calorimetry and Body Composition	48
2.4 <i>In Vivo</i> Lipolysis Assay.....	49
2.5 <i>Ex Vivo</i> Lipolysis Assay	49
2.6 Plasma Parameters.....	50
2.7 <i>In Vivo</i> Glucose Tolerance/Insulin Sensitivity Assays.....	50
2.8 Tissue Histology.....	50
2.9 Immunohistochemistry	51
2.10 Liver Oil Red O Staining.....	51
2.11 Liver Triacylglycerol Levels	52
2.12 Macrophage Migration Assay	52
2.13 cGMP Measurements	53
2.14 Real-time Quantitative PCR (qPCR)	53
2.15 Mitochondrial DNA (mtDNA) Copy Number.....	54
2.16 Western Blotting.....	54
2.17 Tissue-level ROS Quantification.....	55
2.18 Cell Culture Models.....	55
2.18.1 HepG2 Cells	55
2.18.2 Primary Murine Hepatocytes.....	56
2.18.3 3T3-L1 Cells	56
2.18.4 Primary Adipocyte Isolation and Differentiation.....	57
2.19 Cellular-level ROS Quantification	58
2.20 Cell Culture Oil Red O Staining.....	58

2.21 <i>In Vitro</i> Lipolysis Assay	59
2.22 Seahorse Assays	59
2.23 Assessment of Isolated Mitochondria Bioenergetics.....	60
2.24 Preparation of Purified TSP1.....	62
2.25 Preparation of <i>In Vitro</i> Fatty Acid Treatments.....	62
2.26 Statistical Analysis	63
Section 3: SPECIFIC AIM 1	66
3.1 Summary	66
3.2 Introduction	67
3.3 Results.....	69
3.3.1 CD47 deficiency protects mice from diet-induced obesity.	69
3.3.2 CD47 deficient mice on HF diet showed reduced systemic and adipose tissue inflammation.....	70
3.3.3 CD47 deficient mice on HF diet showed improved whole body glucose homeostasis.	72
3.3.4 Energy metabolism in WT or CD47 deficient mice under either LF or HF feeding conditions.....	72
3.3.5 Metabolic gene expression in skeletal muscle from LF or HF fed WT and CD47 deficient mice	73
3.3.6 Morphology and metabolic gene expression in brown adipose tissue from LF or HF fed WT and CD47 deficient mice	74
3.3.7 cGMP/PKG signaling in WT and CD47 deficient mice under either LF or HF feeding conditions.....	75
3.3.8 Characterization of white adipose tissue depots in CD47 deficient mice challenged with HF diet	76
3.3.9 White adipocyte function <i>in vitro</i>	76
3.3.10 Regulation of lipid turnover by CD47	78
3.3.11 FFA-mediated uncoupling of brown adipose tissue mitochondria.....	79
3.4 Discussion	79
Section 4: SPECIFIC AIM 2.....	112
4.1 Summary	112
4.2 Introduction	113
4.3 Results.....	114
4.3.1 TSP1 deficiency protects mice from diet-induced fatty liver	114
4.3.2 TSP1 deficiency alters hepatic genes related to lipid metabolism	115

4.3.3 CD47 deficiency protects mice from diet-induced fatty liver	116
4.3.4 CD47 deficiency reduces obesity-associated hepatic inflammation and fibrosis	117
4.3.5 CD47 deficiency regulates lipogenic gene expression in a diet-induced fatty liver model	119
4.3.6 TSP1 and CD47 deficiency reduces hepatic oxidative stress in a diet-induced fatty liver model	119
4.3.7 CD47 expression is upregulated by high fat diet in the liver	121
4.3.8 CD47 blockade and deficiency are associated with reduced FFA and TSP1-induced ROS development in hepatocytes <i>in vitro</i>	121
4.4 Discussion	122
Section 5: GENERAL DISCUSSION	145
5.1 Summary	145
5.2 TSP1-independent Effects in CD47 Deficient Mice	147
5.3 Differential Effects of CD47 Deficiency on Metabolic Tissues.....	148
5.4 Potential Mechanisms Linking CD47 and Energy Expenditure	150
5.4.1 cGMP/PKG Signaling and Mitochondrial Function	150
5.4.2 Regulation of Mitochondrial Function by c-Myc.....	151
5.4.3 BNIP3-dependent Mitochondrial Dysfunction.....	152
5.5 Role of CD47 in Obesity-associated Inflammation	152
5.5.1 TLR4-dependent Mechanisms.....	153
5.5.2 Activation and Migration of Immune Cells	154
5.5.3 Adipose Tissue Remodeling	155
5.6 Study Limitations.....	156
5.6.1 Limitations of the Whole-body CD47 Deficient Mouse Model.....	156
5.6.2 Limitations in the Exploration of Additional CD47 Ligands/Interactions	157
5.6.3 Limitations of the Diet-induced Fatty Liver Disease Model.....	158
5.7 Future Directions.....	159
5.7.1 Effects of CD47 on cAMP Function in Metabolic Tissues.....	159
5.7.2 Pharmacological Blockade of CD47 <i>in vivo</i>	160
5.7.3 Determine the Specific Effects of CD47 Expression in Hematopoietic Cells <i>in vivo</i>	160
5.8 Clinical Significance	161
5.9 Concluding Remarks.....	163

REFERENCES.....	169
VITA.....	215

LIST OF TABLES

Table 1.1 Comparison of white and brown adipose tissues.....	40
Table 2.1 Primer sequences used in studies.....	64

LIST OF FIGURES

Figure 1.1 Adipose tissue remodeling and inflammation.	41
Figure 1.2 Relationship between obesity and systemic complications.	42
Figure 1.3 Molecular structure of CD47	43
Figure 1.4 Dietary regulation of CD47 mRNA levels in a variety of tissues	44
Figure 1.5 TSP1-mediated activation of CD47 on intracellular signaling	45
Figure 2.1 Seahorse Biosciences Mitochondrial Stress Test Protocol.....	65
Figure 3.1 Weight-related measures after LF/HF diet challenge	87
Figure 3.2 Obesity-associated systemic inflammation.....	89
Figure 3.3 Adipose tissue inflammation and macrophage infiltration.....	91
Figure 3.4 Liver lipid accumulation	93
Figure 3.5 Glucose and insulin tolerance tests	95
Figure 3.6 Metabolic profiles of WT and CD47 deficient mice under either LF or HF feeding conditions.....	97
Figure 3.7 Metabolic gene expression in skeletal muscle from LF or HF feeding WT or CD47 deficient mice.....	99
Figure 3.8 Morphology and metabolic gene expression in BAT from LF or HF fed WT or CD47 deficient mice.....	101
Figure 3.9 cGMP or PKG signaling in BAT and skeletal muscle from LF or HF fed WT or CD47 deficient mice.....	103
Figure 3.10 Characterization of white adipose tissue depots in CD47 deficient mice challenged with HF diet.....	105
Figure 3.11 Adipogenesis and mitochondrial function of white adipocytes	107
Figure 3.12 Regulation of lipid turnover by CD47	109
Figure 3.13 FFA-dependent uncoupling in BAT mitochondria	111
Figure 4.1 Liver phenotype of TSP1 deficient and control mice after 16 week LF/HF diet challenge	130
Figure 4.2 Metabolic gene expression in the livers of TSP1 deficient and WT controls after 16 week LF/HF feeding.....	132
Figure 4.3 Liver phenotype of CD47 deficient and control mice after 16 week LF/HF diet challenge	134

Figure 4.4 Obesity-associated hepatic inflammation	136
Figure 4.5 Obesity-associated hepatic fibrosis	138
Figure 4.6 Metabolic gene expression in the livers of CD47 deficient and WT controls after 16 week LF/HF feeding.....	140
Figure 4.7 Hepatic oxidative stress.....	142
Figure 4.8 FFA and TSP1-induced ROS development in hepatocytes <i>in vitro</i> .	144
Figure 5.1 Tissue-specific regulatory functions of CD47 in adipose tissues, skeletal muscle, and the liver.....	166
Figure 5.2 Comparison of TSP1 deficient and CD47 deficient mice phenotypes after 16-week HF diet challenge	168

LIST OF ABBREVIATIONS

4-HNE, 4-hydroxynonenal; AC, adenylyl cyclase; ACO, acyl-CoA oxidase; ACS, acyl-CoA synthase; ADP, adenosine diphosphate; ALT, alanine transaminase; ASOs, antisense oligonucleotides; ATCC, American Type Culture Collection; ATM, adipose tissue macrophages; ATP, adenosine triphosphate; AUC, area under curve; BAT, brown adipose; BSA, bovine serum albumin; BMI, body mass index; BNIP3, BCL2/adenovirus E1B 19kDa protein-interacting protein 3; BW, body weight; cAMP, cyclic adenosine monophosphate; CCR2, C-C chemokine receptor type 2; CD47^{+/+}, CD47 wildtype littermate mice; CD47^{-/-}, CD47 deficient mice; cGMP, cyclic guanosine monophosphate; ChREBP, carbohydrate response element binding protein; CL, CL 316,243; CoA; coenzyme A; COCVD, Center of Research in Obesity and Cardiovascular Disease; CPT-1, carnitine palmitoyltransferase-1; CVD, cardiovascular disease; DMEM, Dulbecco's Modified Eagle Medium; EAT, epididymal adipose tissue; ECM, extracellular matrix; eNOS/NOS3, endothelial nitric oxide synthase; ER, endoplasmic reticulum; ETC, electron transport chain; FABP, fatty acid binding protein; FATP, fatty acid transport protein; FBS, fetal bovine serum; FCCP, carbonyl cyanide 4-(trifluoromethoxy) phenylhydrazone; FFA, free fatty acid; G6P, glucose 6-phosphatase; GAPDH, glyceraldehyde 3-phosphate dehydrogenase; GTT, glucose tolerance test; GST, glutathione-S-transferase; H₂DCFDA, 2',7'-dichlorodihydrofluorescein diacetate; HCC, hepatocellular carcinoma; HDL, high density lipoprotein; HF, high fat; HIF1, hypoxia inducible factor 1; HSC, hepatic stellate cell; HSL, hormone sensitive lipase; HUVECs, human umbilical vein

endothelial cells; IAP, integrin-associated protein; IBMX, 3-isobutyl-1-methylxanthine; IHC, immunohistochemistry; IL, interleukin; iNOS/NOS2, inducible nitric oxide synthase; i.p., intraperitoneal; Iso, Isoproterenol; ITT, insulin tolerance test; LDL, low density lipoprotein; LF, low fat; LPS, lipopolysaccharide; LXR, liver X receptor; MCD, methionine choline deficient; MDA, malondialdehyde; MEM, Minimum Essential Media; MRI, magnetic resonance imaging; MRS, magnetic resonance spectroscopy; mtDNA, mitochondrial DNA; NAFLD, nonalcoholic fatty liver disease; NASH, nonalcoholic steatohepatitis; nDNA, nuclear DNA; NF κ B, nuclear factor κ B; nNOS/NOS1, neuronal nitric oxide synthase; NO, nitric oxide; ns, no significance; NRF1, nuclear respiratory factor 1; Nrf2, nuclear factor E2-related factor 2; OCR, oxygen consumption rate; PA, palmitate; PAI-1, plasminogen activator inhibitor-1; PCR, polymerase chain reaction; p-eNOS, phosphorylated endothelial nitric oxide synthase; PEPCK, phosphoenolpyruvate carboxykinase; PGC1 α , peroxisome proliferator-activated receptor gamma coactivator 1-alpha; PKA, cAMP-dependent protein kinase/protein kinase A; PKG, cGMP-dependent protein kinase/protein kinase G; PLIC, proteins linking IAP to cytoskeleton; PPAR γ , peroxisome proliferator activated receptor- γ ; RFU, relative fluorescence unit; ROS, reactive oxidative species; RT, room temperature; SAT, subcutaneous adipose tissue; SDS-PAGE, sodium dodecyl sulfate polyacrylamide gel electrophoresis; SE, standard error; SIRP, signal regulatory protein; sGC, soluble guanylyl cyclase; SREBP, sterol regulatory element binding protein; T2DM, type 2 diabetes mellitus; TC, total cholesterol; TG, triglyceride; TGF β , transforming growth factor- β ; TLR, toll like

receptor; TSP1, thrombospondin-1; TSP1^{-/-}, thrombospondin-1 deficient mice; UCP1, uncoupling protein 1; VEGFR2, vascular endothelial growth factor receptor 2; VLDL, very low density lipoprotein; WAT, white adipose; WT, wildtype;

Section 1: BACKGROUND

1.1 Defining Obesity

Over the past thirty years, obesity has become a global health concern. Obesity, or an excessive accumulation of fat (lipid), is a result of significant expansion of adipose tissue depots and the deposition of lipid in other organs. The greatest cause of obesity is increased energy consumption paired with a lack of energy expenditure. As a consequence, serious systemic metabolic dysfunctions occur due to increased lipid deposition. Many obesity-associated comorbidities are a result of impaired adaptive mechanisms to manage increased lipid burden.

Evolutionarily, our bodies have become increasingly efficient at storing excess energy for times of need. Initially, humans could go long periods of time fasting as they hunted and searched for food; relying on the hydrolysis of triglycerides (TGs) in adipose tissue stores to release free fatty acids (FFAs), glycogenolysis (break down of glycogen), gluconeogenesis (conversion of non-carbohydrate sources to glucose), and ketogenesis (production of ketone bodies) for energy. As our food availability has rapidly progressed in comparison to the evolution of biological mechanisms, overweight and obesity have become common concerns due to the redundant mechanisms in place that lead to energy storage.

1.1.1 Prevalence of Obesity

The obesity epidemic is not restricted to a specific population or region of the world. In 2014, the World Health Organization reported that approximately

39% of the global adult population was overweight and 13% were considered obese (290). It is predicted by 2030 that roughly 57% of the global adult population will be either overweight or obese (123). Although obesity is a global issue, certain populations are at a disproportionate risk of developing obesity and its associated complications. Around the world, developing countries adopting elements of western culture, such as increased processed food consumption and sedentary behaviors, are experiencing dramatic increases in obesity rates. For example, it is predicted that over 60% of the world's obese adult population reside in developing or developed nations (182). Within the United States, the rates of obesity in Hispanic and African American populations are 42.5% and 47.8%, respectively (190). What is most concerning about the staggering rates of obesity is that significant adiposity typically serves as a predictor for a number of serious metabolic dysfunctions including type 2 diabetes, cardiovascular disease, and even some cancers.

The most common measurement used to determine obesity prevalence is body mass index (BMI; weight in kilograms divided by height in meters squared). In adults, a BMI of 30 or greater is considered obese. Another simple and reliable method is waist circumference. Men and women with waist circumferences greater than 40 inches (102cm) and 35 inches (88cm), respectively, are considered obese and at increased risk for obesity-associated complications (111). Some suggest waist circumference or waist-to-hip ratios are more accurate metrics for obesity because BMI is unable to distinguish weight as fat or lean mass.

1.1.2 Characteristics of Adipose Tissue

Adipocytes (fat cells) are the primary lipid storage cell within the body. Although they are responsible for 95% of the volume of adipose tissue depots, this cell type only constitutes 25% of the cell population in adipose tissue (140). Other cell types include endothelial cells, pericytes, pre-adipocytes, and immune cells. As FFAs enter the adipocyte, the enzyme acyl CoA synthase (ACS) attaches coenzyme-A (CoA) thioesters to FFAs forming fatty acyl-CoA. Through an esterification process, three fatty acyl-CoA residues are esterified to a glycerol backbone forming triglyceride (TG; triacylglycerol) (48). Due to its hydrophobic nature, the endoplasmic reticulum (ER) packages lipid (TG and cholesterol esters) within the cell into lipid droplets coated with phospholipids and lipid-droplet associated proteins (159). Several extracellular signals can activate hydrolysis of TG within lipid droplets to provide FFAs as an energy substrate for ATP production in times of energy deprivation. Lipolysis is mediated by several lipases including adipose triglyceride lipase (ATGL), hormone sensitive lipase (HSL), and monoglyceride lipase (MGL) (301).

Recent studies have determined that WAT depots are not just inert energy storage depots, but rather dynamic tissues with endocrine and paracrine functions. In addition to their plasticity, adipose tissue can receive both hormonal and afferent neuronal signals suggesting dynamic interactions and crosstalk with other tissues (223). Adipose tissue can respond by secreting molecules involved in regulating a number of pathways including hunger, energy metabolism, and

inflammatory responses. These molecules include growth factors, cytokines, chemokines, acute phase proteins, and adipokines.

During obesity-associated adipose tissue expansion, two primary processes contribute to tissue growth and remodeling. Adipocytes accommodate more lipid by enlarging the storage capacity within a single cell resulting in adipocyte hypertrophy (single cell expansion) (45). Second, resident stem cell-like preadipocytes begin to terminally differentiate resulting in new adipocytes to sequester increased lipid burden within the adipose tissue depot. This expansion in cell number is called hyperplasia (140). Specific adipogenic transcription factors, such as peroxisome proliferator-activated receptor- γ (PPAR γ) and members of the CCAAT/enhancer-binding protein (C/EBP) family, largely mediate the differentiation of new adipocytes (222). As a result, adipocytes are now considered one of the most morphologically dynamic cell types capable of adjusting cell size and number to accommodate increased energy substrate storage.

Lineage tracing studies suggest that the formation of different adipose tissue depots is determined at the level of the stem cell progenitor. Although all adipocyte differentiation mechanisms are largely mediated by PPAR γ and C/EBP family members (222), white adipocytes are derived from different progenitor cells than other types of adipocytes. For example, white adipocytes rise from Myf5-negative progenitors while brown adipocytes more closely resemble skeletal muscle in the Myf5-positive lineage (234).

1.1.2.1 White Adipose Tissue (WAT)

Over the past decade it has been determined that mammals, including humans, have various types of adipose tissue responsible for different functions. As previously described, white adipose tissue (WAT) is primarily responsible for storing lipid until times of need and sequestering excess lipid to prevent lipotoxicity in other tissues. WAT is characterized by adipocytes with large singular lipid droplets (unilocular), low basal energy expenditure, and very little protein/mitochondrial content which contributes to its white morphology.

WAT plays a unique role in regulating food intake, energy expenditure, and metabolic function in other tissues through the production and secretion of several adipokines (secreted from adipocytes). For example, leptin was identified in 1994 as an adipokine in which plasma levels positively correlate to adipose tissue mass (305). Mice lacking the leptin gene are hyperphagic and morbidly obese; however chronic leptin administration drastically reduces body weight, suppresses hunger, and induces fatty acid oxidation (91, 201). Leptin elicits these effects by signaling to the arcuate nucleus, the hunger center of the brain, to suppress food intake and stimulate physical activity. Although leptin seemed like a promising anti-obesity therapeutic in the 1990s and early 2000s, it was soon discovered that obese individuals exhibit hyperleptinemia and develop a form of leptin resistance, which abolishes all anorexigenic effects of the protein on the brain (161, 262).

Another well-characterized adipokine is adiponectin. Unlike leptin, plasma adiponectin levels negatively correlate with BMI and adipose tissue mass. The

primary function of adiponectin is to improve insulin sensitivity, increase skeletal muscle and adipose tissue glucose uptake, and suppress hepatic glucose production (82, 161). In addition to adipokines, cytokines and chemokines may be secreted from resident adipose tissue macrophages (ATMs) that stimulate various effects on other peripheral tissues.

1.1.2.2 Brown Adipose Tissue (BAT)

In addition to WAT depots, brown adipose tissue (BAT) is another type of adipose tissue that has been recently identified in adult humans. BAT was thought to only exist in human infants and other small mammalian species with large surface to volume ratios – reason being the need for mechanisms to regulate whole body temperature homeostasis. However, in 2009, four independent studies confirmed with positron-emission tomography with computed tomography (PET-CT) scans the presence of an adipose tissue depot in humans located in the paracervical and supraclavicular region with enhanced glucose uptake and robust metabolic activity (54, 226, 267, 273).

Once activated, BAT catabolizes lipid and other energy substrates at an accelerated rate to maintain non-shivering thermogenesis (shivering thermogenesis is a result of skeletal muscle heat generation). This specific mechanism unique to BAT is largely dependent on the mitochondrial protein, uncoupling protein 1 (UCP1) (184), which is associated with the inner mitochondrial membrane, is activated by FFAs, and dissipates chemical energy as heat by uncoupling the electron transport chain (ETC) (30). As a result, BAT morphology is different from WAT in that it has high protein content due to

increased mitochondrial density, multiple lipid droplets per cell (multilocular) to increase surface area and fuel accessibility, and enhanced blood flow for lipid oxidation (94).

The most potent activator of BAT-driven energy expenditure is the sympathetic nervous system in response to cold exposure. This mechanism is mediated by the release of norepinephrine and activation of β -adrenergic receptors on the brown adipocyte cell surface. Other physiological activators of BAT activity include fibroblast growth factors, thyroid hormone, bone morphogenetic proteins, certain myokines (e.g. irisin), and abundant FFAs (26, 67, 71, 142, 204, 284). Certain compounds have been identified that activate UCP1-driven energy expenditure in humans including common nutraceuticals (e.g. capsinoids, capsaicin) and β -adrenergic receptor agonists (55, 227). In efforts to pharmacologically stimulate BAT through β -adrenergic stimulation, several studies have been deemed unsuccessful due to off-target effects on the cardiovascular system.

Although studies are inconclusive on whether BAT in humans phenocopies classical interscapular BAT of rodents, it is clear that activated BAT in humans and rodents can regulate whole body lipid homeostasis. In 2011, Bartelt et al. clearly demonstrated that BAT, despite low tissue mass/body weight ratios, can uptake approximately 50% of dietary TGs in rodents (17). They even showed cold-induced BAT activation could protect hyperlipidemic genetic rodent models from deleterious cardiovascular events (17). FFAs are an ideal energy source because they provide abundant energy to sustain constant UCP1-

dependent uncoupling within activated BAT. Studies in humans have shown that only 50g (~0.1lbs) of BAT could contribute to $\leq 20\%$ basal caloric requirements (224). Over the past few years, exploiting the potential of BAT energy expenditure has become a popular target for developing anti-obesity therapeutics.

1.1.2.3 Beige Adipose Tissue

Beige adipose tissue is primarily located within WAT depots; however, it shares several similar characteristics with BAT. These adipocytes are still capable of storing large amounts of lipid, yet respond to cold exposure and β -adrenergic stimulation to drive UCP1-dependent energy expenditure (291). Interestingly, these adipocytes are from the same Myf5 negative lineage as white adipocytes and express unique beige adipocyte markers (Cd137, Tmem26) (234, 291), suggesting they are a distinct cell type not related to brown adipocytes. Further, there are several anatomically-distinct WAT depots in rodents and humans, but beige adipocytes have only been identified in retroperitoneal and subcutaneous depots (223). Some suggest future anti-obesity studies should target beige adipose tissue or the “browning” of white adipose tissue rather than BAT due to the substantial differences in WAT and BAT mass in humans. A comparison of the three distinct forms of adipose tissue can be found in Table 1.1.

1.2 Pathophysiology of Obesity

When examining the pathophysiology of obesity, it is important to understand how body fat distribution in obesity contributes to metabolic

dysfunction. It has been established that visceral or central obesity located in the abdominal trunk is more pathological than other depots such as subcutaneous adipose tissue. It has been well established through numerous longitudinal studies that central adiposity alone is an independent predictor of insulin resistance and cardiovascular disease (35, 134, 192). Visceral adipose tissue has direct access to portal vein circulation; therefore, dysregulated lipolysis leads to increased flux of FFA into circulation reaping deleterious effects on hepatic function and cardiovascular health (20, 23).

It is clear that the development of obesity is multifactorial and negatively impacts a number of tissues and organ systems. As a result of adipose tissue expansion through hypertrophy, the secretion of adipokines and inflammatory molecules become dysregulated. For example, expression of adiponectin, the anti-inflammatory and insulin-sensitizing hormone, is significantly reduced in adipose tissue and in circulation of obese individuals (161).

1.2.1 Obesity-associated Inflammation

It is now widely accepted that obesity is a condition characterized by low-grade chronic inflammation. Adipose tissue remodeling and expansion in response to high fat diet stimulates resident ATMs to secrete several proinflammatory cytokines and chemokines (see Figure 1.1) (141, 281). In 1993, Hotamisligl et al. determined circulating levels and adipose tissue expression of tumor necrosis factor- α (TNF α) were significantly upregulated in obese rodent models (96). Several subsequent studies confirmed a direct role of TNF α in mediating insulin resistance by impairing glucose disposal in liver, muscle, and

adipose tissues (225, 248, 265). It has even been shown that TNF α deficiency in a diet-induced obese rodent model improved peripheral insulin sensitivity compared to controls (265), suggesting a systemic role of TNF α in obesity-associated insulin resistance. Further, it has been determined that ATMs are primarily responsible for recruiting additional immune cells to adipose tissue depots by way of chemokines such as monocyte chemoattractant protein 1 (MCP1) (117). Other cytokines and chemokines implicated in the pathogenesis of obesity-associated inflammation include interleukin-6 (IL-6), plasminogen activator inhibitor-1 (PAI-1), and IL-1 β (70, 196). Together, these mechanisms augment systemic and adipose tissue-specific proinflammatory environments, which promote other obesity-associated complications.

1.2.2 Dyslipidemia

Another characteristic of obesity is the presence of dyslipidemia, or pathological levels of lipid in circulation. Increased circulating FFAs are a result of rampant lipid turnover in adipose tissue. As a result, metabolic tissues such as muscle and liver will utilize FFAs as a preferred energy substrate for ATP production and reduce glucose disposal from circulation (208). In addition, hepatic uptake of plasma FFAs will induce gluconeogenesis further exacerbating hyperglycemic conditions (285). Hypertriglyceridemia and elevated plasma FFA levels will also affect lipoprotein metabolism by increasing very-low density lipoprotein (VLDL) and low-density lipoprotein (LDL) production and suppressing the assembly of protective high density lipoprotein (HDL) particles. To further exacerbate the issue, chronically elevated plasma FFAs commonly observed

under obese conditions impair insulin secretion from the pancreas in response to hyperglycemia blunting glucose disposal by insulin-sensitive tissues (307).

1.2.3 Insulin Resistance

Insulin resistance is another contributor to the pathophysiology of obesity. Insulin, a hormone secreted from beta cells within the pancreas, stimulates glucose uptake and energy storage in muscle, adipose tissue, and the liver in order to maintain tight regulation of blood glucose levels. Several mechanisms work tightly to control blood glucose concentrations at physiological levels in times of fasting (92); however, hepatic insulin resistance perpetuates hyperglycemia even in fed conditions. Once the liver no longer responds to insulin, it is unable to suppress glucose production via gluconeogenesis and glycogenolysis. In addition, insulin resistance in the liver drives deregulated *de novo* lipogenesis and lipid trafficking to peripheral tissues. Adipose tissue is another insulin-responsive tissue. In addition to glucose uptake in adipose tissue, a critical function of insulin is to inhibit hydrolysis of TGs and promote lipid storage. However, in insulin resistant adipose tissue, insulin is unable to blunt lipolysis which leads to an increased flux of FFAs out of adipose tissue into circulation which further propagates dyslipidemic conditions in obesity. This vicious cycle triggers the continued secretion of insulin from the pancreas, ultimately resulting in the development of overt type 2 diabetes mellitus (282), highlighted in more detail in Section 1.2.1.1.

1.2.4 Obesity-associated Brown Adipose Tissue Dysfunction

Knowing adult humans have functional BAT depots, which require increased energy substrates, recent studies have targeted BAT function as an anti-obesity therapeutic strategy to help restore global energy balance. In one study examining differences in BAT activity between lean and overweight/obese adult men, it was determined that BAT activity negatively correlates with BMI and body fat percentage (267). It has also been shown in humans that obesity significantly blunts cold-induced BAT activation and glucose uptake compared with lean controls (197). In addition, rodent models have begun to elucidate the effects of obesity on BAT morphology and function. Although lean and obese rodents have similar BAT mass (156), BAT function is impaired as demonstrated by reduced blood flow and insulin resistance in rodents, as well as suppressed metabolic activity in rodents and humans (197, 215, 237). Several genes implicated in BAT-mediated energy expenditure, including UCP1, are significantly downregulated with HF diet, which augments impaired BAT function in obese rodent models (237). Identifying mechanisms that preserve BAT function under obese conditions could provide novel anti-obesity therapeutic targets.

1.2.5 Obesity-associated Comorbidities

It is clearly evident that the pathology of obesity is not restricted to adipose tissue, but causes deleterious effects on several organ systems and their functions. This is illustrated in Figure 1.2. Obesity increases the risk of developing a number of complications including type 2 diabetes mellitus (T2DM), cardiovascular disease (CVD), non-alcoholic fatty liver disease (NAFLD), stroke,

sleep apnea, certain cancers, gallbladder disease, and gout (21, 72, 203). Further, men and women classified as obese according to BMI are at even greater risk for all-cause mortality (283).

1.2.5.1 Type II Diabetes Mellitus (T2DM)

T2DM is a metabolic condition characterized by hyperglycemia and impaired responses to insulin signaling and reduced glucose disposal. In the United States, it is estimated that approximately 15% of individuals are living with T2DM, whether diagnosed or undiagnosed (50). As previously mentioned, insulin resistance perpetuates a vicious cycle that exacerbates hyperglycemic conditions, causing the pancreas to continuously secrete insulin in response to elevated plasma glucose. Ultimately, the pancreas is unable to compensate for hyperglycemia resulting in impaired insulin release. The presence of T2DM has also been shown to be a strong risk factor for micro- and macrovascular complications including nephropathy, retinopathy, neuropathy, dementia, and cardiovascular disease.

1.2.5.2 Cardiovascular Disease (CVD)

Cardiovascular disease (CVD) is a collective term for dysfunctions associated with the heart and vasculature, which includes coronary heart disease, cerebrovascular disease, and atherosclerosis. Collectively, CVD is the number one cause of mortality worldwide (168). A 26-year follow up of the Framingham Heart Study established that obesity alone was an independent risk factor for the development of CVD in both men and women (99). In combination, obesity and insulin resistance associated with T2DM drastically increase the risk

of an individual developing CVD. To demonstrate the tight association between T2DM and CVD, several studies suggest T2DM is a significant independent risk factor for CVD (287, 288) and it has been determined that the cause of mortality in over two thirds of all individuals diagnosed with T2DM is CVD (86).

1.2.5.3 Non-Alcoholic Fatty Liver Disease (NAFLD)

Due to the dramatic rise in obesity and central adiposity, non-alcoholic fatty liver disease (NAFLD) has become the most common liver disease around the world. NAFLD is defined as lipid accumulation in $\geq 5\%$ of hepatocytes not attributed to alcohol consumption, medications, or other disease states (37). Primarily, diet-induced obesity is the largest known cause for the development of NAFLD. Moreover, NAFLD is considered a progressive disease that can range from simple steatosis and fibrosis, to the development of non-alcoholic steatohepatitis (NASH), cirrhosis, and ultimately hepatocellular carcinoma (HCC) (2). Because of the critical role of the liver in whole body glucose and lipid homeostasis, patients diagnosed with NAFLD are at an increased risk of developing T2DM, CVD, and metabolic syndrome (3, 259).

1.2.5.4 Metabolic Syndrome

Metabolic syndrome is a condition in which an individual presents a combination of pathological metabolic factors that significantly enhance the likelihood of developing CVD and all-cause mortality. Although several definitions for metabolic syndrome have been established by different health organizations over the past several decades, a consensus was reached in 2009 by the International Diabetes Federation, National Institutes of Health, American Heart

Association, World Health Federation, International Atherosclerosis Society, and International Association for the Study of Obesity. This publication stated that the diagnosis of metabolic syndrome would include the presence of three out of five specific components (5). These specific components include 1) increased waist circumference, 2) hypertriglyceridemia ($\geq 150\text{mg/dL}$), 3) reduced HDL cholesterol ($< 40\text{mg/dL}$ in males; $< 50\text{mg/dL}$ in females), 4) hypertension (systolic $\geq 130\text{ mmHg}$ and/or diastolic $\geq 85\text{ mmHg}$), 5) and/or fasting hyperglycemia ($\geq 100\text{mg/dL}$).

1.3 NAFLD: Impacts on Metabolic Health

Like obesity, NAFLD has become a global health concern. Because the prevalence of NAFLD is so tightly linked to obesity, incidence rates have significantly increased over the past few decades. Although the prevalence rates of NAFLD vary depending on diagnostic techniques and the population of interest, it is estimated that one third of the United States adult population present NAFLD (29). Moreover, 20-30% of the adult populations in Europe, the Middle East, and Asia are also thought to have NAFLD (12, 66, 209).

Variability is high in estimating the prevalence of NAFLD around the world due to differences in diagnostic criteria, access to medical technology, and subjectivity to pathological analysis. Primarily, ultrasonography is the most commonly used qualitative measure of hepatic lipid accumulation. Other imaging techniques including computerized tomography (CT), magnetic resonance spectroscopy (MRS) and magnetic resonance imaging (MRI) are also used (7); however, accessibility and cost for more advanced imaging is restricted in some

locations around the world. Alanine transaminase (ALT), a serum biochemical marker upregulated in the presence of liver injury, has been used as an indicator of NAFLD development for a number of years. It has even been shown that elevated serum ALT levels in humans correspond with an increased risk of developing end-stage liver disease (61). More recently, studies suggest monitoring serum ALT levels could grossly underestimate the prevalence of NAFLD because some patients with progressive fatty liver can present normal serum ALT levels (269). Distinguishing cases of NAFLD from more advanced forms of steatosis are very difficult with imaging techniques and serum biomarkers. Liver biopsies are preferred for quantitatively determining the severity of the steatosis yet is a much more involved diagnostic criteria and is still subject to sampling bias and inaccurate interpretation (7).

1.3.1 Hepatic Lipid Metabolism

The liver is a dynamic organ responsible for a number of metabolic processes. In particular, the liver plays an integral role in whole body lipid metabolism and homeostasis. A number of mechanisms are involved in regulating the amount of lipid within the hepatocyte, with the goal to maintain very low levels of intracellular FFAs. These pathways include fatty acid uptake, *de novo* lipogenesis/TG synthesis, fatty acid oxidation, and TG export to peripheral tissues through lipoprotein secretion.

As FFAs arrive at the liver, they are taken up into hepatocytes by fatty acid transport proteins (FATP2, FATP5), fatty acid translocases (FAT/CD36), or they diffuse freely across the plasma membrane due to their lipophilic nature. It is

unclear whether FFA uptake from circulation into the liver is regulated; however, some suggest that the amount of FFA uptake is directly proportional to the FFA concentration in circulation (121). Once in the cell, there are a number of fates for FFAs. Immediately, FFAs are bound to fatty acid binding protein (FABP) or acyl-CoA by way of acyl-CoA synthases (ACS) and are transported to various locations in the cell. Some FFAs function as signaling molecules and activate a number of nuclear receptors and transcription factors implicated in lipid metabolism including sterol regulatory element binding proteins (SREBPs) and liver X receptors (LXRs) (124, 296).

As a highly energetic organ, the liver relies on FFAs as a constant and efficient fuel supply for the production of adenosine triphosphate (ATP) within mitochondria. In hepatic β -oxidation, entry into mitochondria for FFA species 14 carbons or longer is mediated by the enzyme carnitine palmitoyltransferase-1a (CPT1a). This enzyme converts FFA to acyl-carnitine in order to be transported across the mitochondrial membrane. FFA species 12 carbons or less are able to pass through the mitochondrial membrane without a transport system (232). CPT1a serves as the rate-limiting step of β -oxidation, acting as a switch so that the synthesis of FFAs as well as the catabolism of FFAs does not occur simultaneously. To a lesser extent, very long chain FFAs can be catabolized within peroxisomes yielding much less ATP due to their lack of an electron transport chain (ETC).

A critical function of the liver is to assemble lipids into VLDL particles and export them out of the liver to other peripheral tissues either for energy or

storage. The enzyme microsomal triglyceride transfer protein (MTTP) is required for the packaging and secretion of VLDL from the liver. It has even been demonstrated in rodents that genetic and pharmacological interruptions in MTTP function significantly blunt VLDL secretion and result in increased hepatic lipid accumulation (145). This indicates just how critical hepatic lipoprotein assembly is for maintaining hepatic lipid homeostasis.

In excess, FFAs are esterified and stored in the form of TG within the cytosol of the hepatocyte either for future use or as a mechanism to protect the cell from FFA-induced cellular dysfunction. TG synthesis is largely regulated by SREBP-1c, LXRs, carbohydrate regulatory element binding protein (ChREBP), PPAR γ , and the overall energy state within the cell (47, 58). If cellular fuel (ATP) is low, acyl-CoA and FFAs are shunted into the β -oxidation pathway and TG synthesis is repressed (175).

1.3.2 Pathophysiology of NAFLD

Elevated intrahepatic triglyceride associated with NAFLD contributes to an imbalance in lipid, glucose, and lipoprotein metabolism. NAFLD is characterized by increased lipid deposition in hepatocytes, a result of enhanced TG synthesis as well as elevated oxidative stress and inflammation driven by FFA-induced lipotoxicity. Together, these two factors are closely linked to insulin resistance; however, it has not been fully determined whether NAFLD is the cause or simply a result of insulin resistance. Some rodent studies suggest that high fat (HF) diet challenge for acute periods of time (few days) can significantly impair insulin signaling in the liver prior to systemic effects of diet-induced obesity, suggesting

the liver plays a central role in the development of whole body insulin resistance (228).

Oxidative stress and low-grade chronic inflammation are consistently observed in NAFLD and cardiometabolic disorders (69, 221). In NAFLD, elevated FFAs levels in portal circulation from both dietary consumption and increased adipose tissue lipolysis are taken up by hepatocytes, which drive intracellular oxidative stress (180). Oxidative stress is a result of impaired cellular capacity to maintain a balance between detoxifying mechanisms and the production of reactive oxidative species (ROS), molecules with unpaired electrons. Some of the most commonly observed forms of ROS include superoxide anions ($\cdot O_2^-$), hydrogen peroxide (H_2O_2), and hydroxyl radicals ($\cdot OH$).

In lipotoxic conditions, protective mechanisms triggered by the hepatocyte, such as increased mitochondrial respiration and activated antioxidant pathways, are compromised further exacerbating oxidative stress within the cell (115, 231). Mitochondria will respond to increased lipid burden by activating the fatty acid oxidation pathway as a compensatory mechanism to maintain low levels of FFA within the cell. However, after chronic burden, the mitochondria begin to produce ROS through enhanced electron leakage and subsequently contribute to the poor oxidative environment within the cell (230, 243). In addition, nuclear factor E2-related factor 2 (Nrf2), a critical transcription factor that regulates the expression of several cytoprotective enzymes, is significantly downregulated by NAFLD (243). These protective enzymes include glutathione S-transferase (GST) enzymes, NADPH quinone oxidoreductase 1 (NQO1), and heme oxygenase 1

(HO-1) (183). Reduced expression of these genes contributes to the imbalance between detoxification and ROS production classically observed in the presence of fatty liver. Several studies have focused on ways to activate and preserve Nrf2 signaling despite the progression of NAFLD as a potential mechanism to protect against hepatic lipid accumulation and insulin resistance (60, 139, 205)

Many of the deleterious effects of oxidative stress are a consequence of damaged intracellular lipids, proteins, and nuclear and mitochondrial DNA which are highly susceptible in poor oxidative environments. In the case of fatty liver disease where intracellular lipid is elevated, lipid peroxidation is commonly observed and can be measured by the levels of reactive aldehyde species including malondialdehyde (MDA) and 4-hydroxynonenal (HNE). In addition to cellular dysfunction and mutagenic effects, oxidative stress induces the production of proinflammatory cytokines and adhesion molecules (69) further propagating systemic oxidative stress and inflammation under obese conditions.

In efforts to determine the initiating causes of hepatic steatosis, some research has focused on the development of oxidative stress and mitochondrial dysfunction. Not only has oxidative stress been implicated in the progression of obesity and cardiometabolic dysfunction (97, 163), some rodent studies suggest mitochondrial-dependent oxidative stress precedes the development of insulin resistance in early stages of NAFLD pathogenesis (211). Rector et al. demonstrated that obese-prone OLETF rats exhibited altered hepatic mitochondrial function and a pro-oxidative environment prior to the development of NAFLD, suggesting that mitochondrial distress may be a casual mechanism as

well as a consequence of hepatic metabolic dysfunction (211). In addition, hepatic oxidative stress has been shown to consistently drive the progression of diet-induced insulin resistance (163).

1.3.3 Contribution of Other Cell Types to NAFLD Development

Although hepatocytes are the primary cell type in the liver affected by lipid accumulation, other cell types are present that have been implicated in the pathophysiology of NAFLD. Kupffer cells are resident macrophages located in the liver sinusoids. They contribute to the detoxifying functions of the liver by quickly recognizing foreign or dangerous molecules and containing them for degradation (206). Hepatic lipid has been shown to activate Kupffer cells through a number of mechanisms. For example, ballooning of hepatocytes due to lipid overload creates physical restriction on liver sinusoids reducing blood flow and activating Kupffer cell-mediated inflammatory pathways (65). In addition, FFAs in circulation can activate various cell membrane receptors, including members of the toll like receptor (TLR) family, and induce the release of inflammatory markers such as TNF α (125).

Another cell type that contributes to the progression of NAFLD to more serious NASH is the hepatic stellate cells (HSCs). As a result of increased proinflammatory cytokine secretion from Kupffer cells, HSCs become activated and produce substantial amounts of extracellular matrix (ECM) including collagen type I, fibronectin, and proteoglycans resulting in a significant remodeling of cellular structure and stiffening of the liver tissue (289). In addition to fibrosis, HSCs contribute to the proinflammatory environment by secreting additional

cytokines that perpetuate hepatic fibrogenesis. Last, sinusoidal endothelial cells have also been implicated in the pathology of NAFLD. Like other metabolic diseases, NAFLD-associated endothelial dysfunction has been linked to impaired vasoconstriction and vasodilation, which augments the progression of inflammation, oxidative stress, and fibrogenesis.

1.4 The Canonical NO/cGMP Signaling Pathway

The nitric oxide (NO) pathway has been considered a critical signaling mechanism for maintaining vascular tone through the induction of vascular smooth muscle cell relaxation and vasodilation. Within the past five years, the effects of this signaling cascade have been broadened to include cellular metabolism and energy homeostasis. NO, a gaseous signaling molecule, is produced by a family of enzymes called nitric oxide synthases (NOSs) (181). The first in the family, neuronal NOS (nNOS, NOS1), is exclusively expressed within the central and peripheral nervous system. Inducible nitric oxide synthase (iNOS, NOS2) is expressed largely in the immune cell population and produces pathological levels of NO that contribute to a proinflammatory environment. Endothelial nitric oxide synthase (eNOS, NOS3) was named for its high expression level in endothelial cells and its role in vascular tone; however, other studies have identified eNOS as the primary NOS isoform in a number of cell types including adipocytes, hepatocytes, and skeletal muscle (166, 171, 244). NO binds to the β 1 subunit of soluble guanylyl cyclase (sGC), which includes the heme prosthetic group and NO-binding domain. Once activated, sGC converts guanosine monophosphate (GMP) to the active secondary messenger molecule

cyclic GMP (cGMP) (57). In metabolic tissues, the effects of cGMP signaling are primarily facilitated through cGMP-dependent protein kinase (PKG), a serine/threonine protein kinase responsible for phosphorylating several intracellular targets modulating cellular functions (202).

1.4.1 Impacts of NO/cGMP Signaling on Metabolic Health

In vitro studies as well as several knockout and transgenic mouse models have demonstrated the NO/cGMP signaling pathway is critical for maintaining healthy cellular metabolism in insulin-responsive tissues. It has been clearly demonstrated that cGMP promotes adipogenesis and mitochondrial biogenesis in 3T3-L1 cells (immortalized murine preadipocyte cell line) and primary white adipocytes through increased expression of adipogenic markers (171, 235, 304). Some studies suggest that increased cGMP/PKG signaling enhances lipid turnover (133) and drives UCP1-dependent energy expenditure contributing to a browning phenomenon in white adipocytes (24, 171).

Similarly in brown adipose tissue, cGMP/PKG promotes brown adipocyte proliferation and increases PPAR γ and UCP1 expression (187). In loss-of-function studies, brown adipocytes isolated from PKG deficient mice had a significant impairment in brown adipogenesis and UCP1-dependent thermogenic potential (90). Similarly, newborn mice lacking PKG exhibit a significant reduction in BAT mass suggesting PKG regulates BAT differentiation and function *in vivo* (90). On the contrary, gain-of-function studies utilizing PKG transgenic mice exhibit a leaner phenotype, increased mitochondrial biogenesis in BAT and

skeletal muscle, and increased oxygen consumption driven by enhanced mitochondrial respiration (172).

The effects of PKG overexpression in mice challenged with HF diet are less conclusive. Miyashita et al. demonstrated that HF-fed male PKG transgenic mice were protected from diet-induced obesity after just eight weeks of feeding (172). Interestingly, Nikolic et al. saw female PKG transgenic mice, not males, were protected from diet-induced obesity after 16-week diet challenge through increased BAT-dependent energy expenditure (185). Although HF diet composed of 60% kcal from fat were used for both studies, several factors could have contributed to the conflicting reports including differences in mouse strains, length of diet challenge, and temperature of housing conditions.

Numerous rodent studies and in vitro experiments have identified the NO/cGMP/PKG signaling pathway as a therapeutic target for obesity and obesity-associated diseases. Although support is strong for the role of cGMP augmenting healthy metabolic function, the mechanisms contributing to both impaired NO/cGMP synthesis and signaling in obese conditions have not been fully defined. A handful of studies suggests increased reactive oxidative species characteristic of cellular metabolic dysfunction competitively inhibit NO-dependent activation of sGC (167, 245). Studies examining upstream regulators of NO/cGMP signaling have not been explored under obese conditions. Future studies are necessary to further elucidate mechanisms responsible for obesity-induced deregulation of NO/cGMP signaling.

1.5 Thrombospondins: Multi-functional Signaling Molecules

Thrombospondins are a family of secreted extracellular glycoproteins that serve no structural purpose, but are typically expressed in response to stress. Thrombospondins 1-2 are homotrimers (three identical subunits) while 3-5 are homopentamers (1). Each subunit consists of an N-terminal domain, central type 1 repeats, and a C-terminal domain, which are responsible for interacting with various receptors (217). Within the family, thrombospondin 1 (TSP1; also abbreviated Thbs1) has been most extensively studied. In 1971, Baenziger et al. first isolated TSP1 from platelets treated with thrombin, deeming TSP1 a stress response protein (13). Since then, TSP1 has been implicated in inflammatory responses (152), apoptosis, and serves as a major regulator of angiogenesis (101, 113). Further, TSP1 has been identified as the most potent activator of latent transforming growth factor- β (TGF- β) (51).

Transcription of the TSP1 gene is positively regulated by a number of pathways. Interestingly, hyperglycemia and hyperleptinemia, two hallmarks of obesity and metabolic dysfunction, have been identified as positive regulators of TSP1 transcription in a variety of tissues including tumors, vessel walls, cardiac cells, and renal cells (42, 56, 247, 277, 306). Now, the effects of TSP1 are being examined in a variety of cardiometabolic disorders including diabetes and obesity development.

1.5.1 Links Between Thrombospondin 1 (TSP1) and Metabolic Dysfunction

Over the past twenty years, several studies have identified a pathological role for TSP1 in the development of obesity and several of its associated comorbidities. In 2000, Hida et al. first identified TSP1 as being one of thirteen novel genes upregulated in visceral adipose tissue of obese, diabetic rats compared to lean, non-diabetic controls (95). At that time, TSP1 was primarily identified as a protein released from platelets in response to stress and as an inhibitor of angiogenesis that could potentially contribute to cardiovascular disease. From this study, evidence suggested adipose tissue was a source of TSP1 in circulation. However, the cellular source of TSP1 within adipose tissue was yet to be defined.

Following this study, Varma et al. confirmed TSP1 mRNA levels were approximately four-fold higher in adipocyte fractions of human subcutaneous adipose tissue compared to the stromal vascular fraction (endothelial cells, preadipocytes, mesenchymal stem cells, immune cell population) (268). Further, significant positive correlations between human subcutaneous adipose tissue mRNA levels of TSP1 and body mass index (BMI), circulating inflammatory cytokines, and adipose tissue-specific inflammatory markers were observed (268). From these studies, it was concluded that TSP1, a novel adipokine, may contribute to systemic effects of obesity and other peripheral metabolic complications. Further studies by Matsuo et al. showed that TSP1 expression was significantly higher in human visceral adipose tissue compared to

subcutaneous adipose tissue depots and that TSP1 levels positively correlated with BMI, abdominal obesity, and hyperglycemia (162). These findings further supported the idea that robust TSP1 secretion from visceral adipose tissue may mediate global metabolic dysfunction through direct access to systemic circulation via the portal vein.

Several diet-induced obesity studies utilizing whole body TSP1 deficient mice have been completed to further investigate the role of TSP1 in the development of diet-induced body weight gain, inflammation, and insulin resistance. From these studies, there have been discrepancies in whether TSP1 deficiency regulates adiposity in a diet-induced obesity paradigm. Li et al. demonstrated that after 16 weeks of HF diet challenge (60%kCal from fat) TSP1 deficient mice were not protected against diet-induced body weight gain or fat mass accumulation compared to HF-fed wildtype controls (144). Similarly, another group demonstrated no difference in body weight gain in TSP1 deficient and wildtype control mice after 15 week diet challenge (42% kCal from fat) (274). On the other hand, two independent studies observed attenuated weight gain after 20 weeks of diet challenge (45% and 60% kCal from fat) in TSP1 deficient male mice compared to controls (100, 128). Differences in studies have been attributed to various lengths of diet challenge, inconsistent fat content in the diet, and the multiple interactions TSP1 has with a variety of tissues.

Although contradictions in body weight gain have been observed in TSP1 deficient mice, several protective phenotypes have been consistent across studies. First, TSP1 is tightly associated with the development of systemic and

adipose tissue-specific obesity-associated inflammation. Independent of body fat mass, TSP1 deficiency reduces macrophage accumulation within white adipose tissue depots demonstrated by reduced positive Mac2 (100, 128) and F4/80 staining (144). Further, mRNA levels of TNF α , an immunogenic trigger for metabolic dysfunction, were significantly reduced in white adipose tissue of HF-fed TSP1 deficient mice (128, 144). In efforts to further characterize the effects of TSP1 on systemic inflammation, Li et al. demonstrated a significant reduction in TNF α , interleukin-6 (IL-6), MCP1, and the metabolic syndrome biomarker, plasminogen activator inhibitor-1 (PAI-1) in circulation (144). In addition, bone marrow derived macrophages isolated from HF-fed TSP1 deficient mice demonstrated reduced macrophage migration upon stimulation with both lipopolysaccharide (LPS) and MCP1 compared with macrophages isolated from wildtype controls (144). Together, these data strongly suggest TSP1 plays a role in macrophage migration and infiltration into white adipose tissue in obesity as well as serving as a contributor to the systemic proinflammatory state associated with diet-induced obesity.

In addition to inflammation, TSP1 deficiency improves glucose tolerance and insulin sensitivity in diet-induced obese rodent models. Multiple studies have determined that TSP1 deficient mice exhibit reduced plasma insulin levels while maintaining similar glucose levels, suggesting less insulin is required to stimulate glucose disposal (128, 144). Similarly, hyperinsulinemic euglycemic clamp studies confirmed HF-fed TSP1 deficient mice required significantly higher levels of glucose infusion to maintain the same plasma blood glucose levels as controls

supporting the idea TSP1 deficiency enhances glucose tolerance (100). Additional studies have confirmed enhanced insulin-dependent glucose disposal was specific to skeletal muscle and not adipose tissue (100). Studies are lacking in determining the effects of TSP1 deficiency on hepatic glucose tolerance and insulin sensitivity.

Not only has TSP1 been implicated to play a role in inflammation and insulin resistance, several studies have examined other obesity-associated comorbidities including renal dysfunction, cardiovascular disease, and hypertension. Maimaitiyiming et al. determined renal TSP1 expression contributes to fibrosis and obesity-induced hypertension (155). In addition, TSP1 is a critical regulator of vascular tone by inhibiting endothelial-dependent vascular smooth muscle cell relaxation (18, 106). TSP1 expression also correlates with cardiovascular disease risk and promotes inflammation in both atherosclerosis and abdominal aortic aneurysm rodent models (150, 154, 239).

Overall, the role of TSP1 expression in adipose tissue could be attributed to paracrine effects necessary for promoting ECM remodeling, adipose tissue expansion, and lipid loading. As a consequence, systemic effects on other tissues occur because of robust TSP1 secretion in obese conditions. Unfortunately, the mechanisms facilitating these actions are still unknown and require further investigation. Several interactions have been identified that facilitate the actions of TSP1, including extracellular matrix proteins, integrins, CD36, and CD47 (177). Of these, TSP1 binds to CD47 most potently – activating CD47 at picomolar concentrations (physiological levels) (102, 107). In addition,

TSP1 binding to other receptors, such as CD36, requires the presence of CD47 (107, 170) suggesting this specific receptor is critical for regulating multiple TSP1-dependent intracellular signaling cascades in a variety of tissues.

1.6 CD47: Potent Receptor to TSP1

CD47 is an integral glycoprotein cell receptor and is classified in the immunoglobulin superfamily (160). CD47 consists of an extracellular IgV domain, which may be heavily glycosylated and a variably spliced cytoplasmic sequence (118, 242). Because of the post-translational modifications possible, the molecular weight of CD47 ranges from 45-55kDa (198). When CD47 was first identified, it was laterally associated with integrins in the cellular membrane (27), earning it the name integrin-associated protein (IAP), which is still used in some literature to date. Over the past several decades, CD47 has been observed in several other interactions and therefore is used more widespread than its original name, IAP (28, 193).

1.6.1 Structure and Functions of CD47

This cellular receptor contains 5 membrane-spanning domains with multiple disulfide bonds necessary for signaling as demonstrated in Figure 1.3 – one being between the extracellular loop of transmembrane domains 4 and 5 and the N-terminus (164) and the extracellular loop of transmembrane domains 1 and the IgV domain (210). The amino acid sequence of CD47 is moderately conserved between many species with approximately 60-70% homology shared between humans, mice, rats, and bovine (28, 193). More specifically, mice and rats have approximately 84% homology in their amino acid sequences (250). The

C-terminal cytoplasmic tail can be variably spliced into four common isoforms, ranging from 3-36 amino acids (147, 212). The second shortest of the four isoforms with a 16-amino acid long cytoplasmic tail is the most dominant form (212) No sequence motif on the cytoplasmic tail has been identified that exhibits any catalytic activity (28).

Literature examining the regulation of CD47 expression is severely lacking. In tumor cells, CD47 protein expression is significantly upregulated and it has been widely accepted that increased expression acts as a pathological, inhibitory signal for immune cell phagocytosis (110), which impairs the ability of the innate immune system to attack and remove diseased cells. Several transcriptional regulators have been recently identified to regulate this phenomenon. MYC, Hypoxia-inducible factor 1 (HIF1), and a-Pal/nuclear respiratory factor 1 (NRF1) have all been shown to bind to the promoter region of CD47 and induce CD47 gene expression in a number of cancer cell lines (36, 40, 303). Interestingly, just this year Lo et al. demonstrated that CD47 gene expression was tightly upregulated by the proinflammatory nuclear factor κ B (NF κ B) signaling pathway *in vivo* and *in vitro* hepatocellular carcinoma models (151). These studies suggest that transcriptional regulation of CD47 expression is cell-type and condition specific. To date, no other studies have been completed to examine the transcriptional or translational regulation of CD47 expression in healthy tissues or in any other disease states besides cancer models.

CD47 expression can be seen in various tissues and cell types throughout the body, ranging from microglia to red blood cells (28, 193). Relative mRNA levels of CD47 are observed in a variety of tissues. In addition, expression levels are not impacted by 4-month high fat diet challenge in mice, as demonstrated in Figure 1.4. Ubiquitous expression suggests that CD47 is active or necessary in several different cellular pathways, mechanisms, and interactions. Many well-established functions are associated with immunity, self-recognition, cellular adhesion, and vascular tone (242) and are dependent on the ligand or partner receptor associated with CD47. Interestingly, literature suggests that all effects of CD47 activation on intracellular signaling are dependent on activation by the matricellular proteins, thrombospondins – specifically TSP1.

1.6.2 Downstream Signaling Effects of TSP1-CD47 Interaction

Depending on the tissue or cell type, TSP1 activation of CD47 exhibits a variety of effects on intracellular signaling. In endothelial cells, it has been clearly demonstrated that TSP1 binding to CD47 inhibits intracellular calcium flux and subsequently the activation of endothelial nitric oxide synthase (eNOS, NOS3) (18), the enzyme responsible for physiological levels of nitric oxide (NO) production. Another well-defined effect of the TSP1-CD47 interaction is the regulation of cyclic nucleotide synthesis and signaling. Less studied are the effects of CD47 activation on cellular levels of cyclic adenosine monophosphate (cAMP). It has been shown that CD47 deficiency is associated with elevated cAMP levels in vascular, skeletal, and cardiac muscle cells, as well as whole

heart tissue, and that these effects involve G-coupled protein receptors to alter the activation of adenylyl cyclase (AC) (106, 297).

Further, CD47 has been shown to redundantly suppress NO/cGMP synthesis and signaling in a variety of tissues, as depicted in Figure 1.5. First, as previously mentioned, suppression of intracellular calcium reduces the ability of eNOS to produce NO from arginine, which is necessary to stimulate activation of sGC (18). Second, CD47 inhibits the phosphorylation of sGC necessary to convert GMP to cGMP (207). And third, CD47 inhibits the ability of cGMP to activate PKG (108). It is well established that NO/cGMP signaling plays a critical role in regulating vascular tone, enhancing blood flow, and promoting angiogenesis (216). Recent studies have begun to demonstrate that this signaling cascade is also critical for functions in metabolic tissues and could have broad implications on nutrient homeostasis and mitochondrial function in obese conditions.

1.6.3 Other Characterized Interactions of CD47

In addition to thrombospondins, integrins and signal regulatory proteins (SIRPs) uniquely interact with CD47. It has even been shown that all CD47 interactions compete for similar binding sites on the extracellular IgV domain of CD47 (102). These characterized interactions regulate a diverse host of cellular processes including cellular adhesion, stress response, and cell survival.

1.6.3.1 Integrins

Integrins serve as a regulatory protein for cell-cell or cell-extracellular matrix interactions by interacting with a host of cell membrane receptors,

structural proteins or ECM molecules. Integrins are transmembrane receptors comprised of heterodimers and are expressed on all cell types including erythrocytes and platelets (28). As mentioned previously, CD47 was initially identified as integrin-associated protein (IAP). Rather than a cell-cell interaction, CD47 has been shown to laterally associate with specific integrins in a *cis* interaction within the same plasma membrane forming a large signaling complex (28) and that cholesterol-rich portions of the plasma membrane, also known as lipid rafts, are necessary to stabilize the complex (85). Out of the large family of integrins, $\alpha\beta3$ and $\alpha2\beta1$ have been consistently copurified with CD47 from a variety of cell types including smooth muscle cells, erythrocytes, and platelets (77, 278). To demonstrate how CD47 activation induces integrin function, when CD47 is activated by ligands, integrin-mediated cell migration and adhesion are induced. For example, TSP1 binds CD47 and subsequently modulates $\alpha\beta3$ function in human umbilical vein endothelial cells (HUVECs), C32 cells, and tumor cells by promoting chemotaxis and cellular migration (15, 38, 39, 77). Both CD47 and integrins are widely expressed; therefore, additional studies are necessary to fully understand the partnership and functions of this complex in specific cell types.

1.6.3.2 Signal Regulatory Proteins (SIRPs)

Another highly characterized interaction with CD47 is a member of the signal regulatory protein (SIRP) family, SIRP α (commonly identified as SHPS1 and CD172a). Interestingly, CD47 and SIRP α exhibit very different tissue expression profiles. SIRP α expression is restricted to neuronal populations and

myeloid-lineage hematopoietic cells including macrophages and immature dendritic cells (4, 266), whereas CD47 is ubiquitously expressed throughout the body (176). In 2000, Oldenborg et al. determined SIRP α expressed on myeloid-lineage hematopoietic cells interacts with CD47 as a partner receptor to inhibit phagocytosis (195). This receptor-receptor interaction acts as a mechanism to establish self-recognition, especially with red blood cells and macrophages. Wildtype mice transfused with CD47 deficient red blood cells saw rapid clearance by phagocytosis from the bloodstream (194, 195), suggesting CD47 regulates the half-life of red blood cells in circulation by providing a “don’t eat me” signal to macrophages and dendritic cells.

CD47 and SIRP α have also shown increased expression in corresponding regions of the brain, suggesting their partnership may play a role in the central nervous system. Studies suggest CD47 and SIRP α may be involved in memory formation, stress response, and autonomic nervous system function (8, 98, 173). Limited evidence in rodent models and cell culture systems suggest CD47 and SIRP α play specific roles in the brain. No studies have been completed that fully elucidate the relationship of these two receptors in neuronal function. Future studies are warranted to fully determine the role of CD47 and SIRP α in neuronal survival and stress response.

1.7 Statement of the Problem

Metabolic dysfunction in obese conditions is incredibly complex; however, several central underlying pathways have been identified which include the development of proinflammatory and poor oxidative cellular environments.

Increased reactive oxidative species and activated stress response signaling pathways in tissues with high metabolic activity perpetuates a systemic proinflammatory environment, which ultimately results in insulin resistance and dyslipidemia. Some suggest identifying mechanisms that augment inflammation, oxidative stress, and mitochondrial dysfunction in metabolic tissues could be a viable therapeutic target for obesity and its associated complications. It is critical that pathways contributing to metabolic abnormalities are identified so that new therapeutics for obesity and its associated complications may be developed.

The receptor, CD47, is ubiquitously expressed throughout the body. Its expression has been implicated to serve a pathological role in the progression of inflammation and oxidative stress in a number of conditions including cardiovascular disease, pulmonary hypertension, ischemia reperfusion, and transplantation models. Further, it has been well established that the most potent ligand of CD47, TSP1, plays a critical role in facilitating inflammation and metabolic dysfunction in diet-induced obesity. Some previous studies have alluded to the role of CD47 in regulating mitochondrial function, yet no studies have examined the effects of CD47 in diet-induced obesity and its associated comorbidities. We believe the studies included in this dissertation identified novel regulatory roles for CD47 within metabolic tissues.

For our studies, we used both global TSP1 deficient mice and global CD47 deficient mice in a high fat diet-induced obesity paradigm. *The central hypothesis of these studies is that CD47 contributes to obesity-associated*

metabolic dysfunctions through diverse mechanisms including inflammation, energy utilization, and TSP1-mediated oxidative stress.

We know TSP1 expression is upregulated under obese conditions and that TSP1 contributes to obesity-associated inflammation and impairments in glucose homeostasis, but it is unclear how these actions are facilitated. With CD47 being the most potent cell membrane receptor for TSP1, we will explore whether TSP1 activity is mediated by CD47 activation. We hypothesized that lack of CD47 will protect against obesity-associated inflammation and will preserve healthy glucose homeostasis despite high fat diet challenge.

It is also well established that cGMP/PKG signaling is critical for healthy adipocyte function, mitochondrial respiration, and energy homeostasis, yet this signaling pathway is significantly impacted by high fat diet-induced obesity. The mechanisms contributing to this impaired signaling is unknown. Because CD47 activation has been shown to redundantly suppress cGMP/PKG signaling, studies were conducted to examine whether CD47 regulates energy homeostasis in metabolic tissues. We hypothesized that CD47 deficiency would enhance mitochondrial function and preserve energy homeostasis. The following aims were designed to test our hypotheses:

Specific Aim 1: To characterize the global effects of CD47 deficiency on diet-induced obesity in a rodent model

- A. To determine whether CD47 augments obesity-associated systemic and adipose tissue-specific inflammation

B. To define the relative role of CD47 in energy homeostasis within metabolic tissues under obese conditions

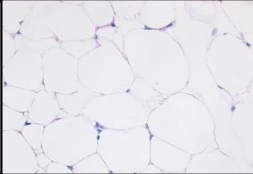
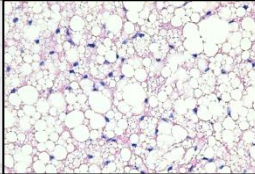
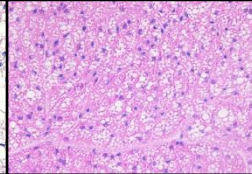
Increased oxidative stress has been shown to be the molecular link between mild steatosis and progression to more severe non-alcoholic steatohepatitis through induction of cellular stress signaling pathways, inflammation, and fibrogenesis. Unfortunately, the exact mechanisms augmenting reactive oxidative species production have not been clearly elucidated. The TSP1-CD47 signaling axis has previously been implicated in the development of hepatic oxidative stress and inflammation in other diseased conditions (hepatic ischemia/reperfusion injury, liver transplantation models), yet its contribution to fatty liver-induced ROS has never been explored. *In vivo* studies with two mouse models and *in vitro* experiments will define the contribution of TSP1-CD47 signaling to hepatic oxidative stress in a non-alcoholic fatty liver rodent model. We hypothesize that TSP1-CD47 activity leads to increased hepatic oxidative stress within a fatty liver model. The following aim was designed to test our hypothesis:

Specific Aim 2: To define the contribution of the TSP1-CD47 axis in the development of non-alcoholic fatty liver disease-associated oxidative stress

1.7.1 Impact

We demonstrate that CD47 deficiency is protective against adiposity, insulin resistance and obesity-associated chronic inflammation. Further, lack of CD47 corresponds with increased energy expenditure *in vivo* and *in vitro*. Additional studies show that reduced TSP1-CD47 signaling may be protective against hepatic oxidative stress and the pathogenesis of NAFLD. As a cell membrane receptor, CD47 may be a viable therapeutic target to reduce obesity-associated oxidative stress, inflammation, and mitochondrial dysfunction. Currently, four clinical trials (NCT02678338, NCT02641002, NCT02367196, NCT02663518) are underway using monoclonal functional blocking antibodies against CD47 as a cancer immunotherapy. Our studies provide new evidence that targeting CD47 could be expanded to include metabolic disorders.

Table 1.1 Comparison of white and brown adipose tissues

<i>Parameter</i>	<i>White</i>	<i>Beige</i>	<i>Brown</i>
Morphology (Mouse; 40x)			
Physiological Function	Energy storage	Energy storage, inducible non-shivering thermogenesis	Non-shivering thermogenesis
Anatomical Location	Pericardial, perirenal, retroperitoneal, mesenteric, subcutaneous, visceral	Retroperitoneal, subcutaneous	Humans: interscapular (newborns), supraclavicular, pericervical (adults) Mice: interscapular, cervical, perirenal
Developmental Origin	Myf5- stem cells	Myf5- stem cells	Myf5+ stem cells
Key Gene Expression	FABP4, LEP, PPAR γ , RETN	Cd137, Tmem26, UCP1	Cidea, Ebf2, PGC1 α , Prdm16, UCP1

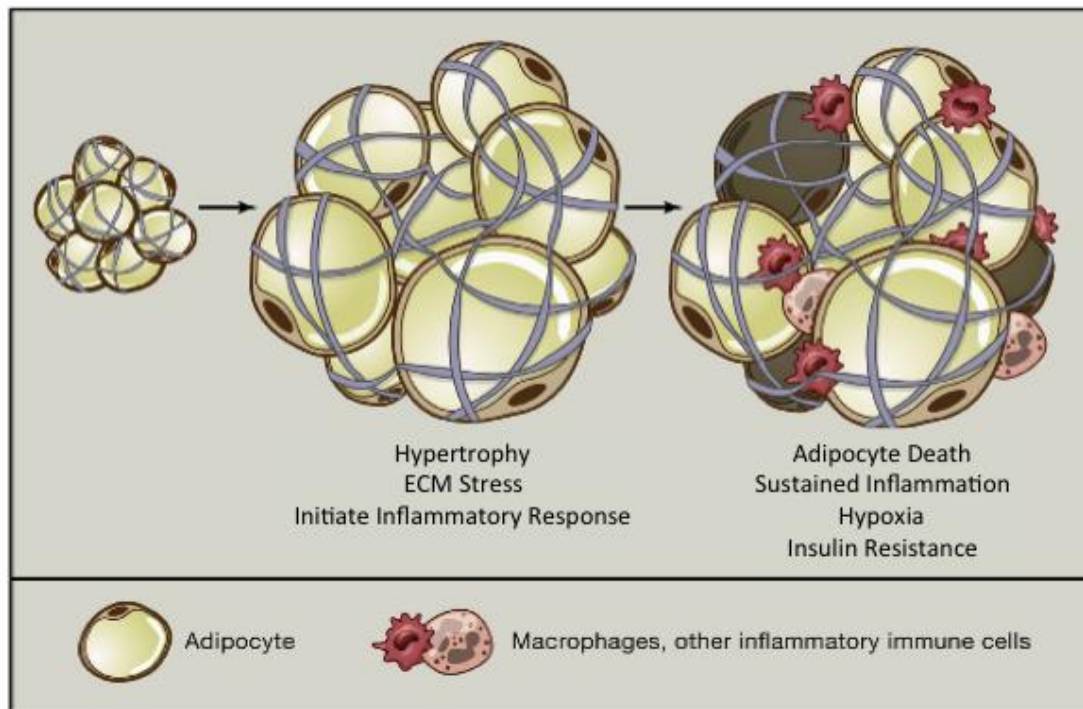


Figure 1.1 Adipose tissue remodeling and inflammation.

Modified cartoon depiction of the effects of obesity on adipose tissue as previously illustrated (223). Adipocytes are dynamic cell types capable of dramatically expanding cell size to accumulate excess lipid. As adipocytes hypertrophy, stress is placed on the ECM resulting in an inflammatory response. Adipocytes and ATMs are capable of secreting proinflammatory proteins, cytokines and chemokines, to stimulate an immune response and recruit additional macrophages to the adipose tissue depot. This mechanism further propagates the inflammatory phenotype commonly observed in obesity and contributes to adipocyte cell death and whole body insulin resistance.

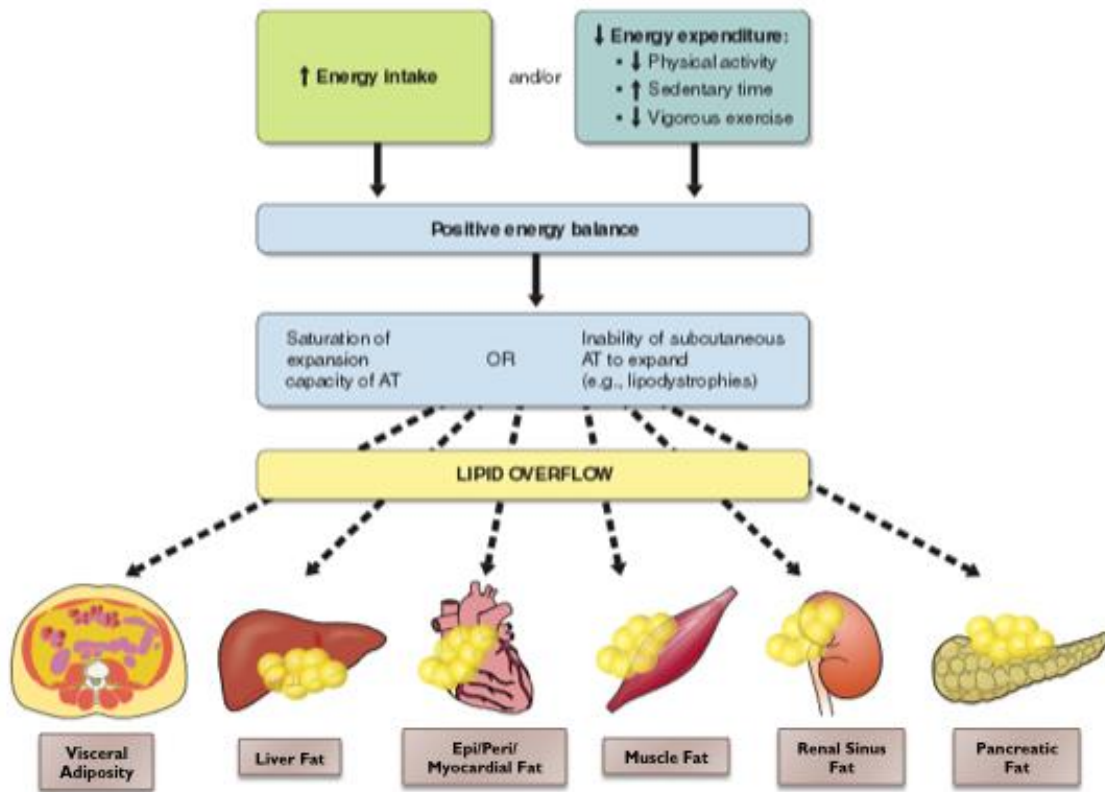


Figure 1.2 Relationship between obesity and systemic complications.

Obesity contributes to metabolic dysfunction in peripheral tissues and ultimately results in increased risk of type 2 diabetes and cardiovascular disease. Adapted schematic diagram of the relationship between obesity and global metabolic dysfunction as previously illustrated (261).

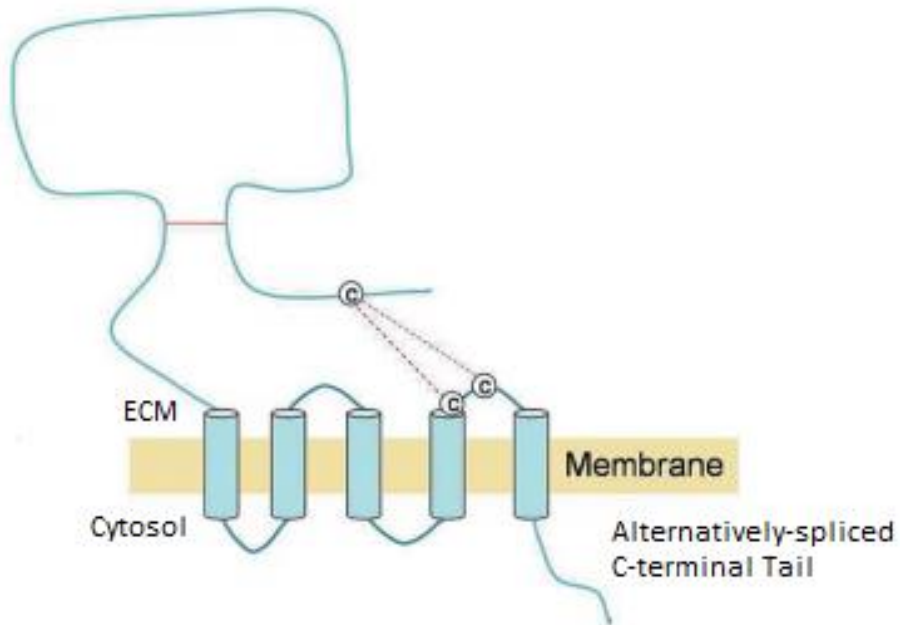


Figure 1.3 Molecular structure of CD47

Modified cartoon depiction of the structure of CD47 (200). CD47 is a unique cell membrane receptor which exhibits both an IgV immunoglobulin domain and 5 membrane-spanning domains with multiple disulfide bonds necessary for signaling. The C-terminal cytoplasmic tail can be variably spliced into four common isoforms, ranging from 3-36 amino acids. Of these four isoforms, the second shortest C-terminal cytoplasmic tail (16 amino acids) is the most commonly observed form.

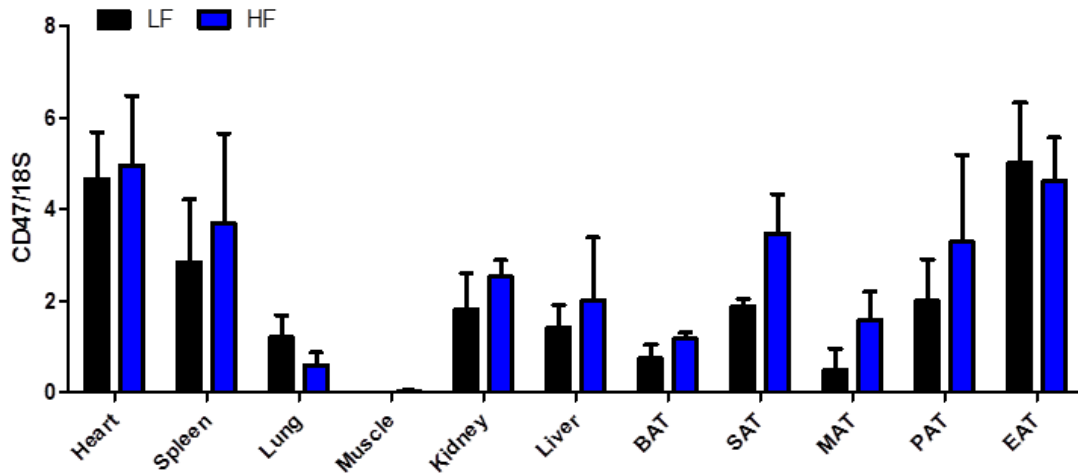


Figure 1.4 Dietary regulation of CD47 mRNA levels in a variety of tissues

Tissue expression profile of CD47 mRNA levels after four months of either LF or HF diet challenge. Expression levels demonstrate no significant diet regulation of CD47 mRNA levels.

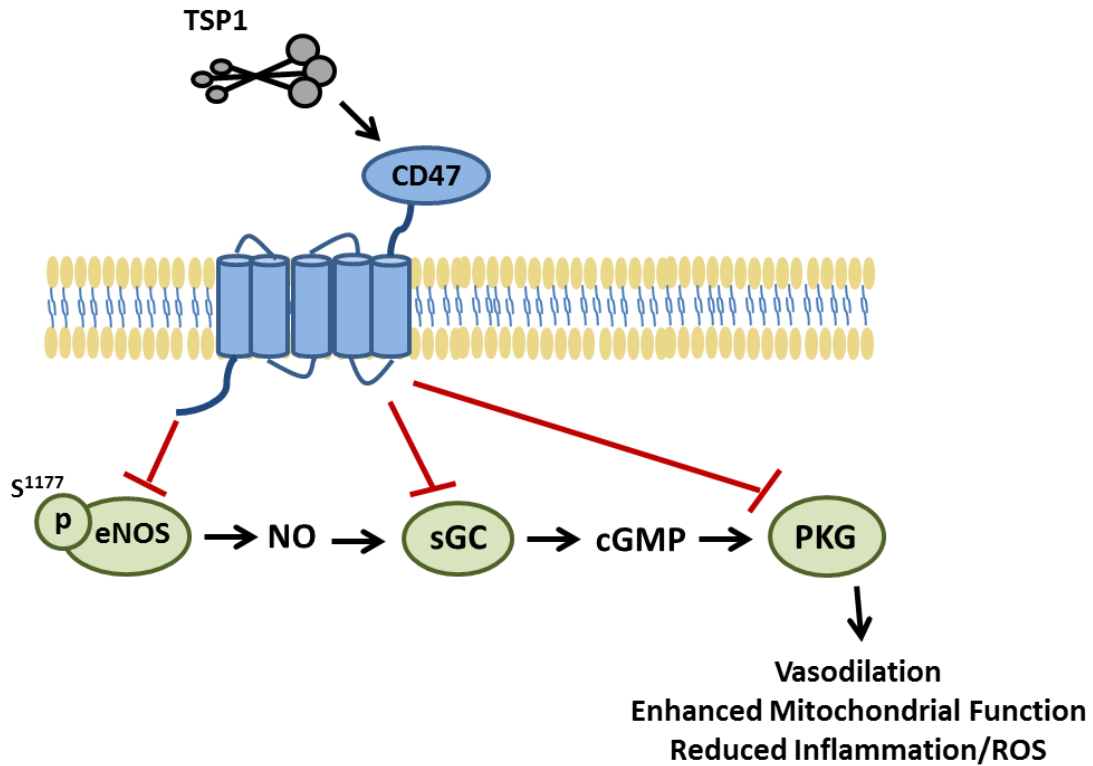


Figure 1.5 TSP1-mediated activation of CD47 on intracellular signaling

Cartoon depiction of intracellular signaling as previously illustrated (218, 219).

First, CD47 activation via TSP1 inhibits the phosphorylation of eNOS (at Ser1177) to produce NO from arginine. Second, CD47 inhibits the NO-mediated activation of sGC necessary to convert GMP to cGMP. And third, CD47 blunts the ability of cGMP to activate PKG. This canonical signaling cascade has been implicated in vascular tone and vasodilation; however, recent studies suggest its regulation in mitochondrial function, energy homeostasis, and obesity-associated inflammation could expand its therapeutic potential to metabolic diseases.

Section 2: METHODS

2.1 Breeding and Genotyping

CD47^{-/-} and wildtype (WT/CD47^{+/+}) littermate controls were generated by breeding heterozygous CD47^{+/-} mice. At approximately two weeks of age, pups were sexed and tail clips were collected for genotyping. DNA was extracted from tail clips using the E.Z.N.A. Tissue DNA Kit (Omega Bio-Tek, Norcross, GA, USA). For genotyping, two specific polymerase chain reaction (PCR) products must be examined per mouse – wildtype (300 base pairs) and mutated (199 base pairs). PCR mixes were prepared using the Kapa 2G Fast HotStart PCR Kit with dNTPs (Kapa Biosystems, Wilmington, MA, USA), common primer 7714, and either wildtype primer 13700 or mutant primer 7297. Primer sequences can be found in Table 2.1. Following PCR, samples were loaded with a 6x Blue/Orange Loading Dye (Promega, Madison, WI, USA) and run on a 2% agarose gel with ethidium bromide with a 100 base pair DNA Ladder (Promega, Madison, WI, USA). Gels were imaged using the PXi Multi-Application Gel Imaging system (Syngene, Frederick, MD, USA). Wildtype samples demonstrated one band at 300 base pairs. Mutant (CD47^{-/-}) mice exhibited one band at 199 base pairs. Heterozygous mice present bands at both 300 and 199 base pairs.

2.2 Animal Experimental Protocols

All experiments involving mice conformed to the National Institutes of Health Guide for the Care and Use of Laboratory Animals and were approved by the University of Kentucky Institutional Animal Care and Use Committee.

2.2.1 Aim 1

All experiments were performed on eight week-old male CD47 deficient mice (C57BL6/J background from Jackson Laboratories) and same sex and age-matched C57BL6/J controls (purchased from Jackson Laboratories). Mice were given a high fat (HF) (60% kcal from fat; D12492, Research Diets, Inc., NJ) or low fat (LF) diet (10% kcal from fat; D12450B; Research Diets, Inc., NJ) for 16 weeks with standard laboratory water. Each group contained 7 mice. Body weight was measured weekly at the same time. Temperature transponders (Implantable Programmable Temperature Transponder 300; BioMedic Data Systems, Seaford, DE) were subcutaneously implanted into mice at the week 8 time point during diet challenge. The wireless reader system was utilized to measure core body temperatures in both the light and dark cycles. At the end of the study, mice were sacrificed. Blood was collected and adipose tissue depots, liver, and muscle were harvested for various analyses.

2.2.2 Aim 2

To examine hepatocyte-specific expression of CD47 after HF diet challenge, C57BL6/J mice (Jackson Laboratories) were fed either a high fat (HF) (60% kcal from fat; D12942, Research Diets, Inc., NJ) or low fat (LF) diet (10% kcal from fat; D12450B; Research Diets, Inc., NJ) for the designated time frame (3, 7, or 14 days) with standard laboratory water. Each group contained 3 mice. Mice were sacrificed and hepatocytes were isolated as described by the two-step perfusion method (see details in Section 2.16.2) (112).

To examine the effects of TSP1 deficiency on the development of NAFLD, eight week old male TSP1 deficient and littermate wildtype controls (WT; on C57BL6/J background from Jackson Laboratories) were challenged with high fat (HF) (60% kcal from fat; D12942, Research Diets, Inc., NJ) or low fat (LF) diet (10% kcal from fat; D12450B; Research Diets, Inc., NJ) for 16 weeks with standard laboratory water. For studies, each group contained 10-15 mice.

To examine the effects of CD47 deficiency on the development of NAFLD, eight week-old male CD47 deficient mice and littermate wildtype controls (WT; C57BL6/J background from Jackson Laboratories) were utilized for all experiments. CD47^{-/-} and wildtype (WT/CD47^{+/+}) littermate controls were generated by breeding heterozygous CD47^{+/-} mice. Mice were fed either a HF or LF diet for 16 weeks with standard laboratory water. Each group contained 7-11 mice. Body weights were measured weekly at the same time. At the end of all studies, mice were sacrificed. Blood and liver tissue were collected for various analyses.

2.3 Indirect Calorimetry and Body Composition

Mice were individually housed in TSE LabMaster chambers (TSE Systems, Inc., Midland, MI, USA) for 5 days for measurement of food intake, water intake, and indirect calorimetry. Body composition including lean and fat mass was measured by EchoMRI (Echo Medical System, Houston, TX, USA) basally and two weeks prior to the end of the studies.

2.4 *In Vivo* Lipolysis Assay

Eight week old CD47 deficient and wildtype littermate control mice were fasted for six hours and then treated with either CL 316,243 (β -agonist; 1mg/kg BW; i.p. injection) or saline (vehicle) as control. Blood was collected via tail vein 15 minutes post injection and plasma glycerol was measured with Free Glycerol Reagent and appropriate standards (Sigma, St. Louis, MO, USA). Each group contained 4-7 mice.

2.5 *Ex Vivo* Lipolysis Assay

Subcutaneous adipose tissue (SAT), epididymal adipose tissue (EAT), and brown adipose tissue (BAT) were excised from eight week old CD47 deficient and wildtype littermate control mice after a six hour fast. Tissue was weighed and kept in ice cold PBS until all tissue was collected. Adipose tissue (80-180mg) was placed in one well of a 24-well plate (n=3 mice/group; all tissue samples from each mouse were triplicated). Tissues were serum starved in Dulbecco's Modified Eagle Medium (DMEM, Gibco, Carlsbad, CA, USA) supplemented with 1% fatty acid-free bovine serum albumin (BSA) for 1 hour at RT. Tissue was then treated with Krebs Ringer Buffer (125mM NaCl, 5mM KCl, 1.8mM CaCl₂, 2.6mM MgSO₄, 5mM HEPES, pH adjusted to 7.2) in the presence of vehicle or isoproterenol (10 μ M, Sigma, St. Louis, MO, USA) as previously described (87). After 2 hours, media was collected to measure glycerol release with the Free Glycerol Reagent and appropriate standards (Sigma, St. Louis, MO, USA). Values were normalized to gram tissue weight.

2.6 Plasma Parameters

Plasma insulin, IL-6, TNF α , IL-10, leptin, and MCP1 (eBioscience, San Diego, CA, USA) were measured by ELISA. Plasma and liver TGs, non-esterified fatty acids (NEFA) and total cholesterol (Wako Chemicals, Richmond, VA, USA) levels were measured enzymatically. Plasma ALT levels were measured by colorimetric kit from BioAssay Systems (Hayward, CA, USA).

2.7 *In Vivo* Glucose Tolerance/Insulin Sensitivity Assays

Glucose tolerance and insulin tolerance were analyzed basally and after 15-weeks of HF or LF feeding. Mice were fasted 6 hours before intraperitoneal injections of glucose (1 g/kg body weight) or insulin (0.5 unit/kg body weight; Novolin R, Novo Nordisk Inc., Plainsboro, NJ, USA). Blood glucose concentrations were measured using a glucometer at 0, 15, 30, 60, and 120 minutes post injection.

2.8 Tissue Histology

Interscapular brown adipose tissues, white adipose tissue depots, and liver tissue from all four groups of animals were embedded in paraffin, sectioned at 4 μ m, and stained with hematoxylin and eosin-stain (H&E) or Sirius Red for fibrosis by standard method through the University of Kentucky Pathology Core services from the Center of Research in Obesity and Cardiovascular Disease (COCVD). All images were acquired with a Nikon Eclipse 55i microscope at 20x objective. Image threshold features of Nikon NIS Elements BR software (Melville, NY, USA) were utilized to quantify percent of total area positively stained with Sirius Red. Four sections per mouse and three mice per group were measured.

Adipocyte area was quantified using the Object Count feature of Nikon NIS Elements BR software (Melville, NY, USA). Forty adipocytes were measured per section (n=3 sections/mouse) from mice in all four groups (n=3 mice/group).

2.9 Immunohistochemistry

Epididymal adipose tissue and liver was fixed and embedded in paraffin. Paraffin-fixed tissues were cut into 4µm sections and placed onto slides. Sections were deparaffinized, rehydrated in graded mixtures of ethanol/water, pretreated by boiling in citrate buffer (pH 6.0), and endogenous peroxidase activity was blocked with 3% H₂O₂ for 30 min at room temperature (RT). The sections were blocked for 1 hour at RT in 3% BSA in phosphate buffered saline (PBS) (blocking solution) and immediately incubated with a rat anti-mouse F4/80 antibody (1:200 dilution; AbD Serotec, Raleigh, NC, USA) in blocking solution for 1 hour at RT. Then, slides were washed, incubated with biotinylated secondary antibody for 30 min, and then washed again with PBS. Finally, peroxidase substrate diaminobenzidine (Vector Lab, Burlingame, CA, USA) was applied and incubated for 30 min. The slides were rinsed and counterstained with hematoxylin. Mounting solution and coverslips were added. Images were acquired with a Nikon Eclipse 55i microscope.

2.10 Liver Oil Red O Staining

Frozen liver tissues were cryostat sectioned at 6µm and fixed in 4% paraformaldehyde in PBS for 10 min at RT. Working Oil Red O solution was prepared by mixing 3 volumes of 0.5% Oil Red O in 100% isopropanol with 2 volumes distilled water and filtering through Whatman 4 filter paper. Slides were

blotted in 60% isopropyl alcohol for 5 min, and then stained with working Oil Red O solution for 15 min at RT. Slides were rinsed once with distilled water, mounted, and cover slipped with warmed glycerol gelatin. Images were acquired with a Nikon Eclipse 55i microscope.

2.11 Liver Triacylglycerol Levels

For analysis of liver TG content, approximately 50 mg of liver was placed into 500 μ L of chilled Krebs Ringer Phosphate (118mM NaCl, 5mM KCl, 13.8mM CaCl₂, 1.2mM MgSO₄, 0.016% KH₂PO₄, 0.211% NaHCO₂) and each sample was sonicated ten times (30 seconds/time). The homogenate was centrifuged at 2,000 \times *g* for 10 min at 4°C, and 10 μ L of the supernatant was then removed for triglyceride analyses. Triglyceride content was measured using Wako triglyceride kit (Richmond, VA, USA).

2.12 Macrophage Migration Assay

Bone-marrow derived cells were isolated from femurs and tibias of male WT and CD47 deficient mice fed with HF diet. These cells were cultured 7 days in RPMI-1640 media containing 20% fetal bovine serum (FBS), 25 ng/ml M-CSF (Sigma, St. Louis, MO, USA), and penicillin/streptomycin to allow differentiation into mature macrophages. Ability of these macrophages to migrate toward MCP-1 (50 ng/ml) was determined using modified Boyden Microchemotaxis Chamber. Briefly, cells were washed twice with PBS, counted and loaded into the upper chambers of a Transwell, while the lower chambers were filled with DMEM media with or without MCP-1 (50 ng/ml). Transwell plates were then incubated at 37°C for 6 hours. The upper inserts with membrane were removed and fixed in cold

methanol and stained with crystal violet (Sigma, St. Louis, MO, USA). Cells were counted from five different fields for each well. Results were expressed as a migration index under the high magnification field.

2.13 cGMP Measurements

cGMP levels in brown fat or skeletal muscles from LF or HF fed WT or CD47 deficient mice were measured by using the cGMP Direct Immunoassay Kit (Colorimetric) from Biovision (Milpitas, CA, USA). Frozen tissues were homogenized and the supernatant was collected. cGMP levels in the supernatant were measured and calculated based on the cGMP standard curve following the instruction manual.

2.14 Real-time Quantitative PCR (qPCR)

Total RNA from frozen adipose tissue, skeletal muscle, liver, and cells were extracted using RNeasy Mini Kit (Qiagen, Hilden, Germany). RNA was reverse transcribed to cDNA by High Capacity cDNA Reverse Transcription Kit (Invitrogen, Carlsbad, CA, USA). Real-time quantitative PCR was performed on a MyiQ Real-time PCR Thermal Cycler with iTaq Universal SYBR Green Supermix from Bio-Rad (Hercules, CA, USA). Relative mRNA expression was calculated using the MyiQ system software as previous reported (144) and normalized to 18s RNA levels. All primers used to examine gene expression were designed and purchased using the PrimerQuest Tool from Integrated DNA Technologies (Coralville, IA, USA). All primer sequences utilized in this study are found in Table 2.1.

2.15 Mitochondrial DNA (mtDNA) Copy Number

DNA was extracted from skeletal muscle and brown adipose tissue by using QIAamp DNA mini kit (Qiagen, Hilden, Germany). The relative mitochondria DNA (mtDNA) copy numbers were determined by real-time PCR as described previously (156) and normalized to nuclear DNA (nDNA/28s). Primer sequences utilized are shown in Table 2.1.

2.16 Western Blotting

Brown fat, skeletal muscle, liver tissue, and cells were homogenized in RIPA buffer (Sigma, St. Louis, MO, USA) plus protease and phosphatase inhibitors (Pierce, Waltham, MA, USA). After concentrations were measured using a BCA Assay (Pierce, Waltham, MA, USA), 30µg protein/well was subjected to SDS-PAGE gel under reducing conditions and transferred onto a nitrocellulose membrane. After blocking, the membrane was incubated with anti-GAPDH (1:5000 dilution; Millipore, Billerica, MA, USA), anti-β-actin (1:5000 dilution; Santa Cruz, Dallas, TX, USA), anti-CD47 (1:1000 dilution; Abcam, Cambridge, MA, USA), anti-TSP1 (1:1000 dilution; BD Biosciences, San Jose, CA, USA), and anti-PKG-I (1:1000 dilution; BD Biosciences, San Jose, CA, USA) antibodies at 4°C overnight. After washing, the membrane was incubated with horseradish peroxidase-conjugated secondary antibodies (Jackson Labs, Bar Harbor, ME, USA). The reaction was visualized by using an enhanced chemiluminescence system (Pierce, Waltham, MA, USA). Immunoblots were analyzed by scanning densitometry and quantified by Quantity One gel Analysis software (Bio-Rad, Hercules, CA, USA).

2.17 Tissue-level ROS Quantification

Hepatic oxidative stress was determined by the conversion of 2'7'-dichlorofluorescein diacetate (H₂DCFDA; Life Technologies, Carlsbad, CA, USA) to the fluorescent label 2'7'-dichlorofluorescein (DCF) in tissue homogenates. Frozen liver tissue was homogenized in 5 volumes of ice cold PBS and centrifuged at 10,000 x g for 10 minutes at 4°C. Supernatants were mixed with equal volume H₂DCFDA (20µM in DMSO) and placed in a flat-bottom microplate. Presence of the fluorescent probe DCF was measured after 10 minutes with a fluorescent plate reader (BioTek Synergy H1 Hybrid Reader, Winooski, VT, USA) at 485nm excitation and 520nm emission. Levels of lipid peroxidation were measured in liver tissue homogenates using the Lipid Peroxidation (MDA) Kit from Sigma (St. Louis, MO, USA). Approximately 10mg of tissue was used according to the manufacturer's protocol.

2.18 Cell Culture Models

2.18.1 HepG2 Cells

HepG2 cells, a human hepatoma cell line, were obtained from American Type Culture Collection (ATCC) and cultured in Minimum Essential Medium (MEM, Gibco, Carlsbad, CA, USA) supplemented with 10% FBS, 1% sodium pyruvate, and 1% penicillin-streptomycin at 37°C with 5% CO₂. For cellular ROS quantification, cells were seeded at a density of 2x10⁴ cells/well of a 96-well flat bottom culture plate.

2.18.2 Primary Murine Hepatocytes

Murine primary hepatocytes were isolated by the two-step perfusion method (85). First, livers were perfused with Ca²⁺/Mg²⁺-free HBSS supplemented with 10mM glucose, 10mM HEPES, and 0.3mM EDTA. Second, livers were digested with HBSS supplemented with 0.05% collagenase type IV (Catalog No. C5138, Sigma, St. Louis, MO, USA), 1.3mM CaCl₂, 0.5mM MgCl₂, 10mM glucose, and 10mM HEPES. Hepatocytes were washed three times with low speed centrifugation at 50 x g for 2 minutes. Cell viability was determined with trypan blue staining (>90% cell viability) and were seeded in 96-well flat bottom culture plates pre-coated with rat tail collagen at 2x10⁴ cells/well and cultured in Williams' Medium E (Gibco, Carlsbad, CA, USA) supplemented with 10% FBS, 2% penicillin-streptomycin, 1% sodium pyruvate, 1% L-glutamine, and 1% insulin-transferrin-selenium at 37°C with 5% CO₂.

2.18.3 3T3-L1 Cells

3T3-L1 mouse preadipocytes were obtained from American Type Culture Collection (ATCC) and cultured in DMEM (Gibco, Carlsbad, CA, USA) supplemented with 10% FBS and 1% penicillin-streptomycin at 37°C with 5% CO₂. Once cells were 100% confluent (Day -2) they were allowed to grow for an additional two days (Day 0). On Day 0, differentiation was induced by treating cells with culture media supplemented with 0.1μM insulin, 1μM dexamethasone, and 0.5mM 3-isobutyl-1-methylxanthine (IBMX). After 2 days (Day 2), cells were treated with culture media supplemented with 0.1μM insulin until Day 8. Media

was refreshed every two days. To avoid cell detachment from the plate during differentiation, cells were not washed with PBS during media changes.

2.18.4 Primary Adipocyte Isolation and Differentiation

White adipose tissue was excised from 8-week old CD47 deficient and wildtype littermate controls, minced, and digested in $\text{Ca}^{2+}/\text{Mg}^{2+}$ -free HBSS supplemented with 0.1% collagenase type II (Catalog No. C6885, Sigma, St. Louis, MO, USA) for 45 minutes in a 37°C shaking water bath. After digestion, cells were centrifuged at 700 x g for 10 minutes at 4° and the supernatant including the adipocyte layer was removed. The pellet was digested a second time with collagenase type II digestion buffer and incubated for 10 additional minutes in a 37°C shaking water bath. Cells were then filtered through a 100µm cell strainer and centrifuged again at 400 x g for 5 minutes at 4°. Cells were suspended in culture media Dulbecco's Modified Eagle Medium (DMEM, Gibco, Carlsbad, CA, USA) supplemented with 10% FBS and 1% penicillin-streptomycin. Cell viability was determined with trypan blue staining (>85% cell viability) and were seeded for various experiments.

For primary white adipocyte differentiation, the following protocol was used. Once cells were 100% confluent (day -2), they were allowed to continue growing for an additional 2 days (day 0) in culture media. On day 0, differentiation was induced by treating the cells with culture media supplemented with 1.7µM insulin, 0.5mM 3-isobutyl-1-methylxanthine (IBMX), and 1µM dexamethasone (induction media; all reagents obtained from Sigma, St. Louis, MO, USA) for three days. On day 3, cells were returned to culture media

supplemented with 1.7 μ M insulin (differentiation media) for the remaining duration of differentiation until day 8. Differentiation media was refreshed every two days. During media changes, cells were not washed with PBS to avoid cell detachment from the plate during differentiation.

2.19 Cellular-level ROS Quantification

HepG2 cells and primary hepatocytes were preloaded with 50 μ M H₂DCFDA and/or IgG Control or anti-human CD47 antibody clone B6H12 (2 μ g/mL; R&D Systems, Minneapolis, MN, USA) where indicated for thirty minutes at 37°C. TSP1 was generated through construction plasmids and purification of GST-fused proteins. After loading, cells were washed 2x with PBS then treated with palmitate (200 μ M), purified GST-fused TSP1 (2 μ g/mL), or GST as control (2 μ g/mL) for 6 hours at 37°C. After treatment, DCF fluorescence was measured with a fluorescent microplate reader (BioTek Synergy H1 Hybrid Reader, Winooski, VT, USA) at 485nm excitation and 528nm emission. *In vitro* experiments were triplicated and results are expressed as relative fluorescence units (RFU) normalized by cellular protein/well. Total protein concentrations were measured using BCA assay (Pierce, Waltham, MA, USA).

2.20 Cell Culture Oil Red O Staining

Primary adipocytes were fixed with 4% paraformaldehyde for 15 minutes at RT. Cells were then washed with PBS for 5 minutes, immediately followed by a 5 minute wash with freshly prepared 60% isopropanol in water. Working Oil Red O solution was prepared by mixing 3 volumes of 0.5% Oil Red O in 100% isopropanol with 2 volumes distilled water and filtering through Whatman 4 filter

paper. Cells were stained with filtered Oil Red O for 30 minutes and subsequently washed an additional 4 times with water. Images were acquired with a Nikon Eclipse 55i microscope. To quantify lipid accumulation, Oil Red O was extracted by carefully washing cells with 100% isopropanol. Extracted Oil Red O samples were loaded in triplicate into a clear, flat-bottom 96-well plate and absorbance was read at 500nm with a microplate reader. Absorbance values were normalized to protein content per well determined by BCA assay and presented as fold change over control.

2.21 *In Vitro* Lipolysis Assay

Lipolysis in fully differentiated 3T3-L1 adipocytes was determined by measuring free glycerol released into the media. After 8 days of differentiation, 3T3-L1 cells were serum starved for 1 hour and pretreated with either IgG control or a CD47 functional blocking antibody clone B6H12 (2 μ g/mL; R&D Systems, Minneapolis, MN, USA) for 30 minutes prior to treatment. Cells were then treated with or without c-CPT-cGMP (200 μ M; Sigma, St. Louis, MO, USA) or isoproterenol (positive control; 10 μ M; Sigma, St. Louis, MO, USA). After three hours, media was collected and glycerol release was measured and normalized to cellular protein content. Free glycerol levels were determined with Free Glycerol Reagent and appropriate standards (Sigma, St. Louis, MO, USA).

2.22 Seahorse Assays

To examine differences in mitochondrial function between WT and CD47 deficient primary adipocytes, the XF Mitochondrial Stress Test by Seahorse Bioscience (Agilent Technologies, Santa Clara, CA, USA) was completed. The

protocol provided by Seahorse Biosciences used for this assay can be found in Figure 2.1. On day 8 of differentiation, cells were seeded in an XF96 Seahorse cell culture plate (Agilent Technologies, Santa Clara, CA, USA) five hours prior to the assay at a density of 1×10^4 cells/well ($n=7$ wells/group). Over the course of the assay, cells were treated with three different compounds and the oxygen consumption rate (OCR) was measured before and after each treatment. First, cells were treated with oligomycin ($1 \mu\text{M}$), which blunts ATP synthesis by blocking ATP synthase. Second, cells were treated with carbonyl cyanide-4-(trifluoromethoxy) phenylhydrazone (FCCP, $2 \mu\text{M}$) which uncouples the electron transport chain and induces high oxygen consumption and energy expenditure without generating ATP. Finally, cells were treated with a combination of rotenone (complex I Inhibitor) and antimycin A (complex III inhibitor) (both $1 \mu\text{M}$). This combination inhibits all mitochondrial respiration and allows the non-mitochondrial respiration of the cell to be measured. Analysis of data was completed with XFe Wave Software (Agilent Technologies, Santa Clara, CA, USA). All values were normalized to cellular protein levels which were determined by BCA Assay (Pierce, Waltham, MA, USA) following the manufacturer's protocol.

2.23 Assessment of Isolated Mitochondria Bioenergetics

Brown adipose tissue mitochondria were isolated using differential centrifugation with some modifications to the previously described methods (253, 254). Briefly, 500-800mg adipose tissues were excised, minced with a blade, and placed in isolation buffer with EGTA (215mM mannitol, 75mM sucrose, 0.1%

BSA, 20mM HEPES, 1mM EGTA, pH adjusted to 7.2 with KOH). Tissues were mechanically homogenized at 300rpm in 4mL ice cold isolation buffer with EGTA. The homogenate was centrifuged twice at 1300 x g for 3 min in a 2mL centrifuge tube at 4°C. Each supernatant fraction was collected in separate tubes and topped off with isolation buffer with EGTA and finally centrifuged at 13,000 x g for 10min. The mitochondrial pellet was then suspended in 1mL isolation buffer without EGTA and centrifuged for 10min at 10,000 x g. Finally, the mitochondrial pellet was resuspended in 30-50µL isolation buffer without EGTA and stored on ice until the time of assay. The protein concentration was determined using the BCA assay kit (Pierce, Waltham, MA, USA) following the manufacturer's protocol.

Mitochondrial respiration was assessed using a Clark-type oxygen electrode (Hansatech Instruments, Norfolk, UK), in a sealed, thermostatically controlled (37°C), and continuously stirred chamber as described previously (253, 255). Mitochondria were added to the chamber to yield a final protein concentration of 50µg/mL respiration buffer (215mM mannitol, 75mM sucrose, 2mM MgCl₂, 2.5mM inorganic phosphates, 0.1% BSA, 20mM HEPES, pH adjusted to 7.2). State II respiration was initiated by the addition of oxidative substrates, pyruvate and malate (5mM and 2.5mM, respectively). State III respiration was initiated by the addition of 120nmol ADP followed by the addition of oligomycin (1µM) to induce state IV respiration. UCP-mediated proton conductance was measured as increased free fatty acid (60µM linoleic acid) induced respiration (253, 255), followed by recoupling of the mitochondria by

sequestration of FFA with the addition of BSA to a final concentration of 3%. Finally, mitochondria were treated with FCCP to allow for quantification of complex I driven, maximal electron transport.

2.24 Preparation of Purified TSP1

The TSP1 encoding gene was amplified by ultra-based PCR using pGEM2-htsp1 as a template and subcloned into expression plasmid vector pGEX-4T-3 after digestion by the restricted endonucleases xho1, Klenow, and Sal1. The expression plasmids were inserted into competent DH5 α cells and expression of proteins were evaluated by 8% sodium dodecyl sulfate polyacrylamide gel electrophoresis (SDS-PAGE). The GST-TSP1 fusion protein expression was induced by IPTG in competent BL21(DE3) E. coli and was purified with a GST column. Endotoxins were removed with a Detoxi-Gel Endotoxin removing column (Pierce, Waltham, MA, USA) and quantified with the LAL Chromogenic Endotoxin Quantitation Kit (Pierce, Waltham, MA, USA). The purified protein was stored in aliquots at -80°C .

2.25 Preparation of *In Vitro* Fatty Acid Treatments

To represent physiological conditions, palmitic acid (PA; Sigma, St. Louis, MO, USA) was conjugated to fatty acid-free BSA prior to all *in vitro* treatments as previously described (114). Stock palmitic acid solution in 100% ethanol (100mM) was added to 10% BSA solution in serum-free media and incubated at 37°C for 30 minutes to prepare a 5mM BSA-PA solution. As indicated, BSA controls were treated with stocks of 10% w/w BSA plus equal volumes of 100% ethanol added to match concentration of palmitate treatment.

2.26 Statistical Analysis

Data are expressed as the mean value \pm standard error (SE). Student's *t*-tests were used for measuring differences between two groups. Data from 3 or more groups with one experimental variable were analyzed by one-way ANOVA (e.g. cell culture treatments). Data were analyzed by a two-way ANOVA when 2 groups with 2 or more variable were present (diet and genotype) and Bonferroni ad hoc tests were used when appropriate to measure significance between all groups, unless otherwise indicated. A *p* value of <0.05 was considered statistically significant. All statistical analyses were completed utilizing GraphPad Prism.

Table 2.1 Primer sequences used in studies

Gene	Forward (5'-3')	Reverse (5'-3')	Accession Number
<i>18s</i>	AGTCGGCATCGTTTATGGTC	CGAAAGCATTGCCAAGAAT	NR_002170
<i>ACO</i>	GACAGAGGTCCACGAATCTTAC	GGCTACTACTGCACCTACAAC	NM_015729
<i>ATPSyn</i>	TGTGTCCCGGGCAAGAAAGATACA	AAGGCTTGTCTGGGAGATGGTCA	NM_016774
<i>CCR2</i>	AGAGAGCTGCAGCAAAAAGG	GGAAAGAGGCAGTTGCAAAG	NM_009915
<i>CD11c</i>	CTGGATAGCCTTTCTTCTGCTG	GCACACTGTGTCCGAACTC	NM_021334
<i>CD36</i>	ACTGGTGGATGGTTTCCTAGCCTT	TTTCTCGCCAACCTCCAGGTACAA	NM_001159555
<i>CD47</i>	AGAATGCTTCTGGACTTGGCCTCA	TCACATGCCATGATGCAGAGACAC	HQ585874
<i>Col 1a1</i>	TTCTCCTGGCAAAGACGGACTCAA	AGGAAGCTGAAGTCATAACCGCCA	NM_007742
<i>Col 1a3</i>	TCCTAACCAAGGCTGCAAGATGGA	TCCTAACCAAGGCTGCAAGATGGA	NM_009930
<i>Col 1a4</i>	AGGGTTCACAGTTCTAA	GCCCAACGTCACCTTTAT	NM_009932
<i>COX1</i>	ACTTGCAACCCTACACGGAGGTAA	TCGTGAAGCACGATGTCAAGGGAT	NC_005089.1
<i>COXIII</i>	TCAGCCCTCCTTCTAACATCAGGT	AATAGGAGTGTGGTGGCCTTGGTA	NC_005089.1
<i>CPT1a</i>	CTCTATGTGGTGTCCAAG	CACAGGACACATAGTCAG	NM_013495.2
<i>CPT1b</i>	ACCTGAGCTGTGCTGAATAAA	ACAGGAGACGGACACAGATA	NM_009948
<i>F4/80</i>	AGTCGGCATCGTTTATGGTC	CGAAAGCATTGCCAAGAAT	X93328
<i>FATP1</i>	GGAGTCTGGAATGCTGAGAAG	ATCAGAACAGAGAGGCCAAAG	NM_011977
<i>FATP2</i>	GACCCAGACAGAGAAGAA	TCCACCGGAAAGTATCTC	AF072757
<i>FATP5</i>	CTGCGGTACTTGTGTAAC	TGGATCCGTAGAATTCCC	AF072760
<i>G6P</i>	CCCAGGTTGAGTTGATCTTC	GACTTCTTGTGTGTCTGTCC	NM_008061.4
<i>MCP1</i>	CAGCCAGATGCAGTTAACGC	GCCTACTCATTGGGATCATCTTG	NM_011333
<i>mtDNA</i>	CCGCAAGGGAAAGATGAAAGA	TCGTTTGGTTTCGGGGTTTC	AP013030.1
<i>MTTP</i>	TCTGCCTATACTGGCTAC	CCGATGTACTGGAAGATG	XM_017319475
<i>nDNA</i>	GCCAGCCTCTCCTGATTTTAGTGT	GGGAACACAAAAGACCTCTTCTGG	NR_003279.1
<i>Pepck</i>	ACACCATCTTCACCAACG	GTCTCCACTCCTTGTCTTC	NM_011044.2
<i>PGC1α</i>	CTGCATGAGTGTGTGCTGTG	CAAATATGTTCCGAGGCTCA	NM_008904
<i>PPARα</i>	CTCCTTGCTGCCAATCAA	CAAACATAGGACCAGCTCTC	NM_011144
<i>PPARγ</i>	TGCTGTTATGGGTGAAACTCTG	CTGTGTCAACCATGGTAATTTCTT	NM_011146
<i>SREBP1c</i>	GGAGCCATGGATTGCACATT	ACAAGGTGCAGGTGTCACC	XM_006532717
<i>TNFα</i>	AGCCGATGGGTTGTACCT	TGAGTTGGTCCCCCTTCT	NM_013693
<i>UCP1</i>	TACCAAGCTGTGCGATGT	AAGCCCAATGATGTTCACT	NM_009463
<i>UCP3</i>	ACCTGGACTGCATGGTAAGG	GAGAGCAGGAGGAAGTGTGG	NM_009464
<i>7714</i>	CAAGCATAAATGAACAGTTGCAG		
<i>7297</i>	CGTTGGCTACCCGTGATATT		
<i>13700</i>	CACCTTACAGCACTCCACA		

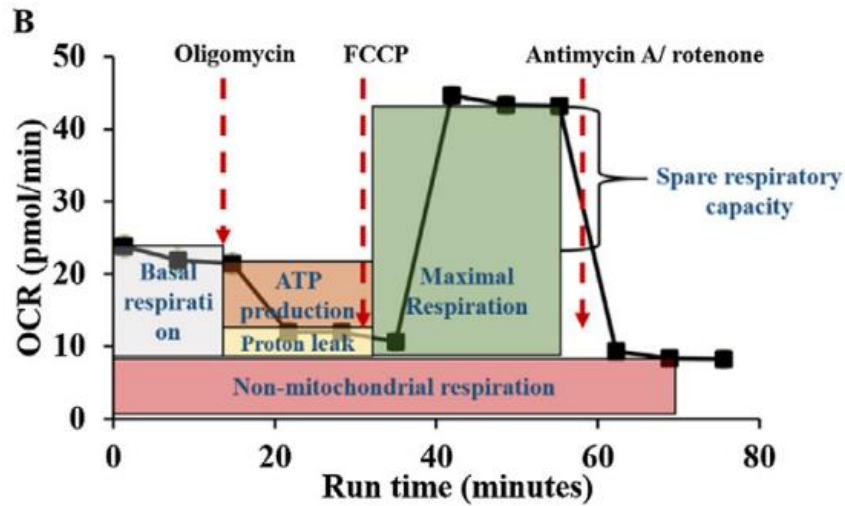


Figure 2.1 Seahorse Biosciences Mitochondrial Stress Test Protocol

Detailed protocol for the XF Mito Stress Test as previously described (88). Fundamental parameters of mitochondrial function, including basal respiration, ATP production, proton leak, maximal respiration, and spare respiratory capacity, can be determined by measuring oxygen consumption rates (OCR) before and after various drug treatments. Oligomycin inhibits ATP Synthase (Complex V). FCCP uncouples the electron transport chain (ETC) by increasing hydrogen ion translocation across the inner mitochondrial membrane. Combinational treatment with rotenone/antimycin A target and disrupt the function of complexes I and III in the ETC.

Section 3: SPECIFIC AIM 1

Portions of this section are reprinted from Macmillan Publishers Ltd: Scientific Reports (156), © 2015. Published under a CC-BY 4.0 Creative Commons license

<http://creativecommons.org/licenses/by/4.0>

3.1 Summary

CD47 is a transmembrane protein with several functions including self-recognition, immune cell communication, and cell signaling. Although it has been extensively studied in cancer and ischemia, CD47 function in obesity has never been explored. In this study, we utilized CD47 deficient mice in a high-fat diet induced obesity model to study for the first time whether CD47 plays a role in the development of obesity and metabolic complications. Age-matched, male CD47 deficient and C57BL6/J wild type (WT) control mice were fed with either low fat (LF) or high fat (HF) diets for 16 weeks. Interestingly, we found that CD47 deficient mice were protected from HF diet-induced obesity displaying decreased weight gain and reduced adiposity. This led to decreased MCP1/CCR2 dependent macrophage infiltration into adipose tissue and reduced inflammation, resulting in improved glucose tolerance and insulin sensitivity. In addition, CD47 deficiency stimulated the expression of UCP1 and carnitine palmitoyltransferase 1b (CPT1b) levels in brown adipose tissue, leading to increased lipid utilization and heat production. Additional studies suggest increased lipid mobilization in white adipose tissue may provide energy substrate for enhanced brown adipose tissue metabolic function in CD47 deficient mice, ultimately contributing to the increased energy utilization and reduced adiposity

observed in these mice. Taken together, these data reveal a novel role for CD47 in the development of obesity and its related metabolic complications.

3.2 Introduction

Obesity and its-associated insulin resistance is rampant within the United States and other developed nations. Previous studies from our lab and others suggest that thrombospondin 1 (TSP1) plays an important role in obesity-associated chronic inflammation and insulin resistance (IR) (100, 128, 144, 268). We demonstrated that TSP1 deficiency did not affect the development of high-fat diet induced adiposity. However, TSP1 deficiency reduced macrophage accumulation in adipose tissue and protected against obesity related inflammation and insulin resistance (144). These data suggest that TSP1 plays an important role in regulating macrophage function and mediating obesity-induced inflammation and insulin resistance. However, the mechanisms of the proinflammatory effect elicited by TSP1 under obese conditions remain to be determined.

TSP1, a 420–450 kDa homotrimer, is a multifunctional matricellular protein composed of several domains that can interact with different cell surface receptors (25, 33, 38, 75, 78, 84, 113, 138, 169, 178, 258, 276). TSP1 is a highly potent ligand for CD47, a trans-membrane glycoprotein cell receptor that belongs to the immunoglobulin superfamily (160). CD47 is expressed in various tissues and cell types throughout the body, ranging from microglia to endothelial cells (28, 193). Wide expression suggests that CD47 is active or necessary in several different cellular pathways including immunity and self-recognition, inflammation,

cellular adhesion, stress response, cell survival, and vascular function (16, 103, 106, 109, 219). It has been shown that the TSP1-CD47 interaction inhibits NO/cGMP/PKG signaling in vascular smooth muscle cells and plays a role in vasoconstriction and inflammation (106, 107, 207, 297). However, it is unknown whether the proinflammatory effect elicited by TSP1 under obese conditions is mediated by CD47.

In the current study, we determined whether TSP1 promotes obesity-associated inflammation and insulin resistance through interaction with its receptor-CD47. We utilized CD47 deficient and WT mice in a diet-induced obesity paradigm. CD47 deficient mice challenged with a HF diet had several protective phenotypes as previously observed in TSP1 deficient mice including decreased obesity-associated inflammation and improved glucose tolerance and insulin sensitivity (144). However, significant reductions in body weight were observed in CD47 deficient mice and not HF-fed TSP1 deficient mice in the previous study (144). Current studies have shown that CD47 deficiency protected mice from HF diet induced obesity; while TSP1 deficiency had no effect on diet-induced obesity after 16 weeks of HF feeding (144). Moreover, CD47 deficiency resulted in tissue-specific effects on metabolic organs *in vivo*. First, CD47 deficient mice exhibited increased energy expenditure, heat production, and core body temperature partially relating to brown adipose tissue and/or skeletal muscle functional changes. These mice also displayed increased white adipose tissue lipolysis which could fuel enhanced brown adipose tissue metabolic activity and contribute to a leaner whole body phenotype. Together, data from

this study revealed a novel role for CD47 in regulation of energy homeostasis and the development of obesity, suggesting that CD47 may serve as a potential therapeutic target to combat obesity and metabolic complications.

3.3 Results

3.3.1 CD47 deficiency protects mice from diet-induced obesity.

To assess the metabolic role of CD47 in mice, CD47 deficient mice and WT controls were challenged with either a low fat (LF, 10% kcal from fat) or high fat (HF, 60% kcal from fat) diet for 16 weeks. Under LF diet conditions, although CD47 deficient mice had a trend of decrease in body weight as compared to WT mice, no significant changes in body weight gain were observed throughout the study (Figure 3.1 A, B). When challenged with HF diet, CD47 deficient mice exhibited significantly reduced body weight starting from 7 weeks' feeding until the end of the study. These mice gained less weight than HF-fed WT mice (Figure 3.1 A, B; $P < 0.05$). At the end of study, body composition was determined in mice by using EchoMRI. There was significantly reduced fat mass in HF-fed CD47 deficient mice as compared to HF-fed WT mice (Figure 3.1 C; $P < 0.05$), which was in agreement with the absolute weight of different adipose tissue depots (Figure 3.1 E; $P < 0.05$ for all white adipose tissue depots). Lean mass was comparable in HF-fed CD47 deficient mice and WT mice (Figure 3.1 D). Consistent with the decreased adiposity, HF-fed CD47 deficient mice had reduced leptin levels (ng/ml, WT HF: 14.4 ± 4.9 vs. CD47^{-/-} HF: 6.8 ± 1.1 , $P < 0.05$). Moreover, plasma total cholesterol (TC) and free fatty acid (FFA) levels were significantly reduced in HF-fed CD47 deficient mice (TC (mg/dl), WT HF:

115.1 ± 7.3 vs. CD47^{-/-} HF: 80.0 ± 7.9, P<0.01; FFA (mEq/L), WT HF: 0.34 ± 0.01 vs. CD47^{-/-} HF: 0.28 ± 0.02, P<0.05). Daily cumulative food consumption was measured and there was no significant difference between either genotype or diet type (Figure 3.6 A). Together, these data suggests that CD47 deficiency protects mice from diet-induced obesity.

3.3.2 CD47 deficient mice on HF diet showed reduced systemic and adipose tissue inflammation.

Systemic and adipose tissue inflammation were determined in four groups of mice. As shown in Figure 3.2 A and B, HF-fed CD47 deficient mice had a significant reduction in plasma TNF α (P<0.01) and IL-6 (P<0.05) levels compared with HF controls. In addition to the reduced plasma proinflammatory cytokines, plasma anti-inflammatory cytokine-IL-10 levels were significantly increased in HF-fed CD47 deficient mice as compared to HF-fed WT mice or to LF-fed CD47 deficient mice (Figure 3.2 C; P<0.05), suggesting that the interaction between diet composition and genotype contributes to the IL-10 secretion.

In addition to systemic inflammation, adipose tissue inflammation status was determined. Visceral adipose tissue has been suggested to be the primary source of cytokine and adipokine release within obesity-associated inflammation (275). Moreover, increased accumulation of adipose tissue macrophages is a significant contributor to obesity-induced chronic inflammation (130, 281, 294). Therefore macrophage infiltration into adipose tissue was determined by immunohistochemical staining for the macrophage marker F4/80. As shown in Figure 3.3 A, HF-fed WT controls had robust positive staining of F4/80 and

crown-like structures, yet HF-fed CD47 deficient mice had minimal positive staining, suggesting a decreased presence of macrophages. We confirmed this staining result with qPCR and demonstrated that HF-fed WT controls had a significant increase in F4/80 expression in adipose tissue, which was reduced in HF-fed CD47 deficient mice (Figure 3.3 B; $P < 0.01$). Moreover, CD11c and TNF- α levels were increased in adipose tissue from HF-fed WT mice compared with LF controls, but decreased in HF-fed CD47 deficient mice (Figure 3.3 B; $P < 0.01$, $P < 0.05$, respectively). Together, these data indicate that CD47 deficient mice had reduced macrophage infiltration into adipose tissue and decreased systemic and adipose tissue inflammation in response to HF diet compared with controls.

To determine the mechanism of reduced macrophage infiltration in adipose tissue from HF-fed CD47 deficient mice, we examined MCP1 and CCR2 levels. MCP1, an inflammatory chemokine responsible for monocyte migration, and its dominant receptor CCR2 are suggested to be responsible for a significant amount of monocyte infiltration into inflamed adipose tissue (281). We found that HF-fed CD47 deficient mice demonstrated a reduction in MCP1 and CCR2 levels in adipose tissue (Figure 3.3 B; $P < 0.05$), which might be due to the reduced adiposity in these mice. In addition, this result could explain the significant decrease in macrophage infiltration in adipose tissue from CD47 deficient mice, which was supported by an *in vitro* migration studies using isolated macrophages from HF fed WT and CD47 deficient mice. We found that WT macrophages had increased MCP1 stimulated migration; while macrophages from CD47 deficient mice showed reduced migration basally ($P < 0.05$) and in response to MCP1

(Figure 3.3 C; $P < 0.01$). Together, these data suggest that CD47 regulates diet-induced adipose tissue macrophage infiltration and inflammation through a MCP1/CCR2 dependent pathway.

3.3.3 CD47 deficient mice on HF diet showed improved whole body glucose homeostasis.

The liver morphology was determined in the current study. We found that CD47 deficiency protected mice from hepatosteatosis when fed with HF diet, which was demonstrated by reduced liver weight, Oil Red O staining in liver sections and liver triglyceride levels (Figure 3.4 A, C; $P < 0.05$). To determine whole body glucose homeostasis, we performed glucose tolerance and insulin sensitivity tests in WT and CD47 deficient mice. As shown in Figure 3.5, glucose tolerance and insulin sensitivity were significantly improved in HF-fed CD47 deficient mice as compared to HF-fed WT mice ($P < 0.05$), suggesting that CD47 deficiency protects mice from diet-induced glucose intolerance and insulin resistance.

3.3.4 Energy metabolism in WT or CD47 deficient mice under either LF or HF feeding conditions

We have shown that CD47 deficiency protects mice from diet-induced obesity. To further elucidate its mechanism, we examined energy balance in both WT and CD47 deficient mice. CD47 deficient mice displayed elevated energy expenditure (normalized to total body mass), heat production, core body temperature, and total activity compared to WT mice in either light or dark cycle (Figure 3.6 B–E). Together, these data suggest that the protection against HF

diet induced weight gain and fat gain in CD47 deficient mice might be due to increased energy utilization.

3.3.5 Metabolic gene expression in skeletal muscle from LF or HF fed WT and CD47 deficient mice

To further determine the mechanism of increased energy utilization in HF-fed CD47 deficient mice, we analyzed the expression of multiple genes in skeletal muscle that relate to mitochondria function and fuel utilization. The rationale for this analysis was based on the previous report showing that skeletal muscle from CD47 deficient mice had greater number of mitochondria and improved function (74), which suggested a possible relationship between skeletal muscle function and the metabolic phenotype observed in the current study. Therefore, mitochondria DNA copy number and expression of a series genes relating to mitochondria oxidative function and fatty acid catabolism were analyzed. Consistent with previous reports (74), the results showed that mitochondria DNA copy number was significantly increased in CD47 deficient mice compared to WT mice under both LF and HF feeding conditions (Figure 3.7 A; $P < 0.05$). However, expression levels of genes related to mitochondria oxidative function and fatty acid catabolism were comparable in CD47 deficient mice compared to WT mice under both LF and HF feeding conditions (Figure 3.7 B), suggesting that skeletal muscle functional changes may not be a major contributor to the increased energy utilization phenotype in HF-fed CD47 deficient mice.

3.3.6 Morphology and metabolic gene expression in brown adipose tissue from LF or HF fed WT and CD47 deficient mice

Recently, brown adipose tissue (BAT) has emerged as an important player in energy metabolism (32). However, whether CD47 regulates BAT function and contributes to diet-induced obesity is unknown. First, we found that diet-induced obesity significantly up-regulated CD47 protein levels in BAT in wild type mice (Figure 3.8 A; $P < 0.05$). Although interscapular BAT weight was not different between WT and CD47 deficient mice under either LF or HF feeding conditions (Figure 3.1 E), histology showed a decrease in intracellular lipid droplet size in BAT of HF-fed CD47 deficient mice compared to HF-fed WT mice, reflected by a decrease in relative lipid area (Figure 3.8 B, C; $P < 0.01$). Moreover, we analyzed mitochondria DNA copy number and a series of genes relating to mitochondria oxidative function and fatty acid catabolism. As shown in Figure 3.8 D, mitochondria DNA copy number in BAT was increased in HF-fed CD47 deficient mice compared to HF WT mice, although not significantly. This suggests that CD47 may regulate mitochondria biogenesis in BAT. In addition, mRNA levels of UCP1 and carnitine palmitoyltransferase 1B (CPT1b) in BAT were significantly increased in HF-fed CD47 deficient mice (Figure 3.8 E; $P < 0.05$, $P < 0.01$, respectively).

BAT expends a large amount of energy through mitochondria β -oxidation and by uncoupling of the mitochondria proton gradient from ATP production. This uncoupling results in heat production or thermogenesis, accomplished by UCP1 located in the inner mitochondria membrane (31, 213). CPT1b, located on the

outer mitochondrial membrane, is the first and rate-limiting step for fatty acid transport into the mitochondria for utilization (233). Therefore, these data suggest that CD47 deficiency-mediated CPT1b expression in BAT may lead to increased fatty acid uptake in mitochondria and subsequent activation of UCP1, resulting in increased uncoupling and heat production (Figure 3.6 C, D).

3.3.7 cGMP/PKG signaling in WT and CD47 deficient mice under either LF or HF feeding conditions

Studies have shown that CD47 activation via TSP1 can disrupt NO/cGMP/PKG signaling in vascular cells (93, 109, 214). Therefore, we determined whether cGMP/PKG signaling in BAT or skeletal muscle was altered in CD47 deficient mice under either LF or HF feeding conditions. As shown in Figure 3.9 A, under LF feeding conditions, cGMP levels in BAT were higher in CD47 deficient mice compared to WT mice ($P < 0.05$). HF diet feeding significantly reduced BAT cGMP levels in both WT and CD47 deficient mice compared to their LF controls ($P < 0.05$); however, levels in HF-fed CD47 deficient mice were comparable to WT mice fed a LF diet. For PKG-I protein levels in BAT, under LF feeding conditions, no difference was found between WT and CD47 deficient mice. However, under HF feeding conditions, BAT PKG-I protein levels were significantly increased in CD47 deficient mice compared to WT mice (Figure 3.9 B; $P < 0.01$).

In addition to brown fat, cGMP/PKG signaling in skeletal muscle was analyzed. We found that cGMP levels or PKG-I protein levels were higher in LF-fed CD47 deficient mice compared to LF-fed WT mice (Figure 3.9 C, D; $P < 0.01$).

However, under HF feeding conditions, there was no difference in cGMP or PKG-I levels between WT and CD47 deficient mice. Together, these data suggest that cGMP/PKG signaling was differentially regulated by CD47 in BAT and skeletal muscle.

3.3.8 Characterization of white adipose tissue depots in CD47 deficient mice challenged with HF diet

In the current studies, we have shown that CD47 deficient mice are protected against the development of diet-induced obesity (Figure 3.1). To further understand the role of CD47 in white adipose tissue expansion under HF conditions, adipocyte size was measured in both subcutaneous adipose tissue (SAT) depots and epididymal adipose tissue (EAT). Similar to the phenotype observed in BAT (Figure 3.8 B), CD47 deficiency was associated with a significant reduction in lipid droplet size under LF and HF conditions in SAT (Figure 3.10 A; $P < 0.05$ between LF groups, $P < 0.01$ between HF groups) and EAT (Figure 3.10 B; $P < 0.05$ between LF and HF groups). This phenotype suggests a unique effect of CD47 on lipid storage independent of diet.

3.3.9 White adipocyte function *in vitro*

Several mechanisms regulate intracellular lipid levels within adipocytes, including the rates of lipogenesis/lipid storage, fatty acid oxidation, and liberation of FFAs from intracellular lipid droplets as a fuel source for metabolically active peripheral tissues. In order to determine the mechanism(s) contributing to a significant reduction in adipocyte size in WAT, *in vitro* studies utilizing primary adipocytes and the immortalized preadipocyte 3T3-L1 cells were completed.

First, stromal vascular fraction was isolated from both 8-week old CD47 deficient and age-matched control white adipose tissue depots, cultured, and differentiated into mature adipocytes as previously described in Section 2.18.4. To determine whether CD47 deficiency impairs adipogenesis and lipid storage in white adipocytes, CD47 deficient and control primary adipocytes were stained with Oil Red O on day 8 of differentiation to assess lipid accumulation. Our studies demonstrated no significant difference in lipid accumulation as indicated by Oil Red O staining of intracellular lipid (Figure 3.11 A, B). These data suggest impaired adipogenesis and lipid storage is not the cause for reduced adipocyte size *in vivo*.

In addition, mitochondrial function was assessed in CD47 deficient and control white adipocytes on day 8 of differentiation using the Seahorse XF96 Flux Analyzer (Agilent Technologies, Santa Clara, CA, USA). Basal respiration, ATP production, non-mitochondrial respiration, and maximal respiratory capacity were determined by measuring oxygen consumption rates (OCR) with the protocol detailed in Figure 2.1. CD47 deficient and control white adipocytes exhibited no significant difference in any mitochondrial function parameters (Figure 3.11.D, E), suggesting increased fatty acid-dependent metabolic activity is not contributing to reduce adipocyte size. Because we saw no differences in lipogenesis or mitochondrial respiration between genotypes *in vitro*, we conclude the smaller adipocyte phenotype *in vivo* (Figure 3.10) may be a result of crosstalk with other metabolic tissues and enhanced global energy requirements.

3.3.10 Regulation of lipid turnover by CD47

It has been previously determined that cGMP/PKG signaling regulates lipolysis by activating lipases critical for the hydrolysis of triglycerides in lipid droplets (185). In addition, it has been well established that activation of CD47 suppresses cGMP/PKG signaling in a number of tissues (93, 109, 214). As a potential mechanism for reduced white adipocyte size, the role of CD47 in white adipocyte lipolysis was examined *in vivo*, *ex vivo*, and *in vitro*. After a six hour fast, eight-week old CD47 deficient and wildtype littermate control mice were intraperitoneally injected with vehicle or CL 316,243 (1mg/kg BW), a β -adrenergic agonist, to induce lipolysis. Independent of treatment, CD47 deficiency significantly increased plasma levels of free glycerol, a common indicator of lipolysis (Figure 3.12 A; $P < 0.05$). *Ex vivo* lipolysis assays determined that lack of CD47 expression, independent of β -adrenergic stimulation, enhanced glycerol release from white adipose tissue depots but not from BAT (Figure 3.12 B; EAT: $P < 0.05$ basally, $P < 0.01$ stimulated; SAT: $p = 0.06$ basally, $P < 0.001$ stimulated).

Further, fully differentiated 3T3-L1 cells were serum starved and pretreated with or without IgG control or a functional blocking antibody targeting CD47 for 30 minutes. Cells were then treated with c-CPT-cGMP (200 μ M), a cGMP agonist, or isoproterenol (10 μ M), a non-specific β -agonist, as a positive control. Our studies show that treatment with cGMP and a CD47 functional blocking antibody (clone B6H12) significantly increase glycerol levels in the media, indicative of lipid mobilization, compared with controls (Figure 3.12 C;

P<0.05). These data suggest that reduced CD47 activity contributes to increased lipid droplet turnover in white adipose tissue.

3.3.11 FFA-mediated uncoupling of brown adipose tissue mitochondria

It is well established that FFAs are an efficient fuel source for enhanced mitochondrial respiration in BAT and directly stimulate uncoupling by interacting with UCP1 (67). In the current studies we have shown that CD47 deficiency is associated with increased CPT1b and UCP1 expression in brown adipose tissue despite HF diet challenge (Figure 3.8). We propose that increased lipid mobilization in CD47 deficient mice drives enhanced FA oxidation and UCP1-mediated uncoupling in BAT. To measure this, mitochondria were isolated from brown adipose tissue of age-matched CD47 deficient and littermate control mice and treated with various compounds to examine mitochondrial bioenergetics. It is clear that mitochondria from WT BAT are uncoupled, which is indicated by the continuous oxygen consumption despite oligomycin treatment, which should blunt all ETC-mediated oxygen consumption and ATP generation (Figure 3.13 A). However, mitochondria isolated from CD47 deficient BAT demonstrated a significant increase in the State IV and FFA-mediated UCP activation (Figure 3.13 B; P<0.05). This indicates that CD47 deficient BAT mitochondria are adapted to consume more oxygen and generate more heat compared to WT.

3.4 Discussion

CD47 is a transmembrane protein with several functions including self-recognition, immune cell communication, and cell signaling (28, 193). Although it

has been extensively studied in cancer and ischemia (165, 238, 241, 286), CD47 function in obesity has never been explored. In this study, we utilized CD47 deficient mice in a high-fat diet induced obesity model to study for the first time whether CD47 plays a role in diet-induced obesity and its associated metabolic complications. As previously reported (74), CD47 deficiency was associated with a leaner phenotype, although not significant, in the LF-fed group through the duration of the study compared with LF controls; however, body weight gain was consistent and no improvements in other metabolic parameters were identified between the two control groups. In our HF-mice, we found that CD47 deficient mice were protected from diet-induced obesity displaying decreased weight gain and reduced adiposity despite comparable daily food consumption and no impairments in intestinal lipid absorption (data not shown). This led to decreased MCP1/CCR2 dependent macrophage infiltration into adipose tissue and reduced inflammation, resulting in improved glucose tolerance and insulin sensitivity. In addition, CD47 deficiency stimulated the expression of UCP1 and CPT1b levels in brown adipose tissue, leading to increased lipid utilization and heat production and contributing to increased energy utilization and reduced adiposity in these mice. To support this, additional studies were completed under basal conditions that demonstrate CD47 deficiency is associated with enhanced white adipose tissue lipolysis and increased FFA-dependent mitochondrial respiration in brown adipose tissue. These data suggest a novel role for CD47 in regulation of metabolic function, energy homeostasis, and its contribution to the development of obesity and dyslipidemia.

CD47 is a receptor for the matricellular protein-thrombospondin 1 (TSP1). Previous studies from our lab and others suggest that TSP1 plays a role in obesity-associated chronic inflammation and insulin resistance (100, 128, 144, 268). Both TSP1 and CD47 expression in adipose tissue was up-regulated under obese conditions (128, 268), suggesting that CD47 may mediate the effects of TSP1 on diet-induced obesity and obesity-associated complications. By feeding CD47 deficient mice with the same diet (10% (LF) and 60% fat (HF) diet) for the same time period (16 weeks) as we did before with TSP1 deficient mice (144), we found that most of the phenotypes observed in the TSP1 deficient mice undergoing HF feeding were replicated in CD47 deficient mice including reduced macrophage infiltration into adipose tissue, reduced inflammation, and improved glucose tolerance and insulin sensitivity. However, one different phenotype was observed between CD47 deficient mice and our previous HF-fed TSP1 deficient mice (144), which was the significant changes in body weight. Current studies showed that CD47 deficiency protected mice from HF diet induced obesity; while TSP1 deficiency had no effect on diet-induced obesity after 16 weeks of HF feeding. This different phenotype suggests that TSP1-CD47 ligation may not be involved in regulation of energy homeostasis under HF feeding conditions. The novel CD47 ligands and their interaction on energy balance and the development of obesity warrant further investigation.

It has been shown that CD47 activation via TSP1 can disrupt the NO-cGMP pathway and that decreased NO/cGMP signaling contributes to vascular inflammation as well as adipose tissue inflammation, resulting in insulin

resistance (93, 214). In agreement with these observations, HF-fed CD47 deficient mice showed decreased levels of circulating proinflammatory cytokines as well as reduced inflammation in adipose tissue. They also had improved glucose tolerance and insulin sensitivity. Moreover, with reduced adiposity in HF-fed CD47 deficient mice, these mice exhibited reduced expression of MCP1 and CCR2 in adipose tissue. This was associated with reduced macrophage infiltration into adipose tissue in HF-fed CD47 deficient mice, which may be secondary to reduced adiposity. Further *in vitro* analysis demonstrated that CD47 deficient macrophages had significantly decreased migration compared to WT cells upon stimulation with MCP1. The importance of MCP1 and CCR2 in adipose tissue macrophage recruitment and their contribution to insulin resistance has been demonstrated by numerous studies (89, 116, 117, 191, 256, 280). Thus, data from our study suggest that the effect of CD47 on macrophage infiltration into adipose tissue and the development of chronic inflammation under obese conditions is MCP1/CCR2 dependent.

In this study, we found that CD47 deficiency protected mice from HF diet induced obesity, which was associated with increased energy utilization. To determine the mechanisms of increased metabolic rate in HF-fed CD47 deficient mice, we analyzed skeletal muscle function since a previous report showed that skeletal muscle from CD47 deficient mice had greater number of mitochondria and improved skeletal muscle function (74). Although we saw increased mitochondrial number in skeletal muscle and increased locomotor activity in HF-fed CD47 deficient mice compared to HF-fed WT mice, the expression of genes

relating to mitochondria oxidative function or fatty acid catabolism in skeletal muscle were comparable between WT and CD47 deficient mice (Figure 3.7). These data suggest that enhanced skeletal muscle function may not be driving the increased energy expenditure phenotype in HF-fed CD47 deficient mice.

The contribution of brown adipose tissue function to the increased metabolic rate in HF-fed CD47 deficient mice was also analyzed. The rationale for such studies is based on previous reports showing that increased cGMP/PKG signaling pathway stimulates brown adipocyte differentiation (90), promotes healthy expansion and browning of white adipose tissue (171), stimulates white adipose tissue lipolysis and cold induced brown fat thermogenesis (185). BAT is highly vascularized, highly innervated by the sympathetic nervous system, and is densely packed with mitochondria. BAT expends a large amount of energy through mitochondria β -oxidation and by uncoupling of the mitochondria proton gradient from ATP production. This uncoupling results in heat production or thermogenesis, accomplished by UCP1 located in the inner mitochondria membrane (31, 213).

It has been well-established that obesity reduces BAT-mediated energy expenditure and UCP1-driven thermogenesis (197, 215, 237). Although WT and CD47 deficient mice exhibited comparable brown fat mass and mitochondrial DNA content, loss of CD47 significantly increased UCP1 mRNA expression in brown fat under HF feeding conditions. Consistently, we found that core body temperature was elevated in HF-fed CD47 deficient mice, indicating increased thermogenesis. We demonstrated that cGMP and/or PKG signaling was up-

regulated in brown fat from CD47 deficient mice, which could augment healthy BAT function despite HF diet challenge. Moreover, the lipid accumulation in brown fat was significantly reduced in HF-fed CD47 deficient mice. UCP1 expression was not found in white fat from either WT or CD47 deficient mice under either LF or HF feeding conditions (data not shown), suggesting there was no browning of white fat and a BAT-specific effect of CD47 deficiency.

Because of the global effect of CD47 deficiency on lipid accumulation, white adipose tissue function was also examined. To elucidate a mechanism for reduced white adipocyte size, *in vitro* studies were completed that determined CD47 deficiency does not impair white adipogenesis/lipid storage and does not enhance white adipocyte mitochondrial function. Moreover, CD47 deficient mice displayed enhanced white adipose tissue lipolysis which could contribute to smaller adipocyte and tissue depot size *in vivo*. Interestingly, CD47 deficient mice were not dyslipidemic or insulin resistant, suggesting enhanced lipolysis is not a result of impaired adipose tissue insulin signaling or contributing to poor cardiovascular health. Rather, enhanced lipid mobilization could be a result of increased metabolic activity in other metabolic tissues.

It is known that fatty acids are an important fuel for thermogenesis. Lipolysis releases fatty acids that can be used for mitochondria oxidation and thermogenesis. We found that carnitine palmitoyltransferase 1b (CPT1b) was up-regulated in BAT from HF-fed CD47 deficient mice compared to HF-fed WT mice. CPT1b, located on the outer mitochondrial membrane, is the first and rate-limiting step for fatty acid transport into the mitochondria for utilization (233).

Therefore, CD47 deficiency may increase fatty acid translocation into mitochondria by fatty acid transporter CPT1b and drive the activation of UCP1 in brown fat and increased heat production. Interestingly, when isolated mitochondria from CD47 deficient BAT were treated with FFA we saw a robust uncoupling effect compared with WT BAT mitochondria supporting our proposal that CD47 deficiency enhances FFA-mediated BAT activation. These findings indicate that CD47 deficient mice have increased respiratory capacity as well as induced uncoupling, which ultimately leads to increased consumption of oxygen and energy. Together, our data suggest that CD47 mediated regulation of white and brown fat function contributes to the metabolic phenotype observed in the current study. However, to demonstrate definitively the effect of brown fat cell derived CD47 on energy metabolism in diet-induced obesity, the tissue specific CD47 deficient mice are required in future studies.

In summary, for the first time, our studies demonstrate an important role for CD47 in regulating energy balance and the development of obesity and its metabolic complications in a tissue-specific manner. CD47 deficiency protects mice from HF diet-induced obesity through stimulation of energy expenditure and heat production. In addition, CD47 deficiency reduces obesity-associated metabolic complications including decreased systemic and adipose tissue inflammation and hepatosteatosis, and improved glucose tolerance and insulin sensitivity. The results from this study suggest that CD47 may serve as a therapeutic target of obesity and its related comorbidities.

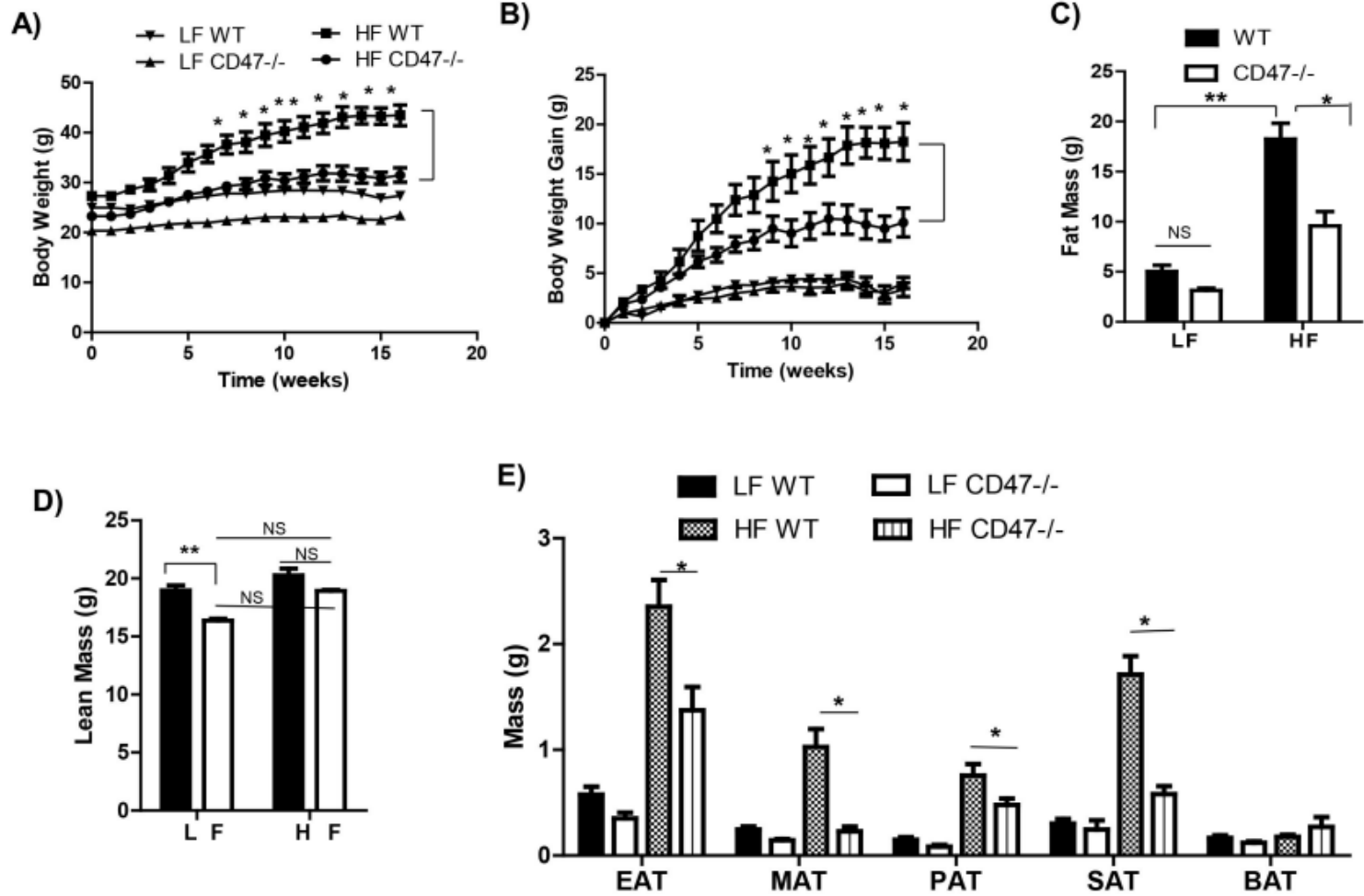


Figure 3.1 Weight-related measures after LF/HF diet challenge

CD47 deficient mice were protected from high fat diet-induced obesity. Eight week old male CD47 deficient mice and wild type C57BL6 controls were fed with low fat (LF) or high fat (HF) diet for 16 weeks. Weekly body weight (A) and body weight gain (B) are shown and were analyzed by two-way repeated measures ANOVA. Fat (C) and lean mass (D) of mice were measured by EchoMRI. Absolute weight of white and brown adipose tissue depots (E) were measured immediately following sacrifice. Data are presented as mean \pm SE (n=5-7 mice/group), *P<0.05, **P<0.01. EAT: epididymal adipose tissue; MAT: mesenteric adipose tissue; PAT: perirenal adipose tissue; SAT: subcutaneous adipose tissue; BAT: brown adipose tissue.

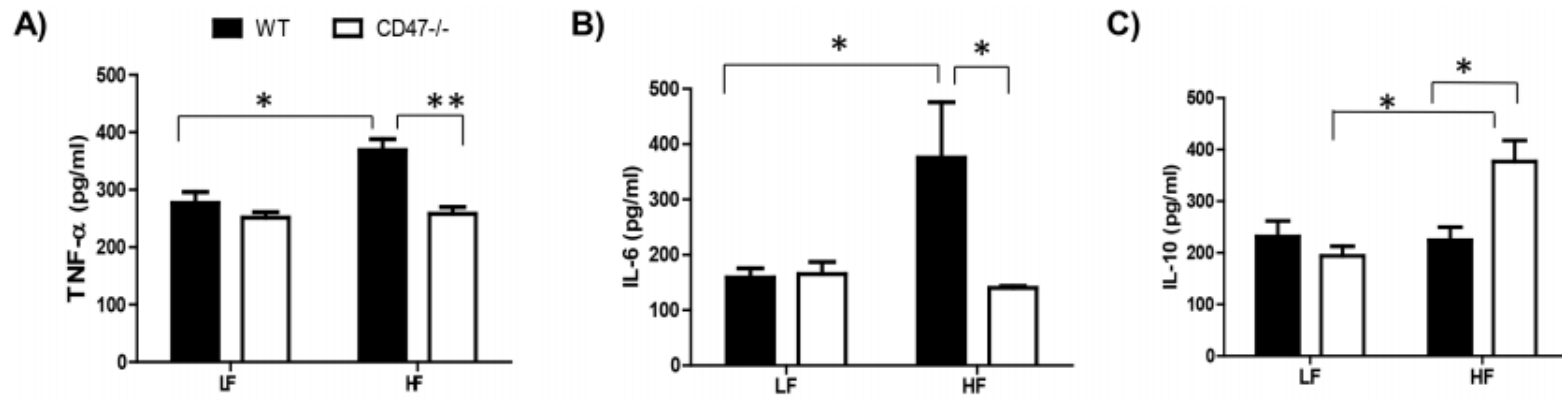


Figure 3.2 Obesity-associated systemic inflammation

HF-fed CD47 deficient mice displayed reduced systemic inflammation compared to HF-fed wild type controls. Plasma TNF α (A), IL-6 (B), and IL-10 (C) levels were measured by ELISA as described in Methods. Data are presented as mean \pm SE (n=5-7 mice/group), *P<0.05 and **P<0.01.

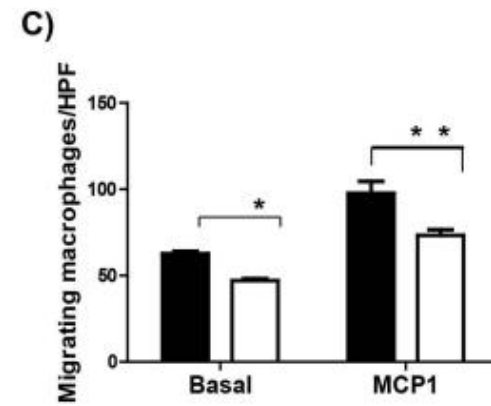
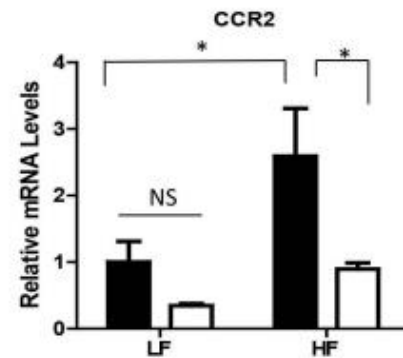
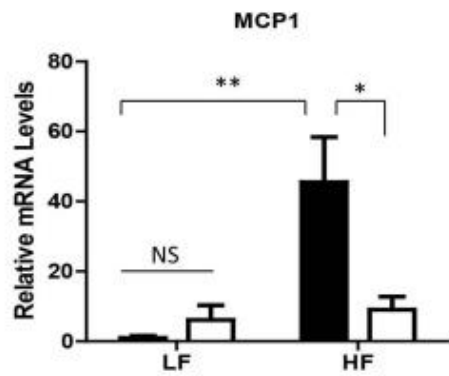
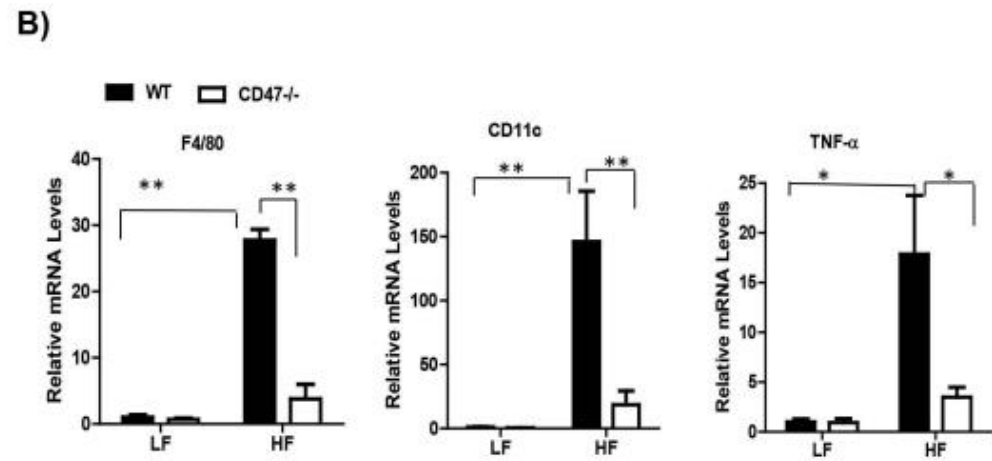
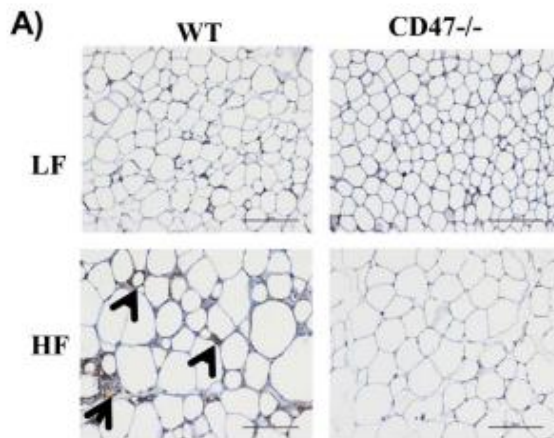


Figure 3.3 Adipose tissue inflammation and macrophage infiltration

HF-fed CD47 deficient mice had decreased adipose tissue macrophage infiltration and inflammation. Macrophage accumulation in epididymal adipose tissue (A) was determined by anti-F4/80 staining. The positive staining showed brown color indicated by arrow head. Representative images are shown. Scale bars represent 100mm. Expression of proinflammatory cytokines in epididymal adipose tissue (B) was determined by real-time PCR and normalized to 18S RNA. Bone marrow cells from HF-fed WT and CD47 deficient mice were isolated and differentiated into macrophages. Migration of these cells were measured basally and upon MCP1 (50 ng/ml) stimulation (C) using modified Boyden Microchemotaxis Chamber. Data are presented as mean \pm SE (n=5-7 mice/group), *P<0.05 and **P<0.01.

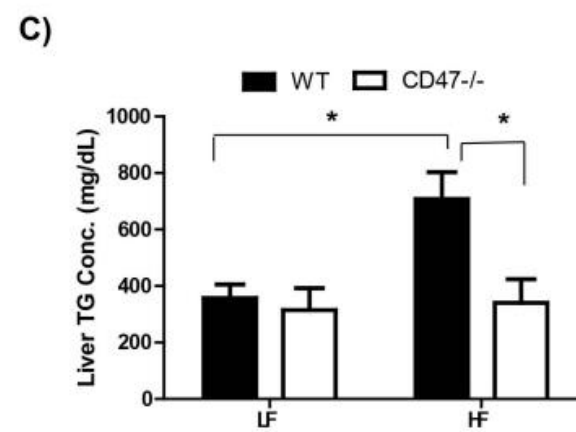
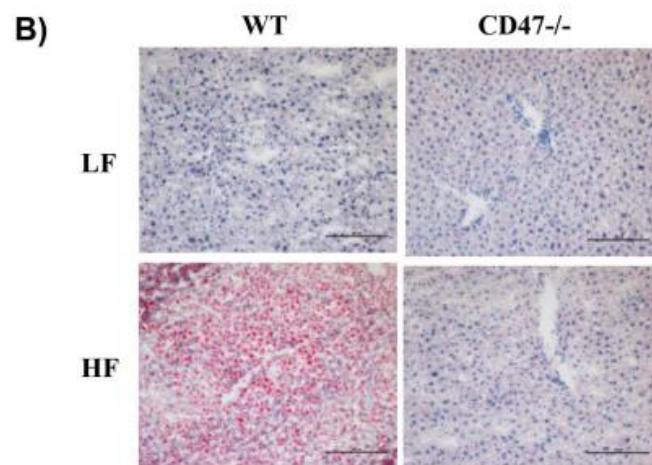
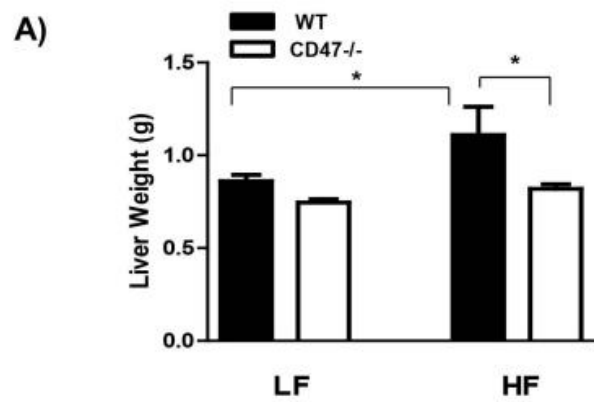


Figure 3.4 Liver lipid accumulation

CD47 deficiency prevents lipid accumulation in liver after HF diet feeding. Lipid accumulation in liver from four groups of mice was determined by measuring liver weight (A), staining liver sections by Oil-red-O (B), and quantification of triglyceride from liver extracts (C). The representative images of Oil Red O staining are shown. Scale bars represent 100 μ m. Data are presented as mean \pm SE (n=5-7 mice/group), *P<0.05.

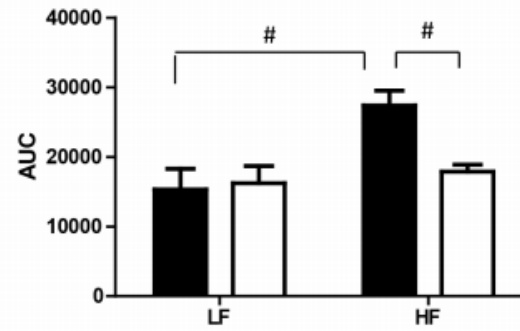
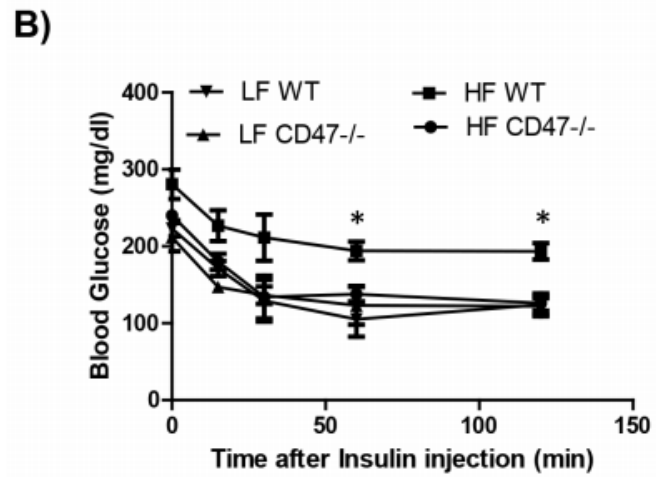
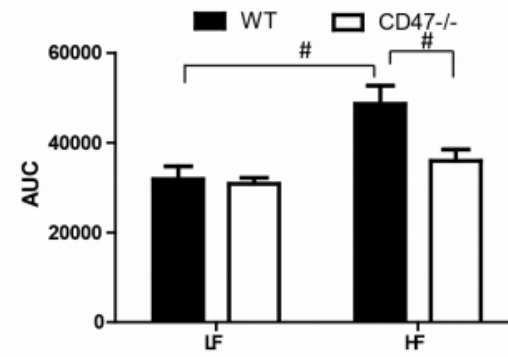
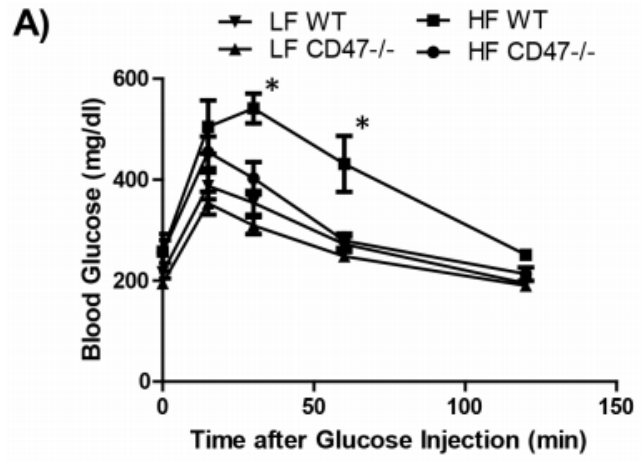


Figure 3.5 Glucose and insulin tolerance tests

HF-fed CD47 deficient mice had improved glucose tolerance and insulin sensitivity compared with HF-fed controls. Intraperitoneal glucose tolerance test (A) and insulin sensitivity test (B) were performed in male CD47 deficient and littermate control mice after 15 weeks of HF or LF feeding. Data are presented as mean \pm SE (n=5-7 mice/group), *P<0.05 vs. HF CD47^{-/-}; #P<0.05; AUC: area under the curve.

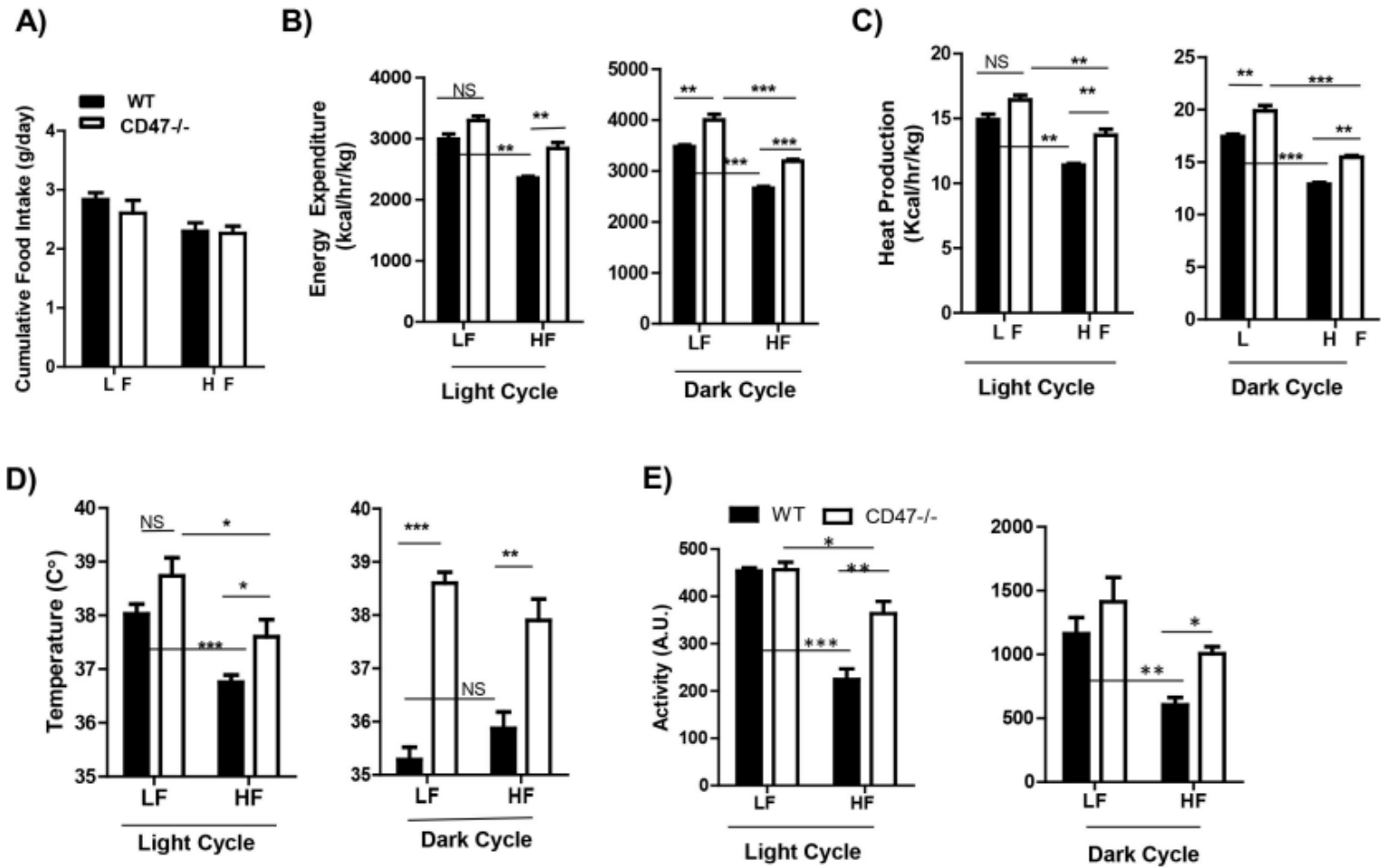
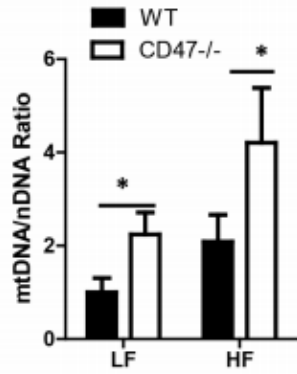


Figure 3.6 Metabolic profiles of WT and CD47 deficient mice under either LF or HF feeding conditions

Eight week old male CD47 deficient mice and wild type littermate controls were fed with LF or HF diet for 16 weeks and individually housed in TSE PhenoMaster chambers for indirect calorimetric analysis. Daily food intake (A) was measured for 6 consecutive days. Energy expenditure (B) was normalized to total body mass during both the light and dark cycles. Heat production (C), core body temperature (D), and activity (E) were shown during both the light and dark cycles. Data are presented as mean \pm SE (n=4-5 mice/group), *P<0.05; **P<0.01; ***P<0.001.

A)



B)

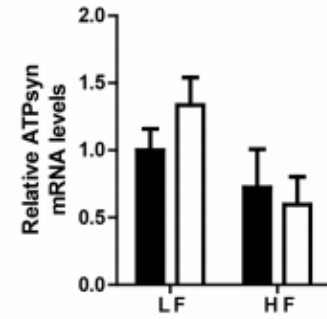
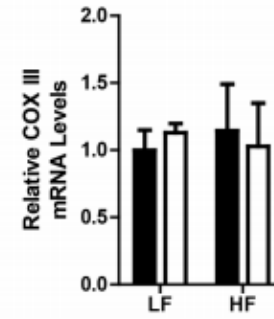
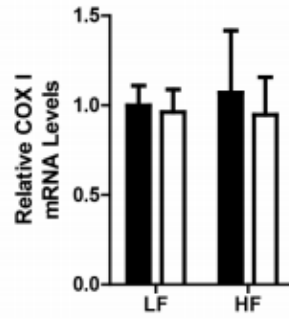
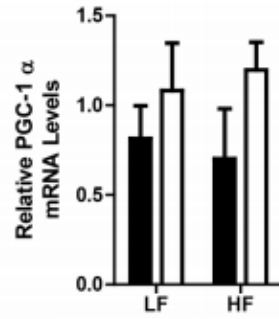
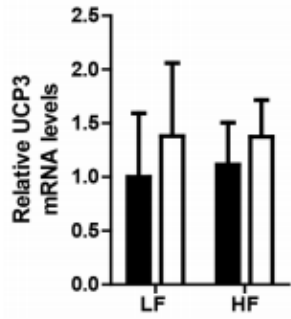
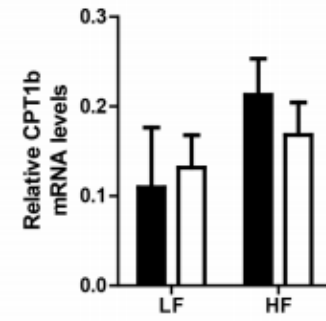
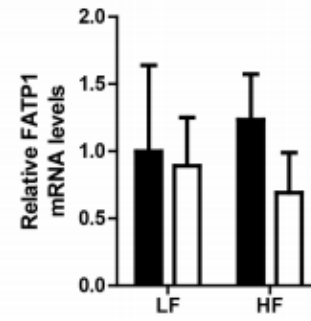
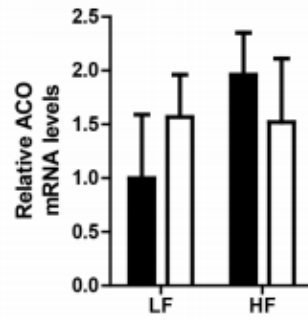


Figure 3.7 Metabolic gene expression in skeletal muscle from LF or HF feeding WT or CD47 deficient mice

After 16 weeks of LF or HF feeding, mitochondria DNA (mtDNA) copy number in skeletal mice (A) from four groups of mice and expression of metabolic genes (B) including acyl-CoA oxidase (ACO), fatty acid transporter protein (FATP1), carnitine palmitoyltransferase 1b (CPT1b), UCP3, PGC-1a, COX I, COX III and ATPsyn were measured by real-time PCR. Data are presented as mean \pm SE (n=5–7 mice/group), *P<0.05.

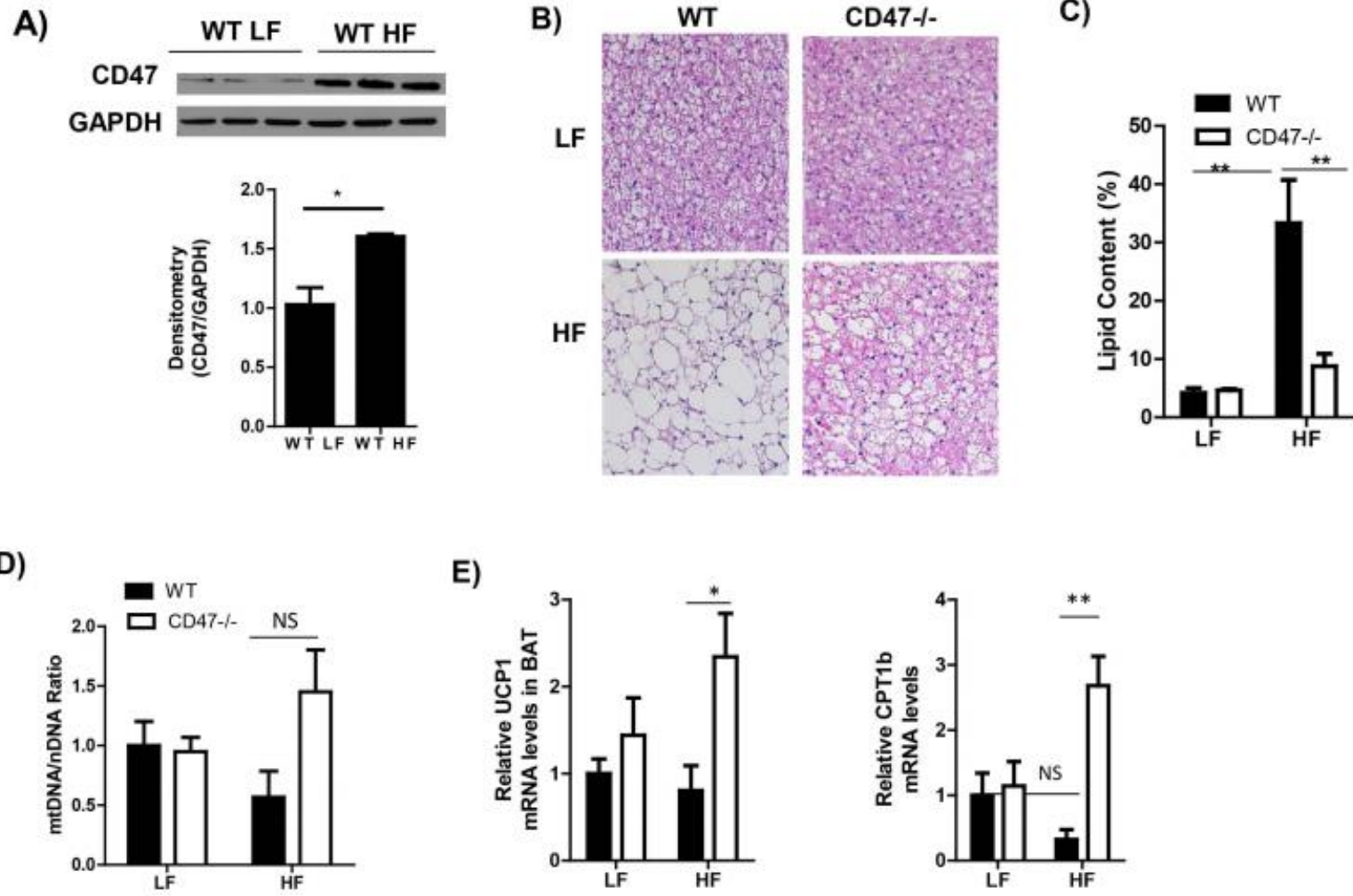
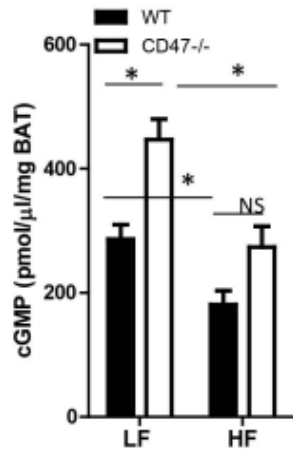


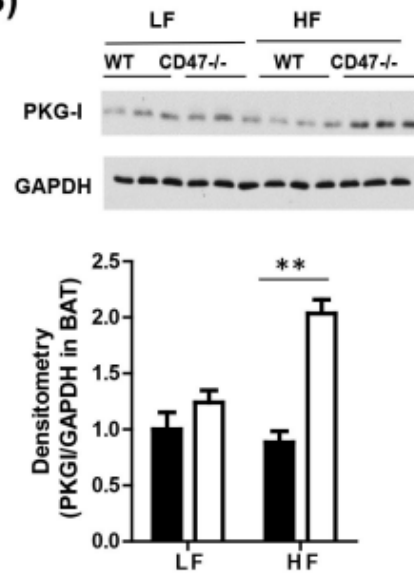
Figure 3.8 Morphology and metabolic gene expression in BAT from LF or HF fed WT or CD47 deficient mice

CD47 protein levels in brown adipose tissue from LF or HF fed WT mice by immunoblotting (A) (Cropped blots were used); Representative images of HE staining of brown adipose tissue (B) from LF or HF fed CD47 deficient and WT mice. Images were obtained at x20. Scale bars represent 100mm; Percentage lipid content in brown adipose tissue sections (C), as quantified using image analysis software. Mitochondria DNA copy number by PCR (D) and expression of metabolic genes (E) by real-time PCR. Data are presented as mean \pm SE (n=5–7 mice/group), *P<0.05 and **P<0.01.

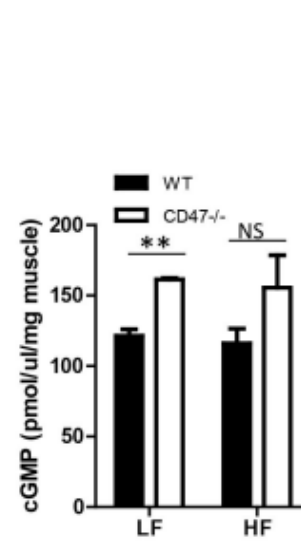
A)



B)



C)



D)

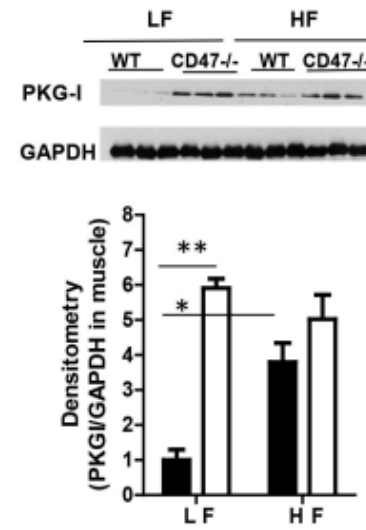


Figure 3.9 cGMP or PKG signaling in BAT and skeletal muscle from LF or HF fed WT or CD47 deficient mice

cGMP levels in brown adipose tissue (A) from LF or HF fed WT mice by direct immunoassay; PKG-I protein levels in brown adipose tissue (B) from LF or HF fed WT mice by immunoblotting (Cropped blots were used); cGMP levels in skeletal muscle (C) from LF or HF fed WT mice by direct immunoassay; PKG-I protein levels in skeletal muscle (D) from LF or HF fed WT mice by immunoblotting (Cropped blots were used). Data are presented as mean \pm SE (n=5-6 mice/group), *P<0.05 and **P<0.01.

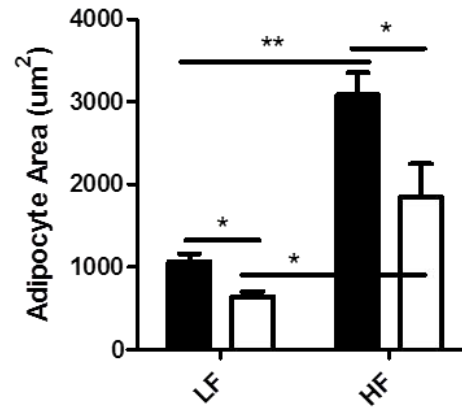
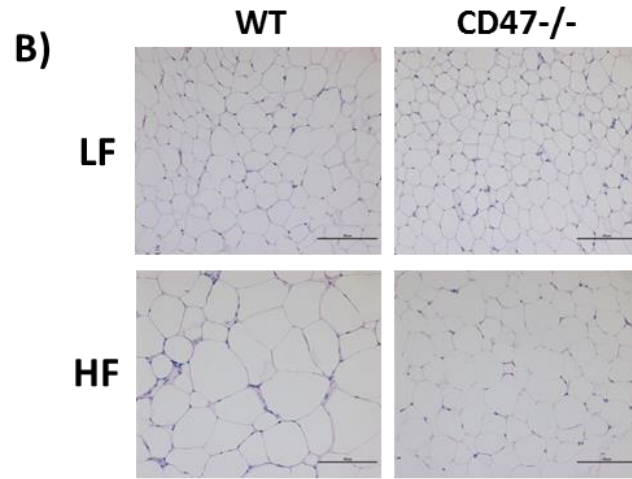
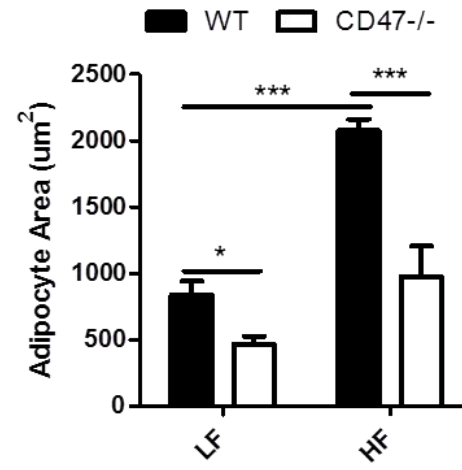
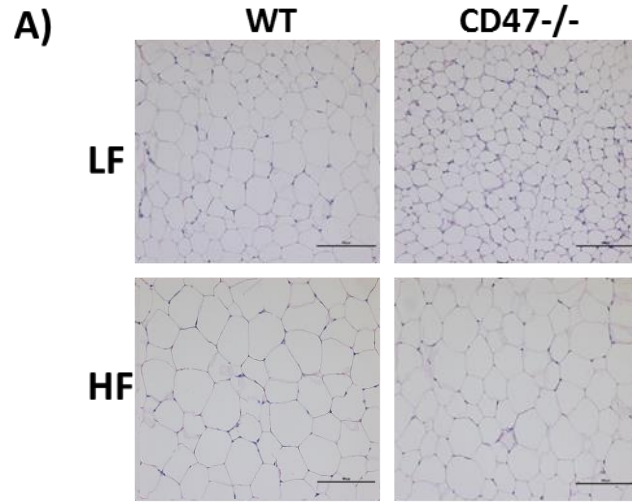


Figure 3.10 Characterization of white adipose tissue depots in CD47 deficient mice challenged with HF diet

CD47 deficiency was associated with a significant reduction in adipocyte size in subcutaneous (A) and epididymal (B) adipose tissue depots independent of diet challenge as demonstrated by H&E staining. Representative images are shown. Scale bars represent 100mm. Adipocyte size was quantified using a Nikon Eclipse 55i microscope and Nikon NIS-Elements BR software. Each group contained three mice. Three sections with 100 adipocytes each were measured per mouse. Data are presented as mean \pm SE. *P<0.05; **P<0.01; ***P<0.001.

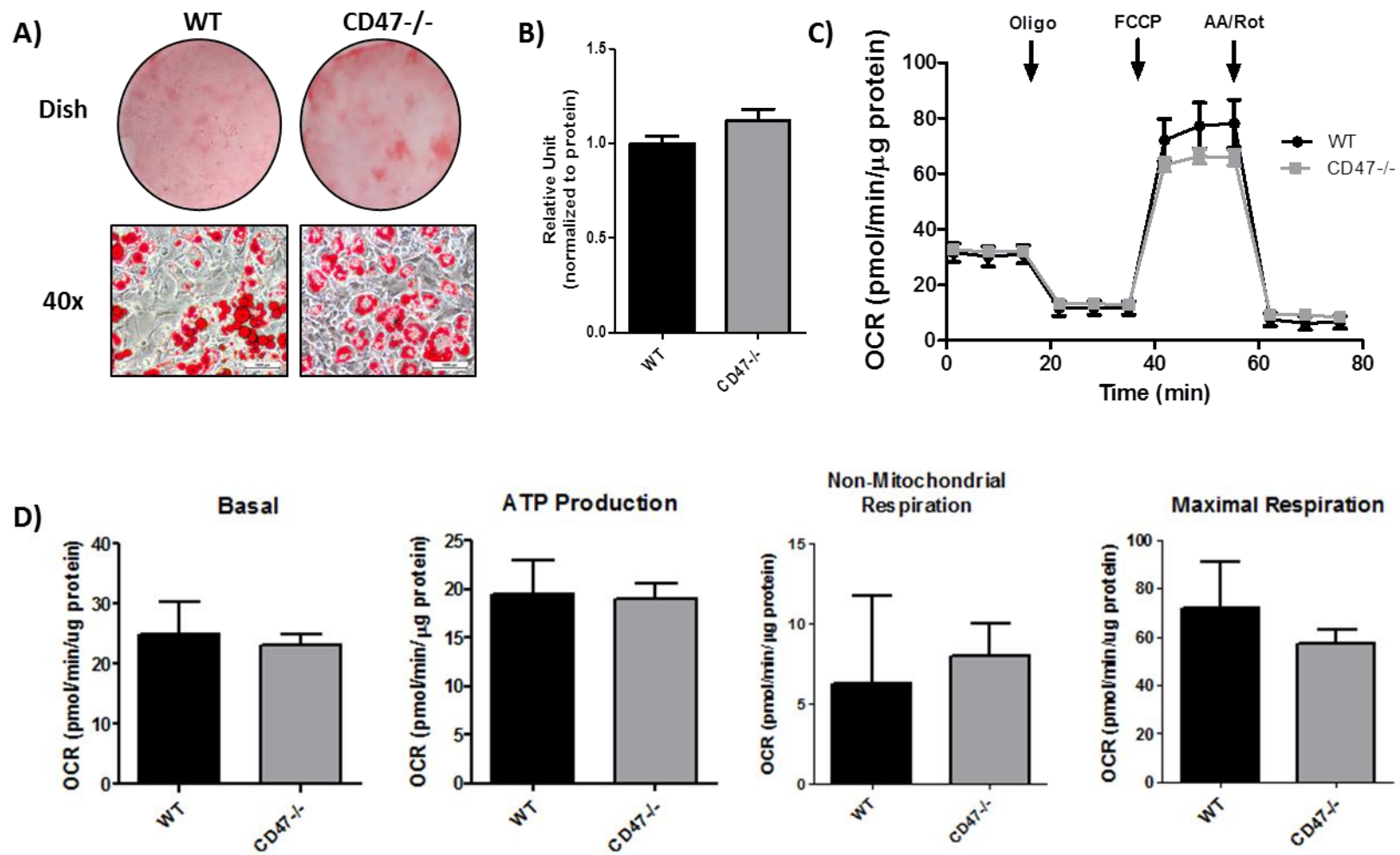


Figure 3.11 Adipogenesis and mitochondrial function of white adipocytes

Primary preadipocytes were isolated from white adipose tissue of eight week old WT and CD47 deficient mice and differentiated into mature adipocytes for 8 days. WT and CD47 deficient adipocytes accumulated comparable levels of lipid demonstrated by Oil Red O staining after 8 days of differentiation (A, B). CD47 deficient and control white adipocytes demonstrate comparable mitochondrial function. A basic mitochondrial stress test using the Seahorse XF96 Flux Analyzer demonstrates no significant difference in mitochondrial function between CD47 deficient and control white adipocytes in response to assay agents at specific time points (C). Basal respiration rates, ATP production, non-mitochondrial respiration, and maximal respiratory capacity (D) are presented as pmol/min of oxygen in assay media. All values are normalized to protein/well. Five to seven replicates were used for each group. OCR: oxygen consumption rates.

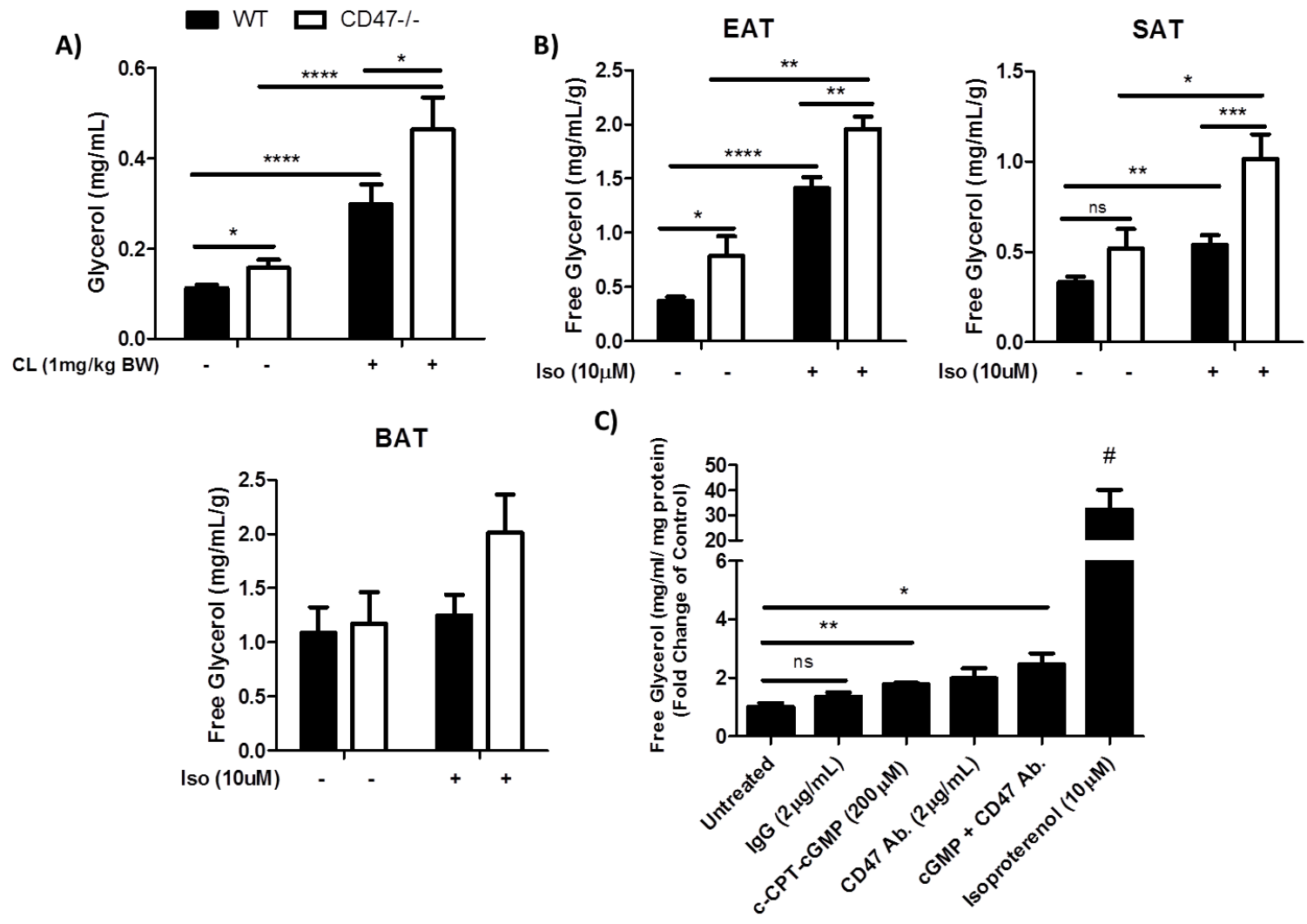


Figure 3.12 Regulation of lipid turnover by CD47

Eight week old CD47 deficient and wildtype littermate control mice were treated with either CL 316,243 (β -agonist; 1mg/kg BW; i.p. injection) or saline (vehicle) after a six hour fast. CD47 deficiency significantly increased plasma glycerol levels basally and with β -agonist stimulation (A) (n=4-7/group). Epididymal adipose tissue (EAT), subcutaneous adipose tissue (SAT), and brown adipose tissue (BAT) were excised from eight week old CD47 deficient and wildtype littermate control mice after a six hour fast (n=3 mice/group; all tissue samples from each mouse were triplicated). Tissues were serum starved for 1 hour and then treated with vehicle or 10 μ M isoproterenol for 2 hours. Glycerol release was measured in the media by colorimetric kit. Lack of CD47 expression significantly increased lipolysis indicated by glycerol content in the media in epididymal and subcutaneous adipose tissue depots independent of treatment (B). Fully differentiated 3T3-L1 adipocytes were serum starved, pretreated with either IgG control or a CD47 functional blocking antibody clone B6H12 (2 μ g/mL) for 30 minutes, then stimulated with c-CPT-cGMP (200 μ M) or isoproterenol (positive control; 10 μ M). After three hours, media was collected and glycerol release was measured and normalized to cellular protein content. Treatment with c-CPT-cGMP and CD47 functional blocking antibody significantly increased glycerol release compared to controls in an additive manner (C). All *in vitro* experiments were triplicated. Data are presented as mean \pm SE; *P<0.05; **P<0.01; ****P<0.0001; #P<0.0001 compared to all groups. Ab: antibody; CL: CL 316,243; Iso: isoproterenol; ns: no significance.

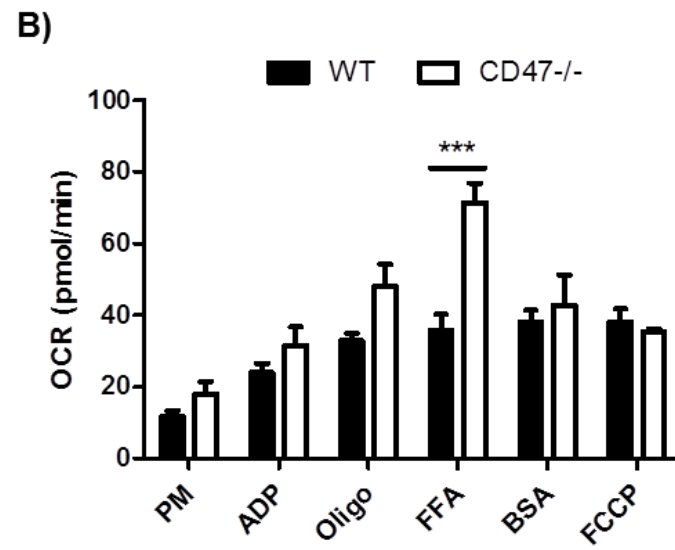
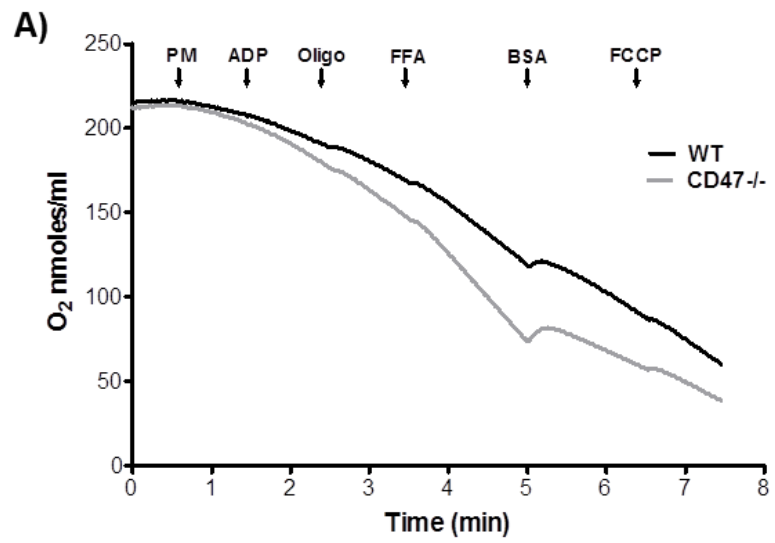


Figure 3.13 FFA-dependent uncoupling in BAT mitochondria

Mitochondria were isolated from BAT of 8-week old CD47 deficient and WT littermate control mice by differential centrifugation. Mitochondrial respiration (presented as oxygen consumption) was measured using a Clark-type oxygen electrode under sealed and isothermic conditions as previously described (255). Over time, mitochondria were treated with various substrates to examine individual bioenergetics states. Pyruvate and malate (PM; 5mM and 2.5mM, respectively) were used to promote oxidation. ADP (120nmol) was used to measure State III respiration and oligomycin (oligo; 1 μ M) was used to induce State IV respiration. FFAs (60 μ M linoleic acid) were added to induce uncoupling-mediated respiration and BSA (3%) was subsequently added to blunt FFA-induced uncoupling by sequestering FFAs. Last, FCCP was added to induce maximal uncoupling. Representative oxygraph traces (A) are presented from WT and CD47 deficient BAT mitochondria. Downward trends of the lines within the graph indicate oxygen consumption. After the addition of each compound, changes in oxygen consumption were quantified (B). Mitochondria isolated from CD47 deficient BAT are highly uncoupled in response to FFA treatment, when respiration is compared to FCCP-induced uncoupling. Data are presented as mean \pm SE (n=4 mice/group); ***P<0.001.

Section 4: SPECIFIC AIM 2

4.1 Summary

Non-alcoholic fatty liver disease (NAFLD), a hepatic manifestation of metabolic syndrome, is driven by elevated oxidative stress and impaired mitochondrial function in the presence of increased lipid. However, specific signaling mechanisms initiating these events are largely unknown. Thrombospondin-1 (TSP1) activity through the transmembrane receptor CD47 has been previously implicated in the development of oxidative stress in rodent hepatic ischemia reperfusion and transplantation models. The aim of our study was to examine for the first time whether TSP1 and CD47 are involved in the pathogenesis of diet-induced fatty liver by mediating oxidative stress. We demonstrated that both TSP1 deficient and CD47 deficient mice challenged with high fat (HF) diet for 16 weeks were protected against hepatic lipid accumulation, inflammation, fibrosis, and oxidative stress typically associated with fatty liver disease. Our studies also demonstrated that hepatic protein levels of TSP1 and CD47 are both upregulated under HF conditions. *In vitro* studies show that TSP1 treatment induces reactive oxidative species (ROS) to levels comparable to free fatty acids (FFAs) in human hepatocyte cell line (HepG2 cells); however, functional blocking antibodies against CD47 attenuated TSP1-induced ROS. Similarly, CD47 deficient primary hepatocytes were protected from FFA and TSP1-induced ROS. Collectively, results from our studies suggest that increased hepatic TSP1 and CD47 expression under HF conditions may contribute to the development of NAFLD by augmenting ROS production.

4.2 Introduction

Nonalcoholic fatty liver disease (NAFLD) is becoming increasingly common due to elevated levels of visceral adiposity and obesity. In the western world, between 10-15% of lean individuals and approximately 70% of obese individuals are affected (73, 270). Unfortunately, increased lipid accumulation within the liver is directly linked to whole body insulin resistance and exacerbates the risk of developing nonalcoholic steatohepatitis (NASH), a full-blown inflammatory and fibrogenic response, which contributes to cirrhosis and hepatocellular carcinoma (HCC) (7).

Recent studies have demonstrated that oxidative stress precedes the development of hepatic insulin resistance, lipodystrophy, and inflammation in high fat-fed rodent models (97, 163, 180). Further, reactive oxidative species (ROS) stimulate inflammatory signaling pathways, reduce mitochondrial biogenesis, and impair the adaptive responses of the mitochondria to manage increased lipid burden under obese conditions (179, 221, 243). However, the specific mechanisms responsible for these initiating events have not been determined. It is suggested that identifying mechanisms which protect against ROS production and preserve mitochondrial function in the presence of increased energy substrate would be a viable therapeutic targets for NAFLD.

CD47, a ubiquitously expressed transmembrane cell surface receptor, regulates several pathways including self-recognition and vascular function (28, 193). Our group and others have identified TSP1 as a contributor to metabolic dysfunction in high fat (HF) diet-induced obesity (53, 100, 128, 144, 162, 268).

Similarly, recent studies from our laboratory suggest CD47 deficiency could be protective against obesity-associated complications (156). Upon activation by picomolar concentrations of thrombospondin-1 (TSP1), CD47 signaling promotes ROS production and inflammation in hepatic ischemia reperfusion injury and liver transplantation models (105, 293). Although the TSP1-CD47 interaction has been implicated in other hepatic conditions and both have been shown to contribute to metabolic dysfunction, this signaling mechanism has never been explored in the progression of NAFLD.

The aim of our study is to determine whether TSP1 and CD47 interaction contributes to ROS production in the development of NAFLD. We determined both TSP1 and CD47 expression is upregulated in the liver under HF conditions. Further, we demonstrated that TSP1 deficiency and CD47 deficiency similarly protected mice from obesity associated fatty liver disease. Moreover, in vitro studies show TSP1-induced ROS is partially facilitated through CD47 and contributes to hepatocyte-specific oxidative stress. This study suggests that the TSP1-CD47 interaction could potentially be a viable therapeutic target for diet-induced fatty liver.

4.3 Results

4.3.1 TSP1 deficiency protects mice from diet-induced fatty liver

It has been well established that expression of TSP1, the most potent ligand of CD47, is significantly elevated in plasma and adipose tissues under obese conditions (268, 277); however TSP1 levels in the liver have not been determined. In our studies, TSP1 protein (Figure 4.1 A; $P < 0.05$) and mRNA

(Figure 4.1 B; $P < 0.05$) levels were significantly upregulated in whole liver tissue from wildtype mice after four month HF feeding compared to LF fed controls. In addition, our lab and others have established a pathological role of TSP1 in obesity and metabolic dysfunction (128, 144, 268). Yet, the effects of TSP1 on obesity-associated fatty liver disease have never been reported. In our studies, TSP1 deficient and wildtype controls (WT) were challenged with either LF or HF diet for 16 weeks. Although TSP1 deficiency did not reduce final body weights (Figure 4.1 C) or liver weights (Figure 4.1 D) after 16-week HF feeding, HF-fed TSP1 deficient mice demonstrated a significant reduction in hepatic triglyceride content (Figure 4.1 E; $P < 0.01$) represented by H&E staining (Figure 4.1 F). Further, TSP1 deficiency was associated with significantly reduced TNF α and collagen I α mRNA levels under HF diet conditions (Figures 4.1 G, H; $P < 0.05$) indicating a protective role against hepatic inflammation and fibrosis, respectively.

4.3.2 TSP1 deficiency alters hepatic genes related to lipid metabolism

To examine what mechanisms in the liver may be contributing to reduced lipid accumulation in TSP1 deficient mice, several metabolic pathways were examined by qPCR. Fatty acid oxidation genes, peroxisome proliferator-activated receptor gamma coactivator 1-alpha (PGC1 α), the coactivator responsible for regulating mitochondrial function, peroxisome proliferator-activated receptor alpha (PPAR α), the key nuclear receptor driving expression of other fatty acid oxidation genes, and carnitine palmitoyltransferase 1A (Cpt1A), an enzyme

responsible for the rate limiting step of fatty acid oxidation, were measured and no differential gene expression was observed between all four groups. This suggests increased lipid oxidation is not contributing to reduced hepatic lipid content (Figure 4.2 A). Key genes associated with gluconeogenesis, phosphoenolpyruvate carboxykinase (Pepck) and glucose-6-phosphatase (G6P), were downregulated in HF-fed TSP1 deficient mice (Figure 4.2 B; $P < 0.05$ for G6P), suggesting enhanced gluconeogenesis is not driving reduced hepatic lipid.

Interestingly, expression of peroxisome proliferator-activated receptor gamma (PPAR γ) and sterol regulatory element-binding protein 1c (SREBP1c), two positive regulators of lipogenesis and lipid storage, were significantly reduced in the livers of HF-fed TSP1 deficient mice compared with HF-fed controls (Figure 4.2 C; $P < 0.01$ and $P < 0.05$, respectively). Moreover, mRNA levels of microsomal triglyceride transfer protein (MTTP), a critical regulator of lipoprotein assembly and triglyceride secretion, was also measured. HF-fed TSP1 deficient mice demonstrated a significant reduction in MTTP (Figure 4.2 D; $P < 0.0001$), which would suggest that enhanced lipoprotein/triglyceride secretion is not preserving hepatic morphology under HF conditions. Finally, key genes implicated in fatty acid uptake in fatty liver disease models were measured. Although a slight reduction, no significant differences were observed in CD36 or fatty acid transport proteins (FATPs) 2 and 5 mRNA levels (Figure 4.2 E).

4.3.3 CD47 deficiency protects mice from diet-induced fatty liver

CD47 is a potent receptor for TSP1. To explore its role in a fatty liver disease phenotype, CD47 deficient and wildtype littermate controls (WT) were

randomized into groups and challenged with either a LF or HF diet for 16 weeks. Consistent with our previously published reports using age-matched CD47 deficient and C57BL/6 control mice (156), HF-fed CD47 deficient mice gained significantly less body weight (Figure 4.3 A; $P < 0.01$) and had significantly smaller livers by absolute weight (Figure 4.3 B; $P < 0.0001$) and as a percentage of body weight (Figure 4.3 B; $P < 0.01$) when compared with HF-fed wildtype littermate controls after 16 weeks of diet challenge. All groups consumed comparable amounts of food daily and no significant differences in plasma lipid parameters (free fatty acids, triglyceride, or total cholesterol levels) were observed (data not shown). In addition, liver morphology and function was examined. Histological H&E and oil red O staining (Figure 4.3 C, D) confirmed the absence of CD47 significantly reduced hepatic triacylglycerol content (Figure 4.3 E; $P < 0.05$) after 16 weeks of HF diet challenge. Moreover, plasma alanine aminotransferase (ALT) levels, a common indicator of hepatic dysfunction, were significantly reduced in HF-fed CD47 deficient mice compared with HF controls (Figure 4.3 F; $P < 0.01$). These studies suggest CD47 deficiency protects mice against diet-induced fatty liver.

4.3.4 CD47 deficiency reduces obesity-associated hepatic inflammation and fibrosis

It has been well-characterized that diet-induced fatty liver is associated with elevated inflammation which drives the development of fibrosis (263). It has also been shown that CD47 deficiency protects against adipose tissue and systemic inflammation under obese conditions, but effects on the liver have not

been explored. To further characterize the liver phenotype observed in our mice, immunohistochemistry (IHC), collagen staining, and quantitative PCR (qPCR) were completed. It has been suggested that fatty liver-associated inflammation is due to an increase in macrophage recruitment rather than resident macrophages (Kupffer cells) (174). Although IHC demonstrates macrophage presence by staining of F4/80 in all groups (Figure 4.4 A), CD47 deficiency significantly reduces the number of macrophages present within the livers of HF-challenged mice to levels comparable to the LF groups (Figure 4.4 B; $P < 0.05$). Moreover, qPCR confirmed HF-fed controls had elevated levels of inflammatory markers $\text{TNF}\alpha$, MCP1, and CD11c, while CD47 deficiency in HF-fed animals completely restored inflammatory markers to that of the LF control animals (Figure 4.4 C; $P < 0.05$).

Further, HF-fed controls have two-fold more collagen deposition as demonstrated by Sirius Red staining compared with HF-fed CD47 deficient mice (Figures 4.5 A, B; $P < 0.05$). We confirmed a reduction in fibrosis with qPCR. Consistently, HF-fed controls had elevated levels of collagen I α 1, collagen III, and collagen IV gene expression (Figure 4.5 C; $P < 0.05$), which have previously been identified as fibrotic markers of NAFLD (34, 64, 229). Together, these data show HF-fed CD47 deficient mice exhibit reduced diet-induced hepatic inflammation and fibrosis.

4.3.5 CD47 deficiency regulates lipogenic gene expression in a diet-induced fatty liver model

To further elucidate the mechanism for reduced lipid deposition within the livers of HF-fed CD47 deficient mice, qPCR was utilized to examine expression of fatty acid oxidation, gluconeogenic, triglyceride secretion, lipogenic, and fatty acid uptake genes. Expression of fatty acid oxidation genes, PGC1 α , PPAR α , and Cpt1A, were comparable between the four groups (Figure 4.6 A), suggesting increased fatty acid oxidation is not contributing to reduced lipid deposition in the liver of HF-fed CD47 deficient mice. Second, key genes associated with gluconeogenesis, Pepck and G6P, were measured and showed no differential regulation between genotypes (Figure 4.6 B). Consistent with HF-fed TSP1 deficient mice (Figure 4.2 C), HF-fed CD47 deficient mice exhibited a significant reduction in both lipogenic genes, PPAR γ and SREBP1c (Figure 4.6 C; $P < 0.01$). No differential expression of MTP was observed indicating reduced lipid within the liver is not a result of elevated triglyceride secretion to peripheral tissues (Figure 4.6 D). Finally, genes involved in fatty acid uptake were measured. CD47 deficiency was associated with a significant reduction in CD36 mRNA levels in HF-fed mice ($P < 0.0001$); however, no differences were observed in fatty acid transport proteins (FATPs) 2 and 5 (Figure 4.6 E).

4.3.6 TSP1 and CD47 deficiency reduces hepatic oxidative stress in a diet-induced fatty liver model

ROS production has been shown to play a causal role in the progression of NAFLD which results in inflammation and insulin resistance (19). Our studies

demonstrate a significant reduction in oxidative stress in both TSP1 and CD47 deficient livers in a diet-induced fatty liver model. TSP1 deficiency under HF conditions was associated with a reduction in the cleavage of H₂DCFDA to DCF, a common indicator of oxidative stress, in liver tissue homogenates (Figure 4.7 A; P<0.001). Lipid peroxidation, the degradation of lipids by free radicals, is another cellular source of ROS that has been implicated in the pathogenesis of fatty liver disease (271). Malondialdehyde (MDA), a potent byproduct of incomplete lipid peroxidation, was measured in whole liver tissue as an indication of lipid peroxidation. As expected, HF diet challenge was associated with a significant increase in MDA levels (P<0.001); however HF-fed TSP1 deficient mice demonstrated a significant reduction in hepatic MDA accumulation compared with HF-fed controls (Figure 4.7 B; P<0.05). Together, these results suggest that TSP1 deficiency is protective against the development of hepatic ROS under obese conditions.

Similarly, HF-fed CD47 deficient mice exhibited a significant reduction in ROS production compared to HF-fed controls demonstrated by the production of DCF in whole liver tissue homogenates (Figure 4.7 C; P<0.05). Moreover, HF-fed controls exhibited a two-fold increase in lipid peroxidation compared with LF controls as indicated by levels of MDA within whole liver tissue (P<0.05). However, HF-fed CD47 deficient mice are protected against hepatic lipid peroxidation (Figure 4.7 D; P<0.05). Together, these studies suggest CD47 deficiency is protective against oxidative stress in the liver under HF conditions.

4.3.7 CD47 expression is upregulated by high fat diet in the liver

Diet regulation of CD47 expression in the liver is largely unknown. HepG2 cells, an immortalized human hepatoma cell line, are commonly utilized as an *in vitro* model for hepatic metabolic function. We were able to demonstrate that CD47 expression is significantly elevated in a dose dependent manner after 24-hour fatty acid treatment (Figure 4.8 A; $P < 0.01$ with 50 μ M palmitate treatment, $P < 0.0001$ with 200 μ M palmitate treatment). In addition, we isolated primary hepatocytes from C57BL6/J mice after 3, 7, and 14 days of LF or HF feeding. CD47 protein expression was significantly increased on hepatocytes from HF-fed mice after just 14 days of diet challenge (Figure 4.8 B; $P < 0.05$). These data suggest CD47 protein expression is upregulated by over-nutrition in the liver.

4.3.8 CD47 blockade and deficiency are associated with reduced FFA and TSP1-induced ROS development in hepatocytes *in vitro*

To define the role of CD47 in hepatocyte function, we performed *in vitro* studies utilizing purified full length TSP1 and fatty acid treatments. It has been previously reported that acute treatment with FFAs triggers ROS production in HepG2 cells (44, 59, 80). Consistent with the literature, we demonstrate an increase in ROS production after 6-hour palmitate treatment in HepG2 cells as indicated by the fluorescent probe DCF (Figure 4.8 C; $P < 0.05$). Similarly, 6-hour TSP1 treatment was sufficient to induce comparable levels of ROS in these cells (Figure 4.8 C; $P < 0.05$). GST had no effect on ROS production. However, pretreatment with a CD47 functional blocking antibody clone B6H12 (2 μ g/mL) for 30 minutes prior to TSP1 treatment attenuated ROS production (Figure 4.8 D;

P<0.05), suggesting TSP1-induced ROS is partially facilitated through CD47 activation.

To confirm the role of CD47 in ROS production within hepatocytes, primary hepatocytes were isolated from age-matched male wildtype, CD47 deficient, and CD36 deficient mice. CD36 deficient primary hepatocytes were also included within this study because some actions of TSP1 in other cell types are facilitated through the scavenger receptor/fatty acid transport protein, CD36, and hepatocyte expression of CD36 positively correlates with lipid accumulation in the liver (104, 129). After 6-hour palmitate treatment, both CD47 deficient and CD36 deficient primary hepatocytes demonstrated a significant reduction in ROS production compared to wildtype cells (Figure 4.8 E; P<0.05). Interestingly, after TSP1 treatment for 6 hours, only CD47 deficient hepatocytes exhibited protection from ROS production (Figure 4.8 F; P<0.01). These data support the idea that CD47 deficiency is protective against both fatty acid and TSP1-induced ROS production within hepatocytes; however, TSP1 activity is dependent on CD47.

4.4 Discussion

CD47, a transmembrane receptor, has been extensively studied in regards to cancer and immune cell function and migration (28, 193). In addition, CD47 activation by thrombospondin 1 (TSP1), a matricellular protein, contributes to oxidative stress in a number of tissues (107, 109). Although oxidative stress has been implicated as a causal mechanism for the development of non-alcoholic fatty liver disease (NAFLD) (122, 189, 199), the role of the TSP1-CD47 axis in hepatic metabolic dysfunction has never been defined. The aim of this

study was to examine whether TSP1 and CD47 are involved in the pathogenesis of diet-induced fatty liver by mediating ROS production. In the current study, we demonstrated for the first time in two separate cohorts of mice that TSP1 and CD47 deficiency protected against hepatic lipid accumulation and suppressed fatty liver-associated inflammation and fibrosis in a HF diet-induced NAFLD model. Moreover, both genotypes were associated with a significant reduction in hepatic ROS production despite HF diet challenge. In addition, hepatic TSP1 and CD47 protein expression positively correlate with HF diet and *in vitro* studies confirmed that CD47 deficiency or pharmacological blockade significantly reduced oxidative stress associated with acute fatty acid or TSP1 treatment. Together, our studies suggest that both TSP1 and CD47 deficiency protect against hepatic lipid accumulation in a rodent NAFLD model by suppressing ROS production.

In the current studies, TSP1 deficient mice when challenged with HF diet did not exhibit reduced body weight or liver size, despite a reduction in liver triglyceride content (Figure 4.1). On the other hand, CD47 deficient mice were significantly protected against diet-induced obesity and demonstrated significantly smaller livers after HF diet challenge (Figure 4.3). Differences in body weight and liver size suggest unique mechanisms within TSP1 deficient and CD47 deficient animals that account for altered lipid partitioning under HF conditions. Although evidence is clear linking the TSP1-CD47 axis to ROS production in the liver, independent effects of TSP1 and CD47 on lipid homeostasis require further investigation.

Hallmarks of NAFLD progression include the accumulation of ectopic fat within hepatocytes, activated inflammatory pathways, and fibrogenesis. In our current studies, both TSP1 deficient and CD47 deficient animals were significantly protected against hepatic lipid deposition. To further characterize the potential mechanisms leading to the protective effects of TSP1/CD47 deficiency, a number of genes that regulate lipid metabolism were examined in both groups of animals. In both *in vivo* studies, no changes in genes relating to fatty acid oxidation or gluconeogenesis were observed, suggesting that reduced lipid accumulation in livers from HF-fed TSP1 deficient and CD47 deficient mice was not due to increased fuel utilization or enhanced glucose production from fatty acid byproducts.

Hepatic CD36 levels were suppressed in HF-fed TSP1 deficient mice and significantly downregulated in HF-fed CD47 deficient mice, suggesting a potential reduction in fatty acid uptake; however, no changes were observed in liver specific fatty acid transport proteins 2 and 5 (FATP2, FATP5) in either group of animals. Because CD36 is a scavenger receptor, the reduction in mRNA levels could be a result of reduced immune cell infiltration into the liver tissue instead of a reduction in hepatocyte-specific expression. Therefore, reduced fatty acid uptake might not be responsible for reduced hepatocyte intracellular lipid accumulation. Interestingly, mRNA levels of MTP were significantly reduced in HF-fed TSP1 deficient livers and no change was observed in HF-fed CD47 deficient livers; nevertheless, enhanced lipoprotein/triglyceride secretion is not contributing to reduced hepatic lipid. Further analysis demonstrated that

expression of lipogenic genes, SREBP1c and PPAR γ , were significantly reduced in both HF-fed TSP1 deficient and CD47 deficient animals. Further analysis demonstrated that downstream target genes of SREBP1c, including Scd1 and Fasn, were not differentially regulated. Together these results suggest that reduced *de novo* lipogenesis might be a contributor to decreased liver fat accumulation. Because SREBP1c activation is driven by insulin, these findings further support the claim that CD47 deficient mice have increased insulin sensitivity due to the reduction in plasma insulin levels after fasting (data not shown).

As expected with a reduction in lipid accumulation, both TSP1 deficient and CD47 deficiency were associated with significant protection from hepatic inflammation under HF conditions. Both TSP1 and CD47 have previously been implicated in obesity-associated inflammation and immune cell recruitment into adipose tissue as a result of HF diet challenge (128, 144, 156). However, the effects of the TSP1-CD47 interaction in diet-induced hepatic inflammation have never been explored. Similar to NAFLD, other disease states such as hepatic ischemia reperfusion injury and liver transplantation models are driven by inflammation (131, 279). Previous reports have linked CD47 deficiency to reduced inflammation in hepatic ischemia/reperfusion models and liver transplantation models (105, 293). Xiao et al. established that CD47 blockade with a monoclonal antibody in a rat liver transplantation model reduced TSP1-mediated expression of several key cytokines (TNF α , IL-1 β , and IL-6) that correlate with liver injury (293). In addition, targeting CD47 with a functional

blocking antibody in steatotic rat livers attenuated ischemia reperfusion injury by suppressing inflammatory responses (292). In alignment with these reports, our *in vivo* studies demonstrated that both TSP1 and CD47 deficiency were associated with a significant attenuation of inflammation in a diet-induced fatty liver model.

Fibrogenesis, or increased collagen deposition within the liver, is a result of activated hepatic stellate cells (HSCs). The presence of fibrosis within the liver is indicative of more severe cases of nonalcoholic steatohepatitis (NASH) and is associated with increased likelihood of developing full blown cirrhosis. HSCs are activated by increased lipid accumulation within hepatocytes and in response to proinflammatory cytokines released by resident immune cells (Kupffer cells) and hepatocytes (289, 295). In our study, the presence of significant collagen deposition in the liver is observed in HF-fed WT mice; however, both TSP1 and CD47 deficiency are associated with downregulated collagen mRNA levels. Most likely, this reduction is secondary to the reduction of lipid accumulation and inflammatory markers observed in the livers of TSP1 and CD47 deficient mice.

Recent studies propose that oxidative stress precedes the onset of NAFLD and drives the development of inflammation, lipid mishandling, and insulin resistance (97). Several mechanisms within the liver may contribute to a deleterious oxidative environment during the development of NAFLD. Our *in vitro* studies utilizing HepG2 cells and primary hepatocytes confirm our *in vivo* findings that TSP1-CD47 contributes to hepatocyte ROS production, yet the mechanism has yet to be determined.

The most common contributor to cytotoxic oxidative stress is mitochondria-derived ROS from compromised substrate oxidation and inability to manage lipid burden (180). In addition, reduced expression and impaired function of antioxidant enzymes augment intracellular oxidative damage (76, 272). Gene expression analysis of downstream targets of Nrf2, a master regulator of antioxidant enzymes, shows no differential regulation in HO-1, GST, or NQO1 (data not shown). This suggests that preservation of antioxidant pathways are not contributing to our reduction in ROS. Interestingly, previous work by Csanyi et al. and Yao et al. demonstrated TSP1 directly activates superoxide production via NADPH oxidases (NOXs) in multiple cell culture models (52, 298); however these effects were presented independent of CD47 activation. In our model, we clearly demonstrated that lack of TSP1 and its receptor, CD47, reduced ROS levels and that acute treatment with TSP1 induced ROS production to levels similar to FFAs which was partially attenuated by a CD47 functional blocking antibody. Our studies are consistent with previous reports presenting TSP1 as a unique, extracellular ligand that may modulate the intracellular oxidative environment. These effects may be through multiple mechanisms - direct activation of oxidative enzymes, such as the NOX family, and through CD47-mediated pathways.

In addition to CD47, CD36 is another receptor for TSP1. It has been shown that uptake of myristic acid via the fatty acid translocase activity of CD36 was inhibited by TSP1 in endothelial cells (104). To further determine whether the effects on ROS production in hepatocytes were specific to CD47, CD47

deficient primary hepatocytes as well as CD36 deficient primary hepatocytes were utilized for *in vitro* studies. Interestingly, we found that both CD47 and CD36 deficiency reduced palmitate-stimulated ROS production, yet only CD47 deficiency protected against TSP1-induced ROS production. Without changes of CD36 levels on CD47 deficient hepatocytes (data not shown), the mechanism of reduced palmitate-stimulated ROS production in CD47 deficient hepatocytes is unknown and warrants further investigation.

In conclusion, our studies suggest a novel role for the TSP1-CD47 interaction in the development of fatty liver-associated oxidative stress. Because hepatic levels of TSP1 and CD47 were elevated under high fat conditions (Figure 4.1, 4.8), we believe TSP1-mediated ROS production through CD47 activation could potentially augment the noxious cellular environment commonly observed in obesity-induced fatty liver models. These findings expand the pathological implications of TSP1-CD47 signaling to include obesity-associated fatty liver disease.

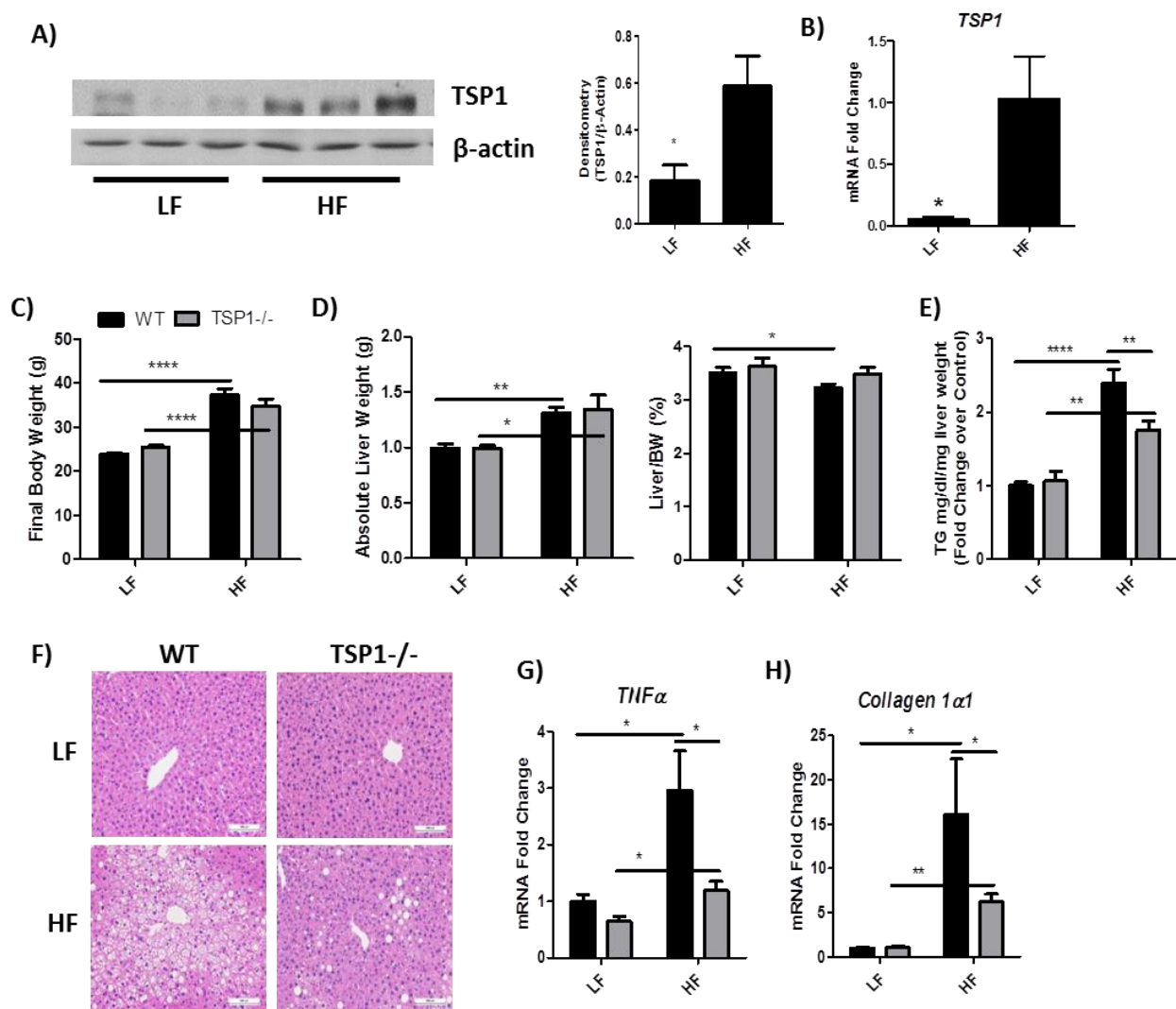
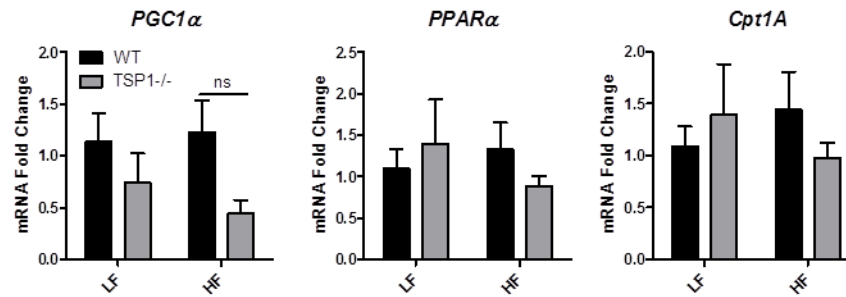


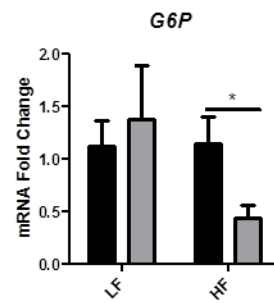
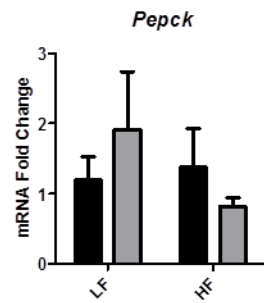
Figure 4.1 Liver phenotype of TSP1 deficient and control mice after 16 week LF/HF diet challenge

WT mice were fed with LF or HF diet for 16 weeks and whole liver tissue TSP1 protein levels (A) and mRNA levels (B) were determined. Body weights (C) and liver weights (D) are presented from WT and TSP1 deficient mice challenged with either LF or HF diet for 16 weeks. Hepatic TG levels were measured by commercial kit (E) and lipid accumulation in the liver was visualized with H&E staining in all four groups of mice (F). Representative images are shown. Scale bars represent 1000 μ m. Gene expression of the proinflammatory cytokine, TNF α , and Collagen 1 α 1 were determined by real-time PCR and the delta CT method (G, H) (n=10-15 mice/group). Data are presented as mean \pm SE, *P<0.05, **P<0.01, ****P<0.0001. LF: low fat; HF: high fat; WT: wildtype; TG: triglyceride

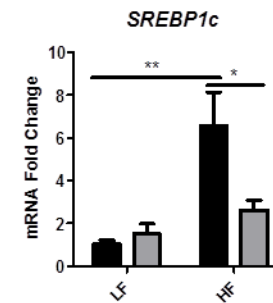
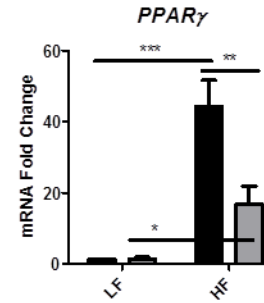
A) Fatty Acid Oxidation



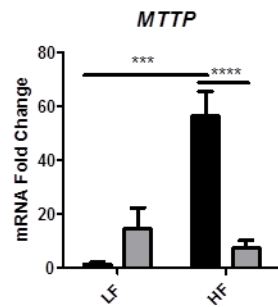
B) Gluconeogenesis



C) Lipogenesis



D) TG Secretion



E) FA Uptake

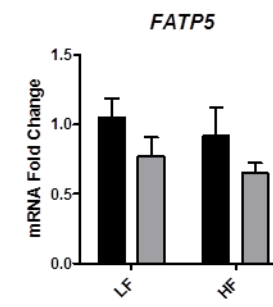
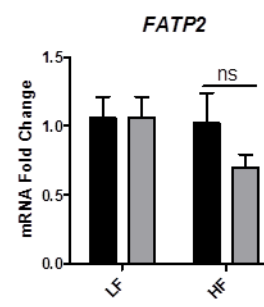
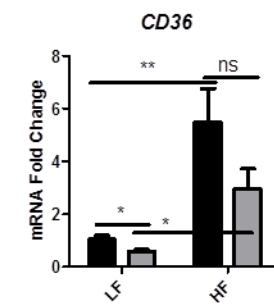


Figure 4.2 Metabolic gene expression in the livers of TSP1 deficient and WT controls after 16 week LF/HF feeding

mRNA levels of genes involved in several hepatic metabolic pathways including fatty acid oxidation (A), gluconeogenesis (B), lipogenesis (C), TG secretion (D), and fatty acid uptake (E) were measured by real-time PCR and the delta Ct method (n=10-15 mice/group). Data are presented as mean \pm SE, *P<0.05, **P<0.01, ***P<0.001, ****P<0.0001. FA: fatty acid; TG: triglyceride.

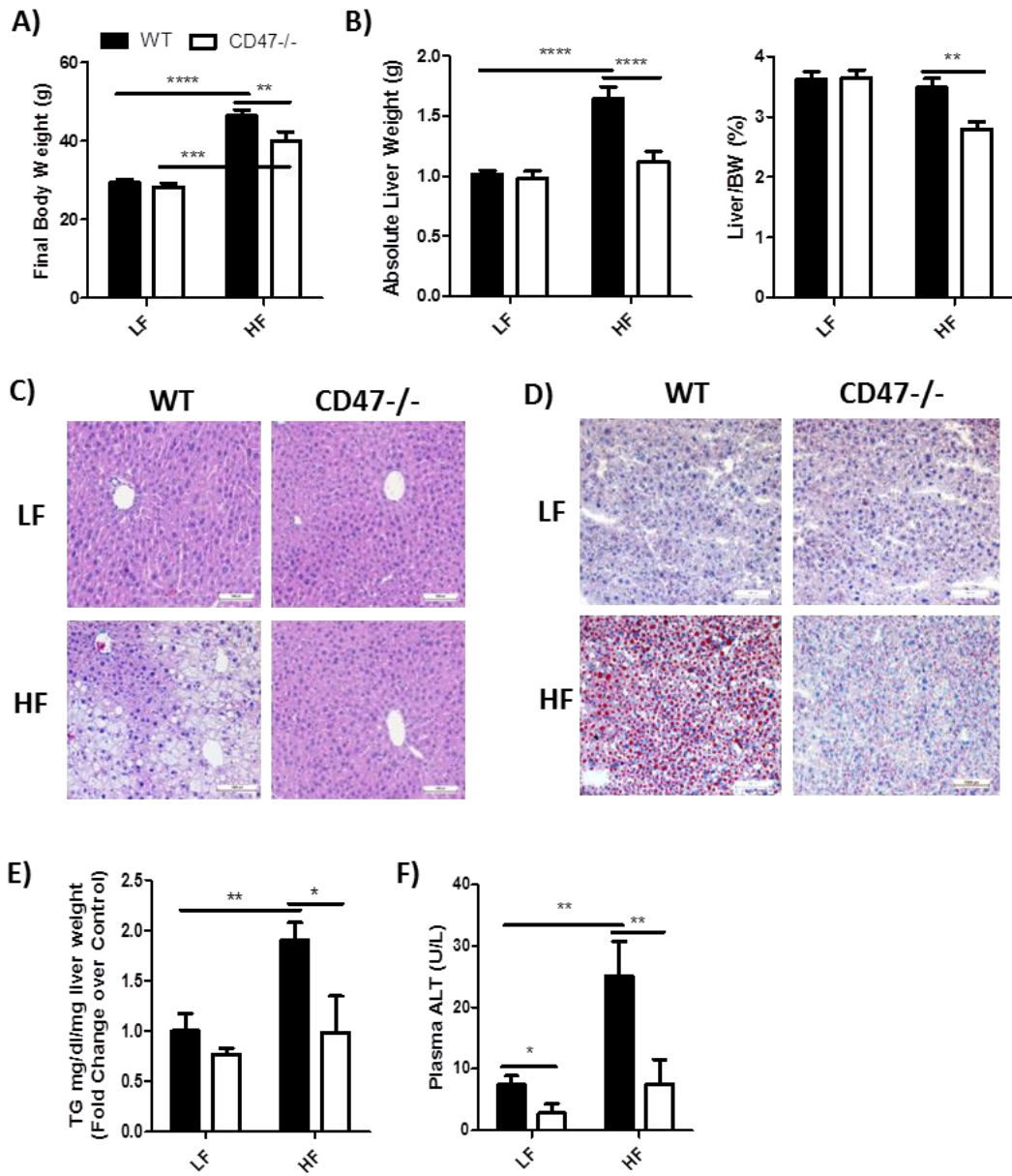


Figure 4.3 Liver phenotype of CD47 deficient and control mice after 16 week LF/HF diet challenge

Body weights (A) and liver weights (B) are presented from WT and CD47 deficient mice challenged with either LF or HF diet for 16 weeks. Lipid accumulation in liver from four groups of mice was visualized by H&E (C) and oil red O staining (D). Representative images are shown. Liver triglyceride levels were quantified (E) and plasma ALT levels were measured by commercial kit as an indicator of hepatic function (F) (n=7-11 mice/group). Scale bars represent 1000µm. Data are presented as mean ± SE, *P<0.05, **P<0.01, ***P<0.001, ****P<0.0001. ALT: alanine aminotransferase; BW: body weight; LF: low fat; HF: high fat; WT: wildtype; TG: triglyceride.

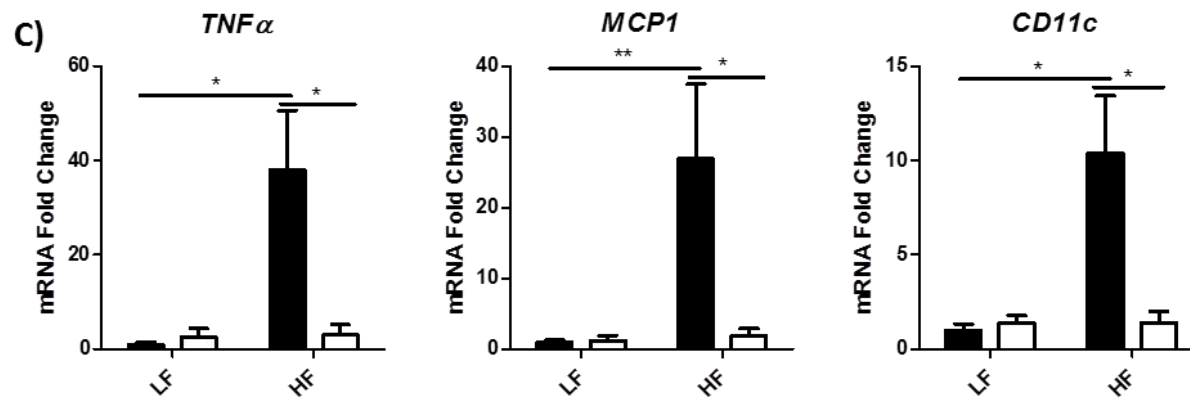
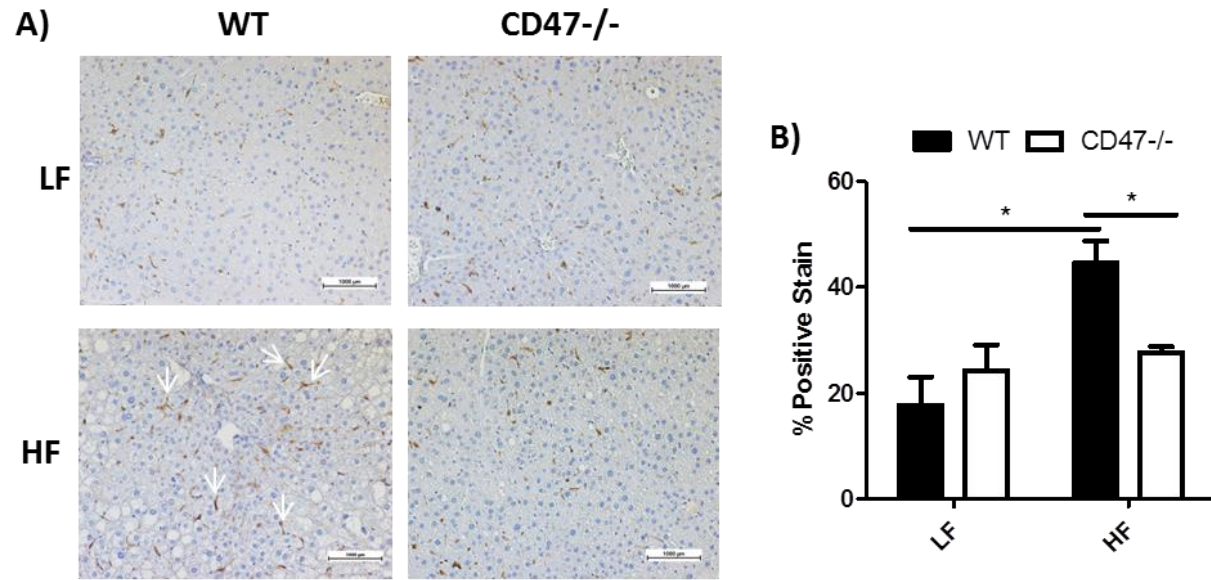


Figure 4.4 Obesity-associated hepatic inflammation

Hepatic macrophage content was determined by anti-F4/80 staining (A). The positive staining is represented by a brown color and indicated by white arrow heads. Representative images for all four groups are shown. Scale bars represent 1000 μ m. The percent of total area positively stained (B) was determined using threshold features of the NIS Elements software by Nikon Instruments. Gene expression for proinflammatory cytokines in the liver (C) was determined by real-time PCR and the delta CT method (n=7-11 mice/group). Data are presented as mean \pm SE, *P<0.05, **P<0.01.

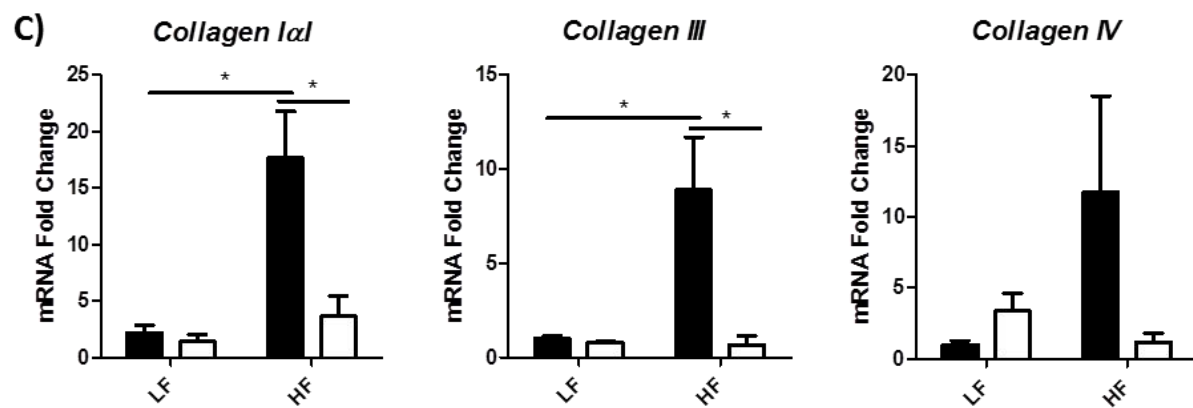
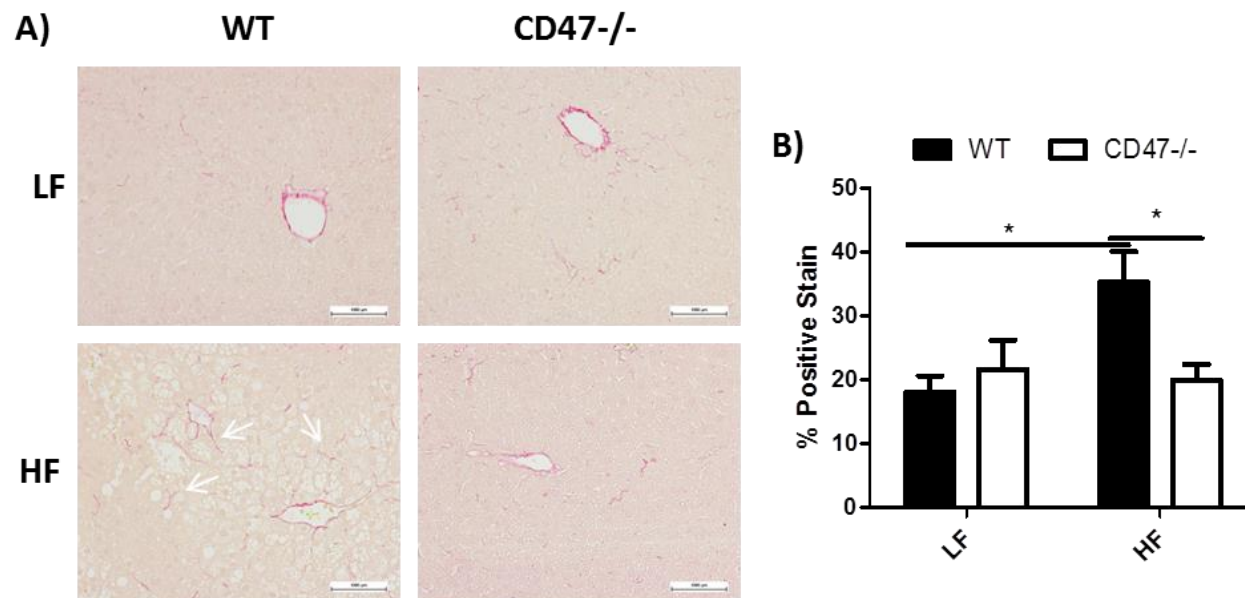
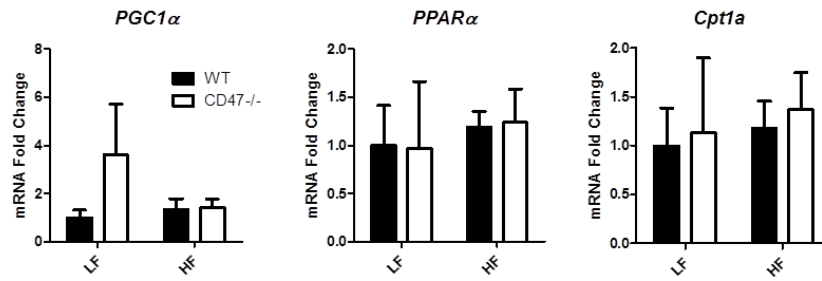


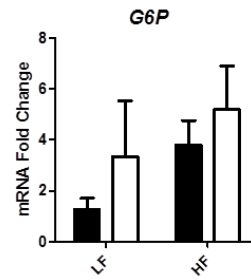
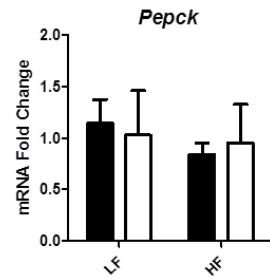
Figure 4.5 Obesity-associated hepatic fibrosis

Collagen deposition in the liver was determined by Sirius red staining (A). The positive stain is represented by a pink color and indicated by white arrow heads. Representative images for all four groups are shown. Scale bars represent 1000 μ m. The percent of total area positively stained (B) was determined using features of the NIS Elements software by Nikon Instruments. Gene expression for collagen (C) in the liver was determined by real-time PCR and the delta CT method (n=7-11 mice/group). Data are presented as mean \pm SE, *P<0.05.

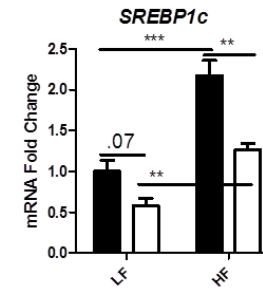
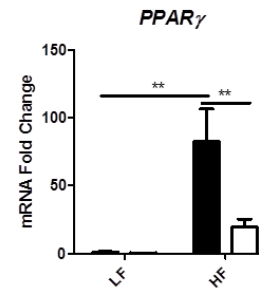
A) Fatty Acid Oxidation



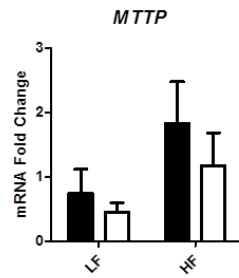
B) Gluconeogenesis



C) Lipogenesis



D) TG Secretion



E) FA Uptake

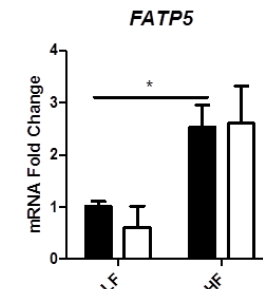
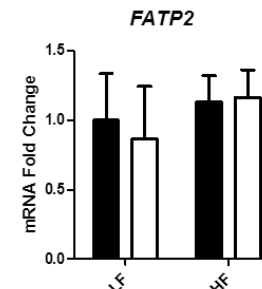
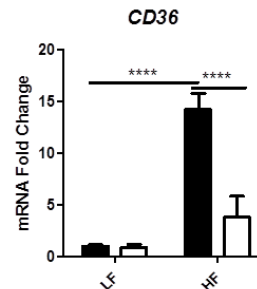


Figure 4.6 Metabolic gene expression in the livers of CD47 deficient and WT controls after 16 week LF/HF feeding

Expression of metabolic genes involved in (A) fatty acid oxidation, (B) gluconeogenesis, (L) lipogenesis, (D) triglyceride secretion, and (E) fatty acid uptake were measured by real-time PCR and the delta Ct method (n=7-11 mice/group). Data are presented as mean + SE, *P<0.05, **P<0.01, ***P<0.001, ****P<0.0001.

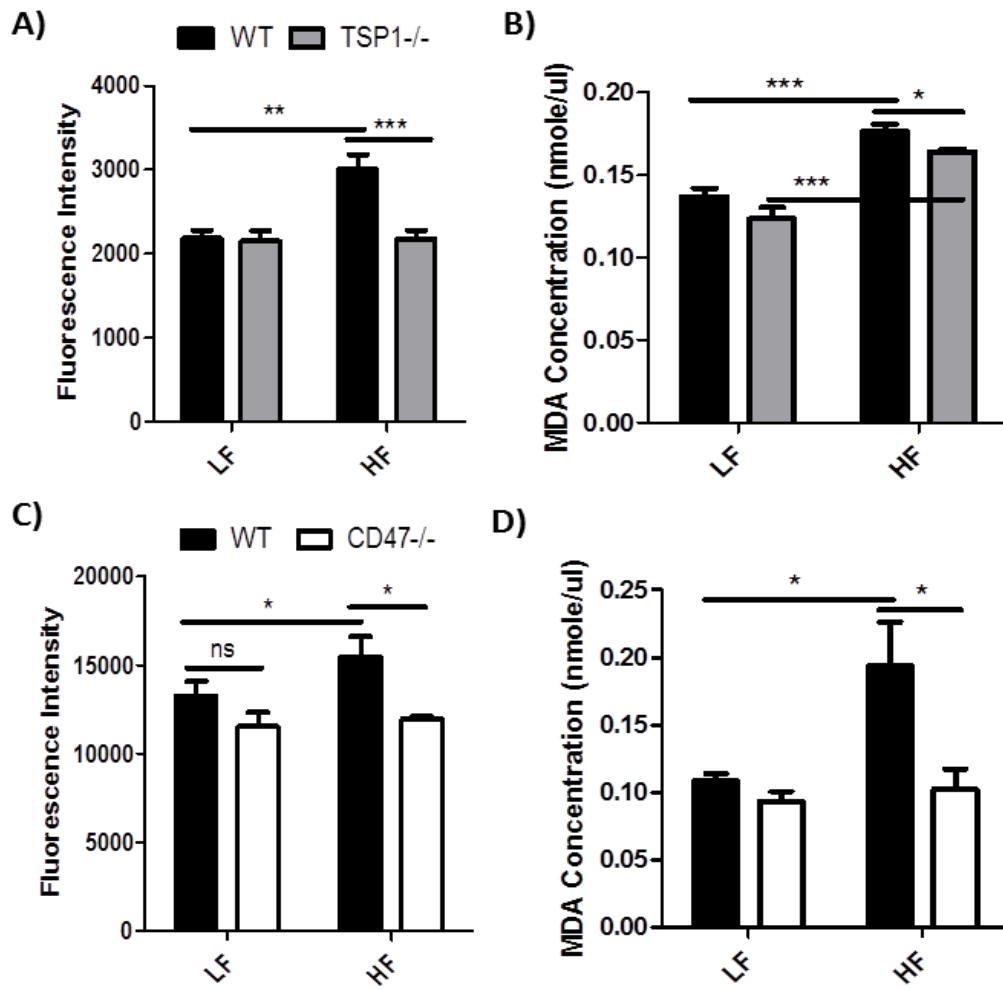


Figure 4.7 Hepatic oxidative stress

ROS was determined by the abundance of DCF and the levels of the lipid peroxidation byproduct, MDA, in whole liver tissue homogenates from both cohorts of mice. HF-fed TSP1 deficient mice (A, B) and CD47 deficient mice (C, D) were protected against the production of ROS and MDA accumulation in whole liver tissue. (n=7-11 mice/group). Data are presented as mean \pm SE, *P<0.05, **P<0.01, ***P<0.001. MDA: malondialdehyde; ns: no significance.

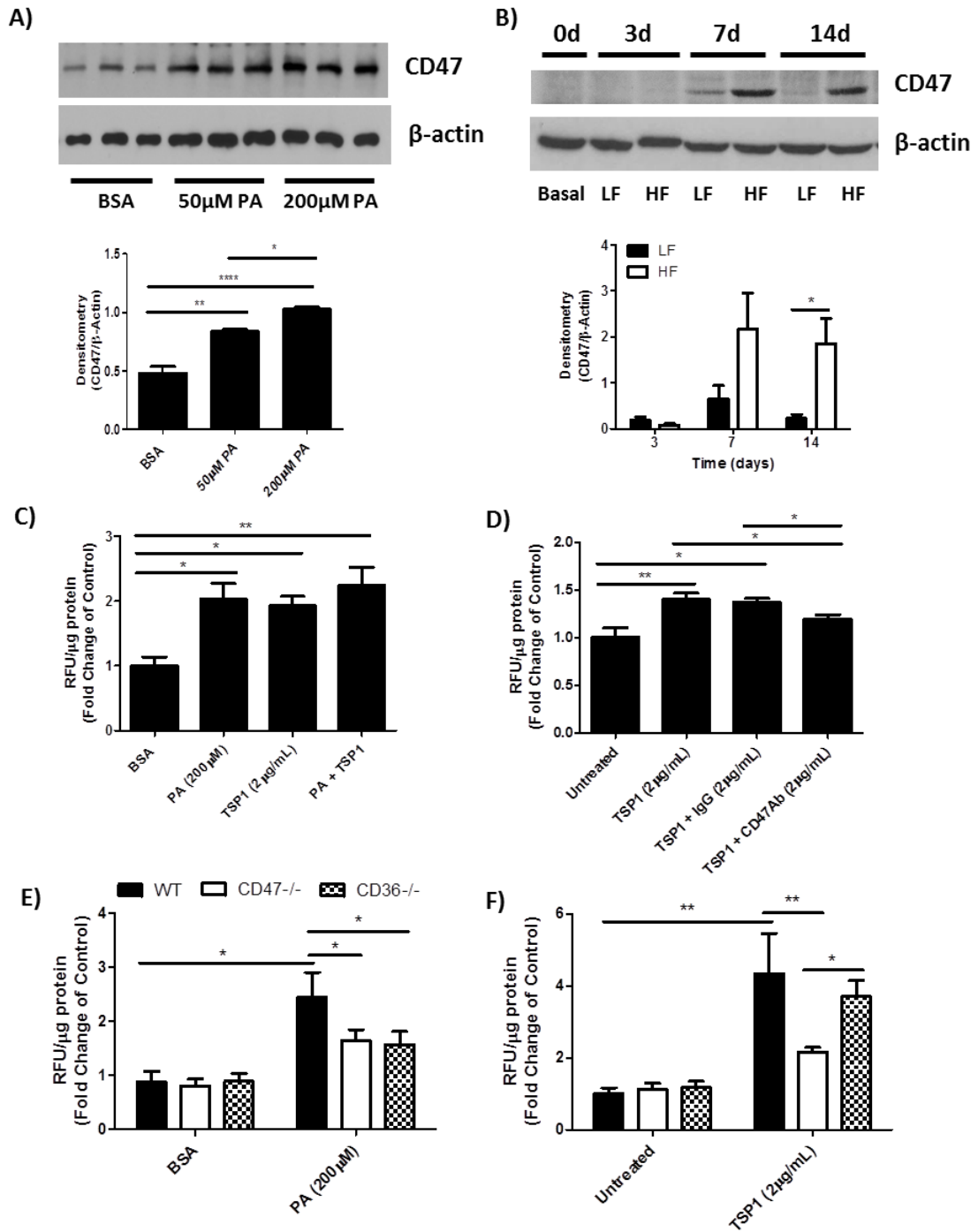


Figure 4.8 FFA and TSP1-induced ROS development in hepatocytes *in vitro*

HepG2 cells were cultured and treated with BSA only, 50 μ M palmitate, or 200 μ M palmitate for 24 hours. CD47 expression in cell lysates was determined by western blotting (A). Wildtype mice were fed with either LF or HF diet for 3, 7, or 14 days and primary hepatocytes were isolated to examine CD47 levels by western blotting (B) (n=3 mice/group). HepG2 cells were seeded at a density of 1x10⁴/well and primary hepatocytes were seeded at a density of 2x10⁴/well of a white, clear-bottom 96-well cell culture plate for ROS quantification. Treatment media for HepG2 cells included serum-free MEM + 0.5% BSA + 1% penicillin-streptomycin to avoid residual TSP1 expression. HepG2 cells were treated with purified TSP1 (2 μ g/mL), BSA, or palmitate (200 μ M) for 6 hours and then DCF in cells was measured by a fluorometric plate reader (C). HepG2 cells were pretreated with either IgG control or a CD47 functional blocking antibody clone B6H12 (2 μ g/mL) for 30 minutes and then treated with purified TSP1 (2 μ g/mL) for 6 additional hours. DCF was measured (D). Treatment media for primary hepatocytes included serum-free Williams Media E + 0.5% BSA + 1% penicillin-streptomycin. Primary hepatocytes isolated from wildtype, CD47^{-/-}, or CD36^{-/-} mice were treated with palmitate (200 μ M) (E) or purified TSP1 (2 μ g/mL) (F) for 6 hours and ROS production indicated by DCF was measured. Data are presented as mean \pm SE (n= 3 experiments), *P<0.05, **P<0.01, ****P<0.0001. Ab; antibody; LF: low fat; HF: high fat; PA: palmitate; BSA: bovine serum albumin; RFU: relative fluorescence unit.

Section 5: GENERAL DISCUSSION

5.1 Summary

Literature suggests that identifying mechanisms that augment inflammation, oxidative stress, and mitochondrial dysfunction in metabolic tissues may be a viable therapeutic target for obesity and its associated complications. The studies included in this dissertation are the first to provide evidence that CD47 may be a novel mechanism contributing to metabolic dysfunction. In addition to its well-established functions, we have demonstrated a unique functional role of CD47 in metabolic tissues including white and brown adipose tissue, skeletal muscle, and the liver, which are exhibited in Figure 5.1. The central hypothesis of these studies is that CD47 contributes to obesity-associated metabolic dysfunctions through diverse mechanisms including inflammation, energy utilization, and TSP1-mediated oxidative stress. Specifically, we hypothesized that lack of CD47 would protect against obesity-associated inflammation, preserve healthy glucose homeostasis, and preserve energy homeostasis despite high fat diet challenge. In addition, we hypothesize that the TSP1-CD47 axis would lead to increased hepatic oxidative stress within a fatty liver model.

In our current studies, CD47 deficiency was consistently associated with a significantly leaner phenotype. Unlike a previous report which suggested that the lean phenotype in CD47 deficient mice under basal conditions was attributed to enhanced skeletal muscle function (74), we saw no change in several genes critical for enhanced mitochondrial respiration in skeletal muscle within a diet-

induced obesity paradigm. This led us to examine other metabolically active tissues.

As described in Section 1, adipose tissue will expand through hypertrophy and hyperplasia to sequester increased lipid burden under obese conditions. Similarly, the liver is highly efficient at storing TG as a mechanism to protect against dyslipidemia. Findings in both aims of this dissertation demonstrate that CD47 deficiency is associated with smaller white adipocyte/adipose tissue depot size, preserved BAT morphology, and reduced hepatic lipid accumulation despite HF diet. It is likely that significantly reduced systemic, hepatic, and adipose tissue inflammation is a result of reduced lipid accumulation and ultimately contributes to the preserved glucose homeostasis and insulin sensitivity demonstrated in CD47 deficient mice after 16 weeks of HF diet challenge.

As demonstrated in Section 3, CD47 deficiency enhanced BAT-dependent energy expenditure through increased UCP1-mediated uncoupling. This specific phenotype may be a result of preserved cGMP/PKG signaling within BAT. Studies with isolated mitochondria confirmed that this increased energy expenditure was driven by FFAs. Together, enhanced white adipose tissue lipolysis perpetuated BAT activation by providing a constant energy source for BAT energy expenditure. From these results, it could be hypothesized that reduced hepatic lipid is also a result of increased peripheral energy needs. It has not been determined whether increased fuel availability drives mitochondrial function in BAT or whether increased energy needs induce rapid lipid turnover in CD47 deficient mice.

Our focus in Section 4 was the contribution of the TSP1-CD47 axis to hepatic oxidative stress under HF conditions. It is difficult to clearly elucidate whether suppressed hepatic ROS production *in vivo* is directly due to TSP1-CD47 or a secondary effect of reduced hepatic lipid accumulation. However, *in vitro* studies clearly show that TSP1 is capable of inducing ROS production in hepatocytes and that blockade of CD47 attenuates this phenomenon. Because these studies were completed in hepatocytes under basal conditions, this supports the idea that TSP1-CD47 regulates hepatocyte oxidative stress independent of obesity. We believe the increased TSP1 and CD47 protein expression in the liver under HF conditions augments ROS production and that these effects may be in conjunction and/or independent of lipid accumulation. In addition, TSP1 deficiency had no effect on body weight/liver weight, whereas CD47 deficiency was associated with a significant reduction in both. However, both models consistently demonstrated improvements in the oxidative environment of the liver, further supporting the idea this mechanism regulates ROS production despite changes in global lipid partitioning. This leads us to conclude that this signaling axis may be a novel mechanism contributing to fatty liver disease-associated oxidative stress.

5.2 TSP1-independent Effects in CD47 Deficient Mice

The justification for our studies using CD47 deficient mice in a diet-induced obesity paradigm was to determine whether this specific cell receptor was facilitating TSP1-mediated metabolic dysfunction under obese conditions. Using the same experimental design for both cohorts of mice, TSP1 deficient and

CD47 deficient mice were protected against obesity-associated complications after 4-month HF diet challenge (100, 128, 144, 156). Several protective phenotypes were shared between the two rodent models; however, some effects were specific to each genotype. These effects are highlighted in Figure 5.2. In both cohorts, mice were protected against obesity-associated inflammation, glucose intolerance, and hepatosteatosis (144, 156). Interestingly, the development of diet-induced obesity was not consistent between studies. TSP1 deficient mice were obese and metabolically healthy, whereas CD47 deficient mice were resistant to obesity development which was attributed to enhanced BAT-mediated energy expenditure. This suggests TSP1-independent effects in CD47 deficient mice contribute to the observed phenotypes when challenged with HF diet. Further studies are warranted to identify novel extracellular ligands or lateral associations/cell receptor complexes for CD47 that may regulate the development of obesity and energy expenditure.

5.3 Differential Effects of CD47 Deficiency on Metabolic Tissues

The effects of CD47 deficiency on metabolic tissues under obese conditions is clearly illustrated in Figure 5.1. Although there seems to be a link between CD47 deficiency and increased mitochondrial biogenesis in liver, muscle, and adipose tissues, metabolic function is altered in a tissue-specific manner in the absence of CD47. For example, CD47 deficiency enhances FFA-mediated uncoupling and energy expenditure in BAT; however, the same effects are not observed in WAT. While the studies included in this dissertation do not define what mechanisms contribute to tissue-specific CD47 function, several

factors have been identified that may contribute to the unique effects of CD47 deficiency in different tissues.

CD47 has been shown to undergo post-transcriptional modifications that may account for varying functions in different metabolic tissues. As a result of alternative splicing, four isoforms (1-4) of CD47 have been established that solely differ by the length of their cytoplasmic tail (147, 212). These isoforms are highly conserved between rodents and humans and vary in length from 3-36 amino acids long. Isoforms 2 and 4 are most commonly observed. Rodent muscle fibers have been shown to express isoforms 1, 2, and 3, while isoforms 2 and 3 are predominantly expressed in the liver (212). To date, specific isoform expression in adipose tissue has not been determined. CD47 may also undergo post-translational modifications as well. Studies have determined that the extracellular N-terminus of CD47 may be highly glycosylated in a tissue-specific manner (28), which would affect the affinity of ligand binding and partner receptor interactions. Tissue-specific isoform expression and structural changes suggest unique functional roles of CD47.

In addition, lateral associations and intramembrane cell receptor complexes including CD47 may differ between cell types. For example, CD47 has been shown to physically associate with the CD14/TLR4 complex in rodent and human macrophages (246) and laterally associates with vascular endothelial growth factor receptor-2 (VEGFR2) in endothelial cells (119). Downstream functions of CD47 activation may be different depending on the lateral associations in various cell types. Finally, varying expression levels of CD47 in

different tissues (Figure 1.4) as well as the concentration of the specific CD47 ligand/binding partner will determine activity levels and function.

5.4 Potential Mechanisms Linking CD47 and Energy Expenditure

5.4.1 cGMP/PKG Signaling and Mitochondrial Function

In the current studies, efforts were made to identify the mechanism contributing to increased mitochondrial number and function in metabolic tissues. It is already well-established that CD47 activation has inhibitory effects on cGMP/PKG signaling in the vasculature (109, 216, 218). These effects are also depicted in Figure 1.4. Now, there are broader implications for cGMP/PKG signaling in metabolic tissues and energy homeostasis. In 2004, Nisoli et al. determined that the NO/cGMP pathway stimulated mitochondrial biogenesis and that reduced eNOS-dependent production of NO in the liver and muscle resulted in reduced mitochondrial area and density (188). Later in 2007, it was determined that inhibiting the degradation of cGMP pharmacologically with the phosphodiesterase-5 inhibitor, sildenafil, enhanced whole body energy expenditure in rodents and protected against diet-induced obesity (10). It was at this time the NO/cGMP signaling cascade was deemed a critical component necessary for systemic regulation of energy and fuel substrate homeostasis through the promotion of mitochondrial biogenesis. Subsequent studies confirmed elevated cGMP/PKG activity is protective against the development of obesity, reduces obesity-associated inflammation, and promotes mitochondrial biogenesis in skeletal muscle (9, 93, 185, 214, 260). Consistent with previous reports (9, 74, 172), CD47 deficiency was associated with increased cGMP/PKG

levels in skeletal muscle basally; however, no differences were observed under HF conditions. This indicates cGMP/PKG-mediated skeletal muscle was not contributing to the protective effects of CD47 deficiency.

Recently, a number of publications have highlighted the role of cGMP/PKG signaling in healthy BAT expansion and energy metabolism. Similar to HF-fed CD47 deficient mice, HF-fed PKG-transgenic mice exhibited significantly smaller adipocytes and elevated mtDNA number in brown adipose tissue and skeletal muscle (172). Haas et al. clearly showed that PKG deficiency blunted brown adipogenesis (90). Further, Balkow et al. demonstrated that cGMP/PKG is necessary for BAT mitochondrial-dependent energy expenditure (14). In our studies, cGMP/PKG levels were reduced in HF-fed WT BAT as expected; however CD47 deficiency was associated with increased levels of cGMP/PKG despite HF diet challenge. This preservation of signaling correlated with enhanced BAT function in CD47 deficient mice. Combining previous studies with our findings, it suggests that impaired cGMP/PKG signaling within BAT could play a causal role in obesity-associated metabolic dysfunction.

5.4.2 Regulation of Mitochondrial Function by c-Myc

Another potential mechanism linking CD47 to increased mitochondrial function is the master regulatory gene, c-Myc. It has been shown that elevated c-Myc expression positively correlates with enhanced mitochondrial function in both hepatocytes and renal cells (143, 302). Interestingly, CD47 deficiency and pharmacological blockade of CD47 significantly upregulate c-Myc expression in a number of cell types (120, 220). Although the focus of these studies was on cell

proliferation and self-renewal, additional studies are necessary to examine whether the regulation of c-Myc expression by CD47 has any implications on mitochondrial density or function in diet-induced obesity models.

5.4.3 BNIP3-dependent Mitochondrial Dysfunction

CD47 has also been shown to modulate intracellular Bcl2/adenovirus E1B 19-kDa interacting protein (BNIP3) activity within the cell (136). Upon activation of CD47 by TSP1, BNIP3 migrates from the cell membrane to the mitochondria and induces mitochondrial dysfunction and subsequent cell death in immune cells (135, 136). Glick et al. demonstrated that BNIP3 is largely expressed in the liver and may be involved in lipid metabolism (83); however, no studies to date have examined the contribution of BNIP3-mediated mitochondrial dysfunction in the liver under obese conditions.

5.5 Role of CD47 in Obesity-associated Inflammation

Although our studies identified a novel role for CD47 in energy homeostasis, CD47 has previously been implicated in inflammatory stress pathways and immune cell migration. The protective phenotype observed in HF-fed CD47 deficient mice could suggest a potential dual function of CD47, regulating both energy homeostasis as well as the inflammatory response to increased lipid burden in obese conditions. Whether these effects on inflammation are secondary to adiposity and lipid deposition has yet to be determined.

5.5.1 TLR4-dependent Mechanisms

It has been confirmed that CD47 is laterally associated with the CD14/toll-like receptor 4 (TLR4) complex in macrophages (246). This specific cell membrane complex is responsible for recognizing pathogens, activating the innate immune system in times of stress through a NF κ B-dependent mechanism, and promoting the secretion of several proinflammatory cytokines/chemokines (153). Recently, reports suggest that in addition to lipopolysaccharide (LPS) recognition, TLR4 can be activated by FFAs in macrophages and adipocytes and may be a novel mechanism linking obesity and inflammation (236, 240). Other groups have shown that TLR4 deficiency and loss-of-function mutations have no conclusive effect on the development of adiposity, yet demonstrate an attenuated inflammatory response in adipose tissue and reduced hepatic dysfunction (158, 236, 251). Additional studies have identified a complex role of CD47 in NF κ B-dependent inflammation. Some groups have shown that the lateral association between CD47 and the CD14/TLR4 complex is necessary for LPS-mediated activation of NF κ B through the canonical TLR4 signaling pathway and that these effects could be independent of TSP1 signaling. It has also been shown that TSP1-mediated activation of CD47 is necessary to stimulate cytokine production in macrophages (246), suggesting that the role of CD47 in inflammation may be tissue and disease condition-specific. In our studies, we determined that whole body CD47 deficiency reduced hepatic, adipose tissue-specific, and circulating levels of proinflammatory cytokines, chemokines, and macrophage markers, including TNF α , MCP1, and CD11c. Knowing many of these genes are

downstream of TLR4 activation, additional studies are necessary to determine whether CD47 expression augments inflammation in the presence of increased FFA so commonly observed in obesity and fatty liver disease.

5.5.2 Activation and Migration of Immune Cells

For several years, it has been widely accepted that CD47 stimulates immune cell activation and chemotaxis. Initially, it was determined that CD47 expression was required for neutrophil transmigration across the endothelial layer into injured tissues (43, 49, 149). Subsequent studies have also shown that T-cell migration into damaged tissues is also mediated by CD47 (11, 160). Not until recently was it shown that CD47 may play a role in stimulating macrophages to secrete proinflammatory cytokines, including IL-1 β (246). Although these studies were not completed in diet-induced obese rodent models, many of these mechanisms are similar to the chronic inflammatory pathways commonly observed in obesity. In addition to macrophage infiltration, T-cell and neutrophil recruitment into adipose tissue have also been shown to perpetuate systemic and adipose tissue-specific inflammation under obese conditions (62, 186).

Previous work from our lab in addition to the studies included in this dissertation show that MCP1/CCR2 dependent recruitment of monocytes to adipose tissue depots is significantly reduced in the absence of both TSP1 (144) and CD47 (Figure 3.3). These findings are similar to the previously mentioned studies that have shown a regulatory function of CD47 in the activation and migration of immune cells in response to stress. Our in vitro migration studies provide evidence to suggest CD47 may contribute to enhanced immune cell

infiltration into adipose tissue and that these effects are independent of the changes in adipocyte physiology. Future studies are critical for discerning whether CD47 is augmenting adipose tissue dysfunction through dual mechanisms – both immune response and alterations in energy storage.

5.5.3 Adipose Tissue Remodeling

A well-established source of inflammation in obesity is from adipose tissue expansion and cellular stress under hypertrophic conditions (252). As adipocytes expand to sequester lipid, stress is placed on the extracellular matrix (ECM). Adipose tissue macrophages (ATMs) respond to this stress by secreting cytokines and chemokines that recruit additional immune cells to the adipose tissue depot (249). Few studies have examined the role of integrins, a molecular link between the cell membrane and extracellular matrix proteins, in the development of obesity. However, some suggest that integrins play a role in the ECM remodeling required for adipocyte hypertrophy (63) and that impaired integrin signaling is protective against diet-induced obesity development through attenuated monocyte recruitment (68).

As a cell membrane protein, CD47 laterally associates with various integrins in a number of cell types including chondrocytes, lymphocytes, microglia, and smooth muscle cells (126, 198, 278, 300). It has even been demonstrated that CD47 expression is necessary for integrin function and integrin-mediated interactions with several ECM structural proteins including fibronectin, vitronectin, and fibrinogen (146). In this case, lack of CD47 expression could impair integrin-mediated expansion of adipose tissue resulting

in smaller adipocytes and a suppressed proinflammatory profile typically associated with obesity. To date, studies examining this interaction under obese conditions have not been completed.

5.6 Study Limitations

5.6.1 Limitations of the Whole-body CD47 Deficient Mouse Model

All *in vivo* studies within Sections 3 and 4 were completed using whole-body CD47 deficient mice on a C57BL/6 background. As mentioned previously, CD47 is ubiquitously expressed throughout the body and regulates a diverse range of functions. When challenged with HF diet, CD47 deficient mice exhibit a number of phenotypes. In order to examine the specific role of CD47 in adipose tissue, inflammatory responses, or hepatic function, cell-specific knockdown of CD47 would be incredibly beneficial to fully elucidate regulatory mechanism. At this time, CD47 floxed mice are not available for cell type-specific knockdown of CD47 via the Cre/LoxP system. An additional model that could be used to examine the translational implications of CD47 *in vivo* includes antisense oligonucleotides (ASOs) targeting highly conserved sequences of CD47 mRNA. Although it has been shown that intraperitoneal injections of ASOs are dispersed systemically, the highest accumulation is observed in the liver (81), providing an alternative to global knockdown of CD47. The use of CD47-targeted oligomers has been previously implemented in rodent ischemia/reperfusion, transplantation, and radiation models.

In culture, ASOs and RNA interference mechanisms can also be used for cellular knockdown of target genes. In addition, other technologies including the

novel CRISPR/Cas system can identify specific DNA sequences and splice genetic elements within target genes. In the current studies, primary cells isolated from CD47 deficient mice (stromal vascular fraction and primary hepatocytes) were used to confirm cell specific functions of CD47 *in vitro*.

5.6.2 Limitations in the Exploration of Additional CD47 Ligands/Interactions

To date, studies have primarily focused on CD47 and its interactions with TSP1 and SIRP α . Our studies examined the TSP1-CD47 interaction in regards to metabolic function; however, evidence suggests our findings related to energy expenditure may be TSP1-independent. When challenged with HF diet for 16 weeks, TSP1 deficient mice exhibit similar adiposity compared with controls (144) whereas CD47 deficient mice are protected from obesity development through enhanced metabolic activity (156). It has been suggested that additional ligands and binding partners could elicit some of the physiological functions observed with CD47 activation. It is well established that other members of the TSP family, including TSP2 and TSP4, have binding capability with CD47 but requires much higher concentrations compared to TSP1 (102). Nevertheless, these interactions have been established yet their tissue-specific functions require additional exploration. Further, it has been proposed that novel ligands could be propagating some of the effects of CD47 activation. Studies examining protein-protein interactions through either yeast two-hybrid screening or affinity purification could be completed to identify any unique interactions with CD47 under obese conditions.

5.6.3 Limitations of the Diet-induced Fatty Liver Disease Model

It is critical that rodent models of NAFLD exhibit similar histology and pathophysiology as fatty liver disease observed in humans. These models should include significant hepatosteatosis, inflammation, and fibrogenesis as well as other peripheral metabolic dysfunctions including obesity, insulin resistance, hyperglycemia, and dyslipidemia (137). Several genetic, nutritional-based, and combinational approaches have been used to study the development and progression of NAFLD and more severe NASH (6). In our studies examining the effects of CD47 deficiency on the development of NAFLD, we utilized a HF (60% kcal from fat) diet-induced fatty liver model. In rodents, HF diet is sufficient to induce obesity, insulin resistance, hepatosteatosis, and other severe comorbidities of NAFLD including fibrosis and necrosis. However, results are highly variable depending on the rodent strain and differing fat compositions found in commonly used HF diets. With this model, long-term dietary interventions are necessary to elicit severe NASH progression.

An alternative to HF diet-induced fatty liver is the Amylin (AMLN) liver NASH model. This diet is composed of 40% kCal from fat, 22% fructose, and 2% cholesterol – most closely resembling the composition of a westernized diet high in fat and added sugar. After ≥ 20 weeks of dietary intervention, severe NAFLD and progression to NASH is observed in rodents (46). Although mice on this diet gain weight, it is not significant or considered obese as demonstrated by 20 or more weeks of HF-diet intervention only. In order to study fibrosis or progression

from NASH to cirrhosis, many believe this rodent model serves as the best histological and pathological representation of fatty liver disease in humans.

Another common model of NAFLD/NASH in rodents uses the methionine/choline deficient (MCD) diet, which impairs hepatic fatty acid oxidation and reduces VLDL secretion resulting in severe steatosis after just 4-10 weeks of dietary intervention (6, 299). In addition, inflammation, oxidative stress, mitochondrial dysfunction, and fibrosis are much more severe in MCD-fed rodents compared to HF-fed models (79); however, this intervention does not mimic the peripheral metabolic dysfunction observed in HF-fed mice (257). On the contrary, mice challenged with MCD diet for greater than 4-6 weeks exhibit significant reductions in body weight. Future studies should consider the MCD or AMLN diets as a model of NAFLD/NASH development in CD47 deficient mice to separate hepatic lipid accumulation from the global effects on lipid deposition and energy metabolism *in vivo*.

5.7 Future Directions

5.7.1 Effects of CD47 on cAMP Function in Metabolic Tissues

Activated cAMP-dependent protein kinase (PKA) via cAMP directly regulates the rate-limiting step of lipolysis, hormone sensitive lipase (HSL), in both WAT and BAT. This signaling cascade liberates FFAs through hydrolysis of intracellular TG stores by phosphorylating HSL and promoting the remodeling of lipid droplet proteins (132). It has been previously demonstrated that not only cGMP, but also cAMP, levels are elevated in CD47 deficient tissues (106, 297). The current studies propose that elevated cGMP/PKG signaling in brown adipose

tissue and the liver promotes enhanced energy expenditure and non-shivering thermogenesis; however, it is critical to explore the canonical cAMP/PKA pathway. Additional studies examining cAMP signaling in CD47 deficient mice under HF conditions are necessary to determine whether there is dual regulation of secondary messenger signaling in CD47 deficient mice. Further, studies inhibiting PKG and/or PKA are necessary to determine what contribution each pathway has on lipid mobilization and utilization in CD47 deficient tissues. These findings could identify CD47 as a novel regulatory mechanism for secondary messenger signaling in metabolic tissues under obese conditions.

5.7.2 Pharmacological Blockade of CD47 *in vivo*

To support the clinical applications of targeting CD47 in obesity and its associated metabolic complications, *in vivo* studies with wildtype mice treated with a functional blocking antibody for CD47 or vehicle control should be completed. To determine whether impaired CD47 signaling enhances metabolic activity, animals could be treated after HF diet challenge to see whether enhanced energy expenditure reduces adiposity post diet challenge. In addition, mice could be treated simultaneously with HF diet challenge and metabolic parameters could be assessed. These studies could potentially shed light on any off-target effects of monoclonal antibody treatment targeting CD47 *in vivo*.

5.7.3 Determine the Specific Effects of CD47 Expression in Hematopoietic Cells *in vivo*

It has been well characterized that CD47 is ubiquitously expressed throughout the body on insulin-sensitive tissues such as muscle and liver. In HF-

fed whole body CD47 deficient mice, both white and brown adipocyte morphology and function was preserved, suggesting a role for CD47 in regulating adipocytes function and contribution to obesity-associated metabolic dysfunction. However, as previously highlighted in section 5.3.2, immune cells express CD47 and may contribute to inflammatory-specific effects under HF conditions. Therefore, it is necessary to determine whether CD47 deficiency in non-hematopoietic cells, specifically adipocytes, protects mice from HF diet-induced obesity and other metabolic dysfunction *in vivo* by utilizing a bone marrow transplantation approach to generate a chimeric mouse model. These experiments would separate the effects of CD47 expression on energy homeostasis and obesity-associated inflammation in metabolic tissues.

5.8 Clinical Significance

CD47 has been highly investigated as an anti-cancer therapeutic target, because of its accessibility as a cell membrane receptor. Strong evidence suggests that CD47 expression is significantly upregulated on tumor cells ranging from non-Hodgkin lymphoma to acute myeloid leukemia as a protective mechanism to avoid detection and phagocytosis by innate and adapted immune responses (41, 157). Further, CD47 expression has been deemed a prognostic marker in determining clinical outcomes for tumorigenesis. In a more recent study in mice, the downregulation of phagocytic function by macrophages in atherosclerotic lesions was attributed to the upregulation of CD47 expression and activity in the vasculature (127). It has been demonstrated clearly in rodents and non-human primates that functional blocking antibodies targeting CD47 are

capable of triggering a phagocytic response and activating anti-tumor T-cell responses *in vivo* without deleterious off-target effects (41, 148, 157, 264, 286). With such promising results, four clinical trials have begun using monoclonal anti-CD47 antibodies against both solid and hematological malignancies (NCT02678338, NCT02641002, NCT02367196, NCT02663518).

In addition to the promising therapeutic potential of targeting CD47 in cancer patients, our findings suggest an additional clinical implication for CD47. Antagonizing CD47 with a functional blocking antibody may protect against deleterious effects of metabolic dysfunction by preserving mitochondrial health and function in states of overnutrition. Looking at preclinical animal models with anti-CD47 antibodies, body weight is commonly reported as a measure of drug tolerance and off-target effects. In many of these models, no changes in body weight or body composition were reported and claimed as a positive indicator of drug tolerance. From these data, it is very difficult to discern the effects of pharmacological CD47 blockade on body weight and energy expenditure because of differences in species, dosages, length of intervention, and varying disease states and conditions. Preclinical studies are necessary to examine the effects of pharmacological CD47 blockade in a diet-induced obesity model.

There are challenges to expanding the clinical implications of CD47 to metabolic function. First, CD47 is highly expressed in the vasculature including red blood cells, leukocytes, platelets, and endothelial cells. There is risk that administration of functional blocking antibodies for CD47 would accumulate in the circulation and very low levels would reach target tissues requiring highly

concentrated doses or frequent administration. Second, it is feared that hemolytic anemia or rapid clearance of native cells in circulation by phagocytosis would be a result of antagonizing CD47. It has been shown that the SIRP α binding site on CD47 is competitively blocked by commonly used functional blocking antibodies (102). Impaired SIRP α -CD47 signaling reduces the body's innate ability to recognize foreign from native cell types (22) and ultimately could result in a weakened response to infection. Current clinical trials will shed light on these concerns.

5.9 Concluding Remarks

Together, these studies provide evidence to suggest CD47 may augment metabolic dysfunction in a tissue-specific manner and that the pathological roles of CD47 function could expand to include obesity and its associated comorbidities. More broadly, *in vivo* studies demonstrate CD47 deficiency is protective against diet-induced adiposity, reduces systemic inflammation, and preserves glucose homeostasis despite HF diet challenge. Many of these protective effects are driven by enhanced brown adipose tissue-dependent energy expenditure and increased lipid mobilization from white adipose tissue. Subsequent studies also identified a unique role of the TSP1-CD47 axis in non-alcoholic fatty liver disease. Together, this interaction contributes to the poor oxidative environment so commonly observed in fatty liver disease. Future studies should examine whether targeting CD47 with a functional blocking antibody *in vivo* protects against cellular metabolic dysfunction and enhances energy expenditure despite HF diet challenge. Results from these studies

support the clinical application of targeting CD47 in obesity and its associated comorbidities.

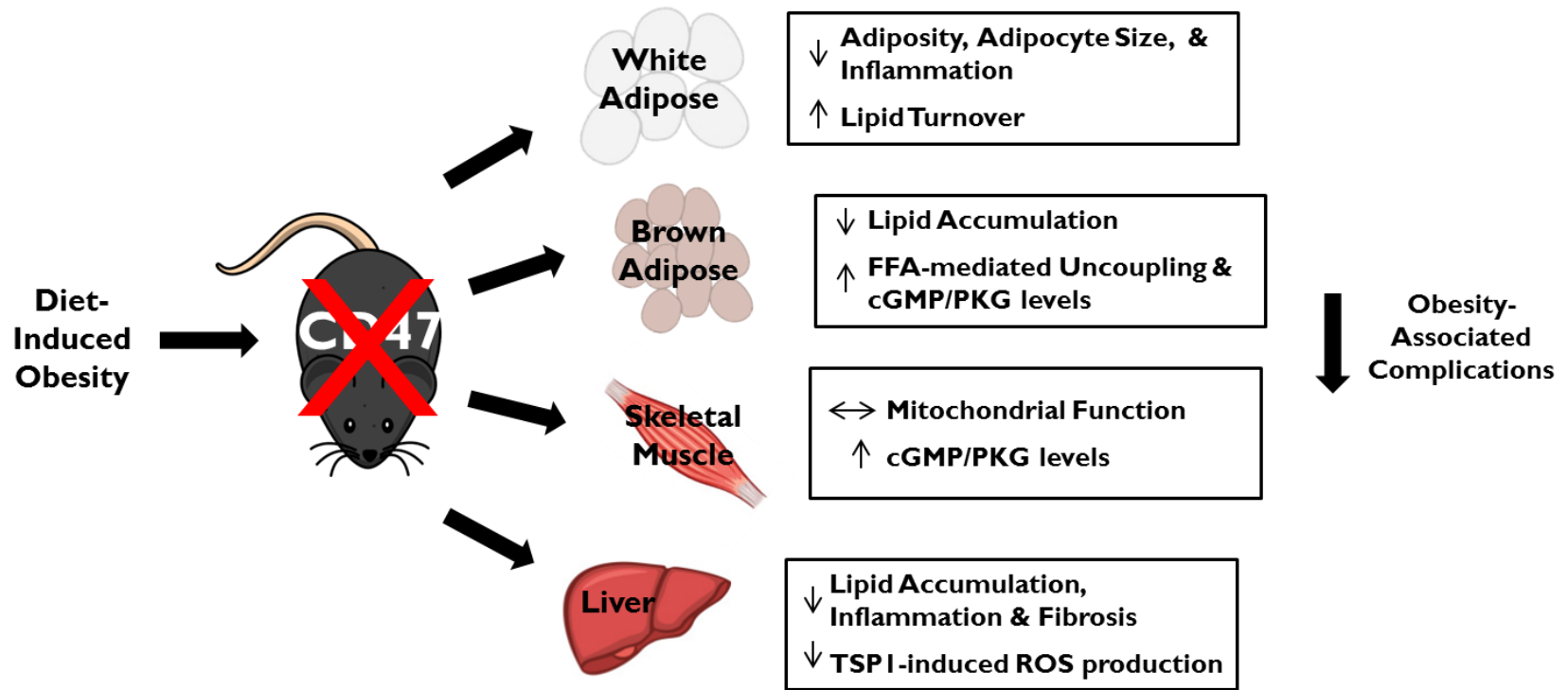


Figure 5.1 Tissue-specific regulatory functions of CD47 in adipose tissues, skeletal muscle, and the liver

Under HF diet conditions, CD47 deficient mice exhibit several protective phenotypes in different metabolic tissues. Together, these effects significantly reduced obesity-associated complications in CD47 deficient mice.

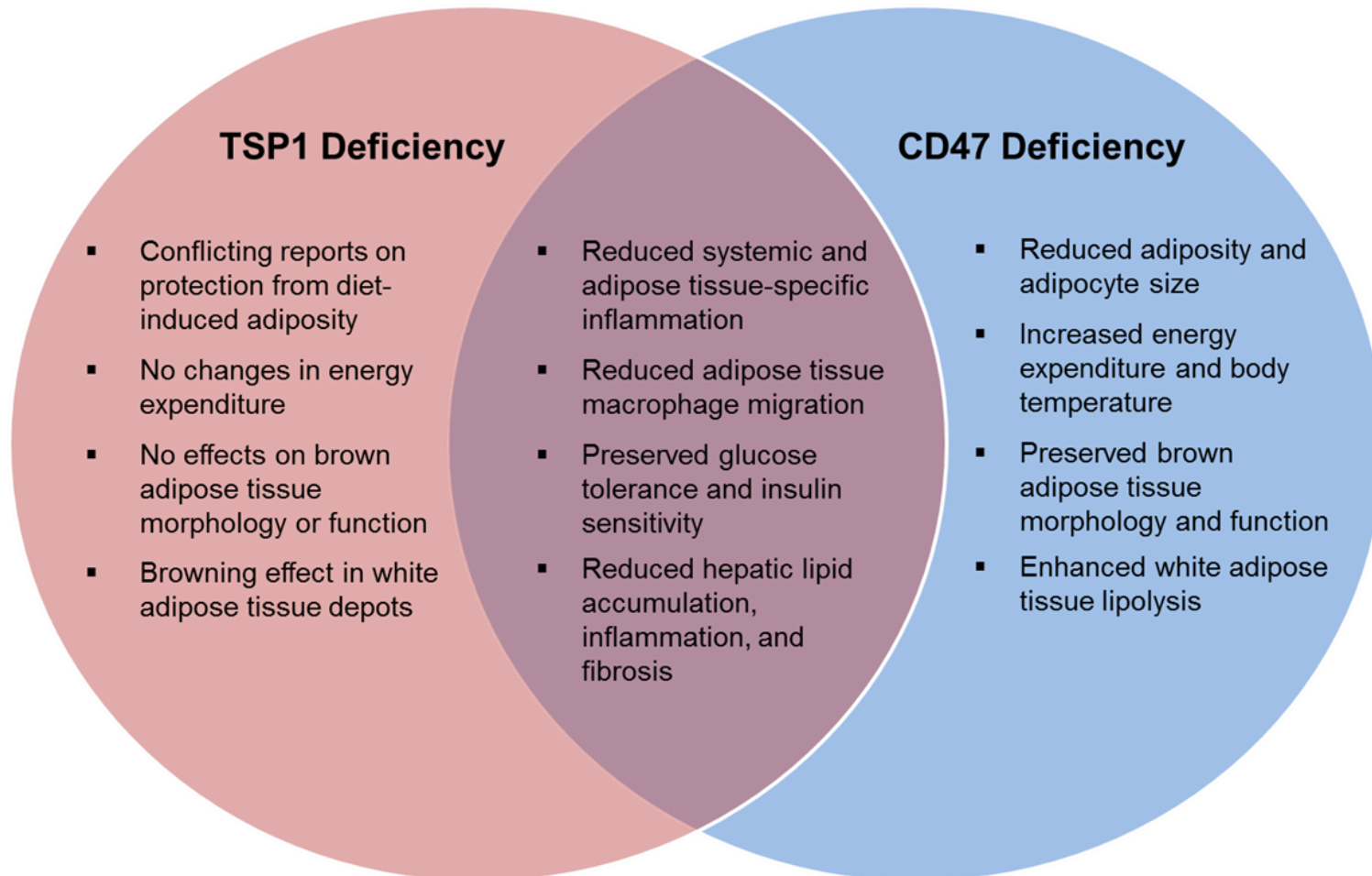


Figure 5.2 Comparison of TSP1 deficient and CD47 deficient mice phenotypes after 16-week HF diet challenge

This Venn diagram compares and contrasts the unique phenotypes between the two cohorts of mice when challenged with HF diet (100, 128, 144, 156). It should be noted that studies conducted with TSP1 deficient mice used different HF diets (45-60% kCal from fat) and diet challenges ranged from 16-20 weeks. With the CD47 deficient mice, the diet was composed of 60% kCal from fat and was administered for 16 weeks.

REFERENCES

1. **Adams JC, and Lawler J.** The thrombospondins. *The international journal of biochemistry & cell biology* 36: 961-968, 2004.
2. **Adams LA, Lymp JF, St Sauver J, Sanderson SO, Lindor KD, Feldstein A, et al.** The natural history of nonalcoholic fatty liver disease: a population-based cohort study. *Gastroenterology* 129: 113-121, 2005.
3. **Adams LA, Waters OR, Knuiaman MW, Elliott RR, and Olynyk JK.** NAFLD as a risk factor for the development of diabetes and the metabolic syndrome: an eleven-year follow-up study. *The American journal of gastroenterology* 104: 861-867, 2009.
4. **Adams S, van der Laan LJ, Vernon-Wilson E, Renardel de Lavalette C, Dopp EA, Dijkstra CD, et al.** Signal-regulatory protein is selectively expressed by myeloid and neuronal cells. *Journal of immunology (Baltimore, Md : 1950)* 161: 1853-1859, 1998.
5. **Alberti KG, Eckel RH, Grundy SM, Zimmet PZ, Cleeman JI, Donato KA, et al.** Harmonizing the metabolic syndrome: a joint interim statement of the International Diabetes Federation Task Force on Epidemiology and Prevention; National Heart, Lung, and Blood Institute; American Heart Association; World Heart Federation; International Atherosclerosis Society; and International Association for the Study of Obesity. *Circulation* 120: 1640-1645, 2009.
6. **Anstee QM, and Goldin RD.** Mouse models in non-alcoholic fatty liver disease and steatohepatitis research. *International journal of experimental pathology* 87: 1-16, 2006.

7. **Anstee QM, Targher G, and Day CP.** Progression of NAFLD to diabetes mellitus, cardiovascular disease or cirrhosis. *Nature reviews Gastroenterology & hepatology* 10: 330-344, 2013.
8. **Araki T, Yamada M, Ohnishi H, Sano SI, and Hatanaka H.** BIT/SHPS-1 enhances brain-derived neurotrophic factor-promoted neuronal survival in cultured cerebral cortical neurons. *Journal of neurochemistry* 75: 1502-1510, 2000.
9. **Ashmore T, Roberts LD, Morash AJ, Kotwica AO, Finnerty J, West JA, et al.** Nitrate enhances skeletal muscle fatty acid oxidation via a nitric oxide-cGMP-PPAR-mediated mechanism. *BMC biology* 13: 110, 2015.
10. **Ayala JE, Bracy DP, Julien BM, Rottman JN, Fueger PT, and Wasserman DH.** Chronic treatment with sildenafil improves energy balance and insulin action in high fat-fed conscious mice. *Diabetes* 56: 1025-1033, 2007.
11. **Azcutia V, Stefanidakis M, Tsuboi N, Mayadas T, Croce KJ, Fukuda D, et al.** Endothelial CD47 promotes vascular endothelial-cadherin tyrosine phosphorylation and participates in T cell recruitment at sites of inflammation in vivo. *Journal of immunology (Baltimore, Md : 1950)* 189: 2553-2562, 2012.
12. **Babusik P, Bilal M, and Duris I.** Nonalcoholic fatty liver disease of two ethnic groups in Kuwait: comparison of prevalence and risk factors. *Medical principles and practice : international journal of the Kuwait University, Health Science Centre* 21: 56-62, 2012.

13. **Baenziger NL, Brodie GN, and Majerus PW.** A thrombin-sensitive protein of human platelet membranes. *Proceedings of the National Academy of Sciences of the United States of America* 68: 240-243, 1971.
14. **Balkow A, Jagow J, Haas B, Siegel F, Kilic A, and Pfeifer A.** A novel crosstalk between Alk7 and cGMP signaling differentially regulates brown adipocyte function. *Molecular metabolism* 4: 576-583, 2015.
15. **Barazi HO, Li Z, Cashel JA, Krutzsch HC, Annis DS, Mosher DF, et al.** Regulation of integrin function by CD47 ligands. Differential effects on alpha vbeta 3 and alpha 4beta1 integrin-mediated adhesion. *The Journal of biological chemistry* 277: 42859-42866, 2002.
16. **Barclay AN, and Van den Berg TK.** The interaction between signal regulatory protein alpha (SIRPalpha) and CD47: structure, function, and therapeutic target. *Annual review of immunology* 32: 25-50, 2014.
17. **Bartelt A, Bruns OT, Reimer R, Hohenberg H, Ittrich H, Peldschus K, et al.** Brown adipose tissue activity controls triglyceride clearance. *Nature medicine* 17: 200-205, 2011.
18. **Bauer EM, Qin Y, Miller TW, Bandle RW, Csanyi G, Pagano PJ, et al.** Thrombospondin-1 supports blood pressure by limiting eNOS activation and endothelial-dependent vasorelaxation. *Cardiovascular research* 88: 471-481, 2010.
19. **Begrache K, Massart J, Robin MA, Bonnet F, and Fromenty B.** Mitochondrial adaptations and dysfunctions in nonalcoholic fatty liver disease. *Hepatology (Baltimore, Md)* 58: 1497-1507, 2013.

20. **Bergman RN, Van Citters GW, Mittelman SD, Dea MK, Hamilton-Wessler M, Kim SP, et al.** Central role of the adipocyte in the metabolic syndrome. *Journal of investigative medicine : the official publication of the American Federation for Clinical Research* 49: 119-126, 2001.
21. **Bhaskaran K, Douglas I, Forbes H, dos-Santos-Silva I, Leon DA, and Smeeth L.** Body-mass index and risk of 22 specific cancers: a population-based cohort study of 5.24 million UK adults. *Lancet (London, England)* 384: 755-765, 2014.
22. **Bian Z, Shi L, Guo YL, Lv Z, Tang C, Niu S, et al.** Cd47-Sirpalpha interaction and IL-10 constrain inflammation-induced macrophage phagocytosis of healthy self-cells. *Proceedings of the National Academy of Sciences of the United States of America* 113: E5434-5443, 2016.
23. **Bjorntorp P.** "Portal" adipose tissue as a generator of risk factors for cardiovascular disease and diabetes. *Arteriosclerosis (Dallas, Tex)* 10: 493-496, 1990.
24. **Bordicchia M, Liu D, Amri EZ, Ailhaud G, Dessi-Fulgheri P, Zhang C, et al.** Cardiac natriuretic peptides act via p38 MAPK to induce the brown fat thermogenic program in mouse and human adipocytes. *The Journal of clinical investigation* 122: 1022-1036, 2012.
25. **Bornstein P.** Thrombospondins as matricellular modulators of cell function. *The Journal of clinical investigation* 107: 929-934, 2001.
26. **Broeders EP, Vijgen GH, Havekes B, Bouvy ND, Mottaghy FM, Kars M, et al.** Thyroid Hormone Activates Brown Adipose Tissue and Increases Non-

Shivering Thermogenesis--A Cohort Study in a Group of Thyroid Carcinoma Patients. *PLoS one* 11: e0145049, 2016.

27. **Brown E, Hooper L, Ho T, and Gresham H.** Integrin-associated protein: a 50-kD plasma membrane antigen physically and functionally associated with integrins. *The Journal of cell biology* 111: 2785-2794, 1990.

28. **Brown EJ, and Frazier WA.** Integrin-associated protein (CD47) and its ligands. *Trends in cell biology* 11: 130-135, 2001.

29. **Browning JD, Szczepaniak LS, Dobbins R, Nuremberg P, Horton JD, Cohen JC, et al.** Prevalence of hepatic steatosis in an urban population in the United States: impact of ethnicity. *Hepatology (Baltimore, Md)* 40: 1387-1395, 2004.

30. **Cannon B, and Nedergaard J.** Brown adipose tissue: function and physiological significance. *Physiological reviews* 84: 277-359, 2004.

31. **Cannon B, and Nedergaard J.** Metabolic consequences of the presence or absence of the thermogenic capacity of brown adipose tissue in mice (and probably in humans). *International journal of obesity (2005)* 34 Suppl 1: S7-16, 2010.

32. **Cannon B, and Nedergaard J.** Studies of thermogenesis and mitochondrial function in adipose tissues. *Methods in molecular biology (Clifton, NJ)* 456: 109-121, 2008.

33. **Carlson CB, Lawler J, and Mosher DF.** Structures of thrombospondins. *Cellular and molecular life sciences : CMLS* 65: 672-686, 2008.

34. **Carmiel-Haggai M, Cederbaum AI, and Nieto N.** A high-fat diet leads to the progression of non-alcoholic fatty liver disease in obese rats. *FASEB journal : official publication of the Federation of American Societies for Experimental Biology* 19: 136-138, 2005.
35. **Casassus P, Fontbonne A, Thibult N, Ducimetiere P, Richard JL, Claude JR, et al.** Upper-body fat distribution: a hyperinsulinemia-independent predictor of coronary heart disease mortality. The Paris Prospective Study. *Arteriosclerosis and thrombosis : a journal of vascular biology / American Heart Association* 12: 1387-1392, 1992.
36. **Casey SC, Tong L, Li Y, Do R, Walz S, Fitzgerald KN, et al.** MYC regulates the antitumor immune response through CD47 and PD-L1. *Science (New York, NY)* 352: 227-231, 2016.
37. **Chalasani N, Younossi Z, Lavine JE, Diehl AM, Brunt EM, Cusi K, et al.** The diagnosis and management of non-alcoholic fatty liver disease: Practice guideline by the American Association for the Study of Liver Diseases, American College of Gastroenterology, and the American Gastroenterological Association. *The American journal of gastroenterology* 107: 811-826, 2012.
38. **Chandrasekaran L, He CZ, Al-Barazi H, Krutzsch HC, Iruela-Arispe ML, and Roberts DD.** Cell contact-dependent activation of alpha3beta1 integrin modulates endothelial cell responses to thrombospondin-1. *Molecular biology of the cell* 11: 2885-2900, 2000.
39. **Chandrasekaran S, Guo NH, Rodrigues RG, Kaiser J, and Roberts DD.** Pro-adhesive and chemotactic activities of thrombospondin-1 for breast

carcinoma cells are mediated by alpha3beta1 integrin and regulated by insulin-like growth factor-1 and CD98. *The Journal of biological chemistry* 274: 11408-11416, 1999.

40. **Chang WT, and Huang AM.** Alpha-Pal/NRF-1 regulates the promoter of the human integrin-associated protein/CD47 gene. *The Journal of biological chemistry* 279: 14542-14550, 2004.

41. **Chao MP, Alizadeh AA, Tang C, Myklebust JH, Varghese B, Gill S, et al.** Anti-CD47 antibody synergizes with rituximab to promote phagocytosis and eradicate non-Hodgkin lymphoma. *Cell* 142: 699-713, 2010.

42. **Chavez RJ, Haney RM, Cuadra RH, Ganguly R, Adapala RK, Thodeti CK, et al.** Upregulation of thrombospondin-1 expression by leptin in vascular smooth muscle cells via JAK2- and MAPK-dependent pathways. *American journal of physiology Cell physiology* 303: C179-191, 2012.

43. **Chin AC, Fournier B, Peatman EJ, Reaves TA, Lee WY, and Parkos CA.** CD47 and TLR-2 cross-talk regulates neutrophil transmigration. *Journal of immunology (Baltimore, Md : 1950)* 183: 5957-5963, 2009.

44. **Chong LW, Hsu YC, Lee TF, Lin Y, Chiu YT, Yang KC, et al.** Fluvastatin attenuates hepatic steatosis-induced fibrogenesis in rats through inhibiting paracrine effect of hepatocyte on hepatic stellate cells. *BMC gastroenterology* 15: 22, 2015.

45. **Cinti S, Mitchell G, Barbatelli G, Murano I, Ceresi E, Faloia E, et al.** Adipocyte death defines macrophage localization and function in adipose tissue of obese mice and humans. *Journal of lipid research* 46: 2347-2355, 2005.

46. **Clapper JR, Hendricks MD, Gu G, Wittmer C, Dolman CS, Herich J, et al.** Diet-induced mouse model of fatty liver disease and nonalcoholic steatohepatitis reflecting clinical disease progression and methods of assessment. *American journal of physiology Gastrointestinal and liver physiology* 305: G483-495, 2013.
47. **Coleman RA, and Lee DP.** Enzymes of triacylglycerol synthesis and their regulation. *Progress in lipid research* 43: 134-176, 2004.
48. **Coleman RA, Lewin TM, and Muoio DM.** Physiological and nutritional regulation of enzymes of triacylglycerol synthesis. *Annual review of nutrition* 20: 77-103, 2000.
49. **Cooper D, Lindberg FP, Gamble JR, Brown EJ, and Vadas MA.** Transendothelial migration of neutrophils involves integrin-associated protein (CD47). *Proceedings of the National Academy of Sciences of the United States of America* 92: 3978-3982, 1995.
50. **Cowie CC, Rust KF, Byrd-Holt DD, Gregg EW, Ford ES, Geiss LS, et al.** Prevalence of diabetes and high risk for diabetes using A1C criteria in the U.S. population in 1988-2006. *Diabetes care* 33: 562-568, 2010.
51. **Crawford SE, Stellmach V, Murphy-Ullrich JE, Ribeiro SM, Lawler J, Hynes RO, et al.** Thrombospondin-1 is a major activator of TGF-beta1 in vivo. *Cell* 93: 1159-1170, 1998.
52. **Csanyi G, Yao M, Rodriguez AI, Al Ghouleh I, Sharifi-Sanjani M, Frazziano G, et al.** Thrombospondin-1 regulates blood flow via CD47 receptor-

mediated activation of NADPH oxidase 1. *Arteriosclerosis, thrombosis, and vascular biology* 32: 2966-2973, 2012.

53. **Cui W, Maimaitiyiming H, Qi X, Norman H, and Wang S.**

Thrombospondin 1 mediates renal dysfunction in a mouse model of high-fat diet-induced obesity. *American journal of physiology Renal physiology* 305: F871-880, 2013.

54. **Cypess AM, Lehman S, Williams G, Tal I, Rodman D, Goldfine AB, et al.** Identification and importance of brown adipose tissue in adult humans. *The New England journal of medicine* 360: 1509-1517, 2009.

55. **Cypess AM, Weiner LS, Roberts-Toler C, Franquet Elia E, Kessler SH, Kahn PA, et al.** Activation of human brown adipose tissue by a beta3-adrenergic receptor agonist. *Cell metabolism* 21: 33-38, 2015.

56. **Daniel C, Wiede J, Krutzsch HC, Ribeiro SM, Roberts DD, Murphy-Ullrich JE, et al.** Thrombospondin-1 is a major activator of TGF-beta in fibrotic renal disease in the rat in vivo. *Kidney international* 65: 459-468, 2004.

57. **Denninger JW, and Marletta MA.** Guanylate cyclase and the .NO/cGMP signaling pathway. *Biochimica et biophysica acta* 1411: 334-350, 1999.

58. **Dentin R, Denechaud PD, Benhamed F, Girard J, and Postic C.** Hepatic gene regulation by glucose and polyunsaturated fatty acids: a role for ChREBP. *The Journal of nutrition* 136: 1145-1149, 2006.

59. **Dong Y, Gao G, Fan H, Li S, Li X, and Liu W.** Activation of the Liver X Receptor by Agonist TO901317 Improves Hepatic Insulin Resistance via

Suppressing Reactive Oxygen Species and JNK Pathway. *PloS one* 10: e0124778, 2015.

60. **Du J, Zhang M, Lu J, Zhang X, Xiong Q, Xu Y, et al.** Osteocalcin improves nonalcoholic fatty liver disease in mice through activation of Nrf2 and inhibition of JNK. *Endocrine* 53: 701-709, 2016.

61. **Ekstedt M, Franzen LE, Mathiesen UL, Thorelius L, Holmqvist M, Bodemar G, et al.** Long-term follow-up of patients with NAFLD and elevated liver enzymes. *Hepatology (Baltimore, Md)* 44: 865-873, 2006.

62. **Elgazar-Carmon V, Rudich A, Hadad N, and Levy R.** Neutrophils transiently infiltrate intra-abdominal fat early in the course of high-fat feeding. *Journal of lipid research* 49: 1894-1903, 2008.

63. **Farnier C, Krief S, Blache M, Diot-Dupuy F, Mory G, Ferre P, et al.** Adipocyte functions are modulated by cell size change: potential involvement of an integrin/ERK signalling pathway. *International journal of obesity and related metabolic disorders : journal of the International Association for the Study of Obesity* 27: 1178-1186, 2003.

64. **Farrell GC, and Larter CZ.** Nonalcoholic fatty liver disease: from steatosis to cirrhosis. *Hepatology (Baltimore, Md)* 43: S99-s112, 2006.

65. **Farrell GC, Teoh NC, and McCuskey RS.** Hepatic microcirculation in fatty liver disease. *Anatomical record (Hoboken, NJ : 2007)* 291: 684-692, 2008.

66. **Farrell GC, Wong VW, and Chitturi S.** NAFLD in Asia--as common and important as in the West. *Nature reviews Gastroenterology & hepatology* 10: 307-318, 2013.

67. **Fedorenko A, Lishko PV, and Kirichok Y.** Mechanism of fatty-acid-dependent UCP1 uncoupling in brown fat mitochondria. *Cell* 151: 400-413, 2012.
68. **Feral CC, Neels JG, Kummer C, Slepak M, Olefsky JM, and Ginsberg MH.** Blockade of alpha4 integrin signaling ameliorates the metabolic consequences of high-fat diet-induced obesity. *Diabetes* 57: 1842-1851, 2008.
69. **Fernandez-Sanchez A, Madrigal-Santillan E, Bautista M, Esquivel-Soto J, Morales-Gonzalez A, Esquivel-Chirino C, et al.** Inflammation, oxidative stress, and obesity. *International journal of molecular sciences* 12: 3117-3132, 2011.
70. **Ferrante AW, Jr.** Obesity-induced inflammation: a metabolic dialogue in the language of inflammation. *Journal of internal medicine* 262: 408-414, 2007.
71. **Fisher FM, Kleiner S, Douris N, Fox EC, Mepani RJ, Verdeguer F, et al.** FGF21 regulates PGC-1alpha and browning of white adipose tissues in adaptive thermogenesis. *Genes & development* 26: 271-281, 2012.
72. **Ford ES, Williamson DF, and Liu S.** Weight change and diabetes incidence: findings from a national cohort of US adults. *American journal of epidemiology* 146: 214-222, 1997.
73. **Fotbolcu H, and Zorlu E.** Nonalcoholic fatty liver disease as a multi-systemic disease. *World journal of gastroenterology* 22: 4079-4090, 2016.
74. **Frazier EP, Isenberg JS, Shiva S, Zhao L, Schlesinger P, Dimitry J, et al.** Age-dependent regulation of skeletal muscle mitochondria by the thrombospondin-1 receptor CD47. *Matrix biology : journal of the International Society for Matrix Biology* 30: 154-161, 2011.

75. **Frazier WA, Gao AG, Dimitry J, Chung J, Brown EJ, Lindberg FP, et al.** The thrombospondin receptor integrin-associated protein (CD47) functionally couples to heterotrimeric Gi. *The Journal of biological chemistry* 274: 8554-8560, 1999.
76. **Furukawa S, Fujita T, Shimabukuro M, Iwaki M, Yamada Y, Nakajima Y, et al.** Increased oxidative stress in obesity and its impact on metabolic syndrome. *The Journal of clinical investigation* 114: 1752-1761, 2004.
77. **Gao AG, Lindberg FP, Dimitry JM, Brown EJ, and Frazier WA.** Thrombospondin modulates alpha v beta 3 function through integrin-associated protein. *The Journal of cell biology* 135: 533-544, 1996.
78. **Gao AG, Lindberg FP, Finn MB, Blystone SD, Brown EJ, and Frazier WA.** Integrin-associated protein is a receptor for the C-terminal domain of thrombospondin. *The Journal of biological chemistry* 271: 21-24, 1996.
79. **Gao D, Wei C, Chen L, Huang J, Yang S, and Diehl AM.** Oxidative DNA damage and DNA repair enzyme expression are inversely related in murine models of fatty liver disease. *American journal of physiology Gastrointestinal and liver physiology* 287: G1070-1077, 2004.
80. **Garcia-Ruiz I, Solis-Munoz P, Fernandez-Moreira D, Munoz-Yague T, and Solis-Herruzo JA.** In vitro treatment of HepG2 cells with saturated fatty acids reproduces mitochondrial dysfunction found in nonalcoholic steatohepatitis. *Disease models & mechanisms* 8: 183-191, 2015.

81. **Geary RS, Norris D, Yu R, and Bennett CF.** Pharmacokinetics, biodistribution and cell uptake of antisense oligonucleotides. *Advanced drug delivery reviews* 87: 46-51, 2015.
82. **Ghoshal K, and Bhattacharyya M.** Adiponectin: Probe of the molecular paradigm associating diabetes and obesity. *World journal of diabetes* 6: 151-166, 2015.
83. **Glick D, Zhang W, Beaton M, Marsboom G, Gruber M, Simon MC, et al.** BNip3 regulates mitochondrial function and lipid metabolism in the liver. *Molecular and cellular biology* 32: 2570-2584, 2012.
84. **Goicoechea S, Orr AW, Pallero MA, Eggleton P, and Murphy-Ullrich JE.** Thrombospondin mediates focal adhesion disassembly through interactions with cell surface calreticulin. *The Journal of biological chemistry* 275: 36358-36368, 2000.
85. **Green JM, Zhelesnyak A, Chung J, Lindberg FP, Sarfati M, Frazier WA, et al.** Role of cholesterol in formation and function of a signaling complex involving alphavbeta3, integrin-associated protein (CD47), and heterotrimeric G proteins. *The Journal of cell biology* 146: 673-682, 1999.
86. **Grundy SM, Benjamin IJ, Burke GL, Chait A, Eckel RH, Howard BV, et al.** Diabetes and cardiovascular disease: a statement for healthcare professionals from the American Heart Association. *Circulation* 100: 1134-1146, 1999.
87. **Guo CA, Kogan S, Amano SU, Wang M, Dagdeviren S, Friedline RH, et al.** CD40 deficiency in mice exacerbates obesity-induced adipose tissue

inflammation, hepatic steatosis, and insulin resistance. *American journal of physiology Endocrinology and metabolism* 304: E951-963, 2013.

88. **Gupta P, Jordan CT, Mitov MI, Butterfield DA, Hilt JZ, and Dziubla TD.**

Controlled curcumin release via conjugation into PBAE nanogels enhances mitochondrial protection against oxidative stress. *International journal of pharmaceutics* 511: 1012-1021, 2016.

89. **Gutierrez DA, Kennedy A, Orr JS, Anderson EK, Webb CD, Gerrald**

WK, et al. Aberrant accumulation of undifferentiated myeloid cells in the adipose tissue of CCR2-deficient mice delays improvements in insulin sensitivity.

Diabetes 60: 2820-2829, 2011.

90. **Haas B, Mayer P, Jennissen K, Scholz D, Berriel Diaz M, Bloch W, et al.**

Protein kinase G controls brown fat cell differentiation and mitochondrial biogenesis. *Science signaling* 2: ra78, 2009.

91. **Halaas JL, Gajiwala KS, Maffei M, Cohen SL, Chait BT, Rabinowitz D,**

et al. Weight-reducing effects of the plasma protein encoded by the obese gene. *Science (New York, NY)* 269: 543-546, 1995.

92. **Han HS, Kang G, Kim JS, Choi BH, and Koo SH.** Regulation of glucose metabolism from a liver-centric perspective. *Experimental & molecular medicine* 48: e218, 2016.

93. **Handa P, Tateya S, Rizzo NO, Cheng AM, Morgan-Stevenson V, Han**

CY, et al. Reduced vascular nitric oxide-cGMP signaling contributes to adipose tissue inflammation during high-fat feeding. *Arteriosclerosis, thrombosis, and vascular biology* 31: 2827-2835, 2011.

94. **Harms M, and Seale P.** Brown and beige fat: development, function and therapeutic potential. *Nature medicine* 19: 1252-1263, 2013.
95. **Hida K, Wada J, Zhang H, Hiragushi K, Tsuchiyama Y, Shikata K, et al.** Identification of genes specifically expressed in the accumulated visceral adipose tissue of OLETF rats. *Journal of lipid research* 41: 1615-1622, 2000.
96. **Hotamisligil GS, Shargill NS, and Spiegelman BM.** Adipose expression of tumor necrosis factor-alpha: direct role in obesity-linked insulin resistance. *Science (New York, NY)* 259: 87-91, 1993.
97. **Houstis N, Rosen ED, and Lander ES.** Reactive oxygen species have a causal role in multiple forms of insulin resistance. *Nature* 440: 944-948, 2006.
98. **Huang AM, Wang HL, Tang YP, and Lee EH.** Expression of integrin-associated protein gene associated with memory formation in rats. *The Journal of neuroscience : the official journal of the Society for Neuroscience* 18: 4305-4313, 1998.
99. **Hubert HB, Feinleib M, McNamara PM, and Castelli WP.** Obesity as an independent risk factor for cardiovascular disease: a 26-year follow-up of participants in the Framingham Heart Study. *Circulation* 67: 968-977, 1983.
100. **Inoue M, Jiang Y, Barnes RH, 2nd, Tokunaga M, Martinez-Santibanez G, Geletka L, et al.** Thrombospondin 1 mediates high-fat diet-induced muscle fibrosis and insulin resistance in male mice. *Endocrinology* 154: 4548-4559, 2013.

101. **Iruela-Arispe ML, Lombardo M, Kruttsch HC, Lawler J, and Roberts DD.** Inhibition of angiogenesis by thrombospondin-1 is mediated by 2 independent regions within the type 1 repeats. *Circulation* 100: 1423-1431, 1999.
102. **Isenberg JS, Annis DS, Pendrak ML, Ptaszynska M, Frazier WA, Mosher DF, et al.** Differential interactions of thrombospondin-1, -2, and -4 with CD47 and effects on cGMP signaling and ischemic injury responses. *The Journal of biological chemistry* 284: 1116-1125, 2009.
103. **Isenberg JS, Frazier WA, Krishna MC, Wink DA, and Roberts DD.** Enhancing cardiovascular dynamics by inhibition of thrombospondin-1/CD47 signaling. *Current drug targets* 9: 833-841, 2008.
104. **Isenberg JS, Jia Y, Fukuyama J, Switzer CH, Wink DA, and Roberts DD.** Thrombospondin-1 inhibits nitric oxide signaling via CD36 by inhibiting myristic acid uptake. *The Journal of biological chemistry* 282: 15404-15415, 2007.
105. **Isenberg JS, Maxhimer JB, Powers P, Tsokos M, Frazier WA, and Roberts DD.** Treatment of liver ischemia-reperfusion injury by limiting thrombospondin-1/CD47 signaling. *Surgery* 144: 752-761, 2008.
106. **Isenberg JS, Qin Y, Maxhimer JB, Sipes JM, Despres D, Schnermann J, et al.** Thrombospondin-1 and CD47 regulate blood pressure and cardiac responses to vasoactive stress. *Matrix biology : journal of the International Society for Matrix Biology* 28: 110-119, 2009.
107. **Isenberg JS, Ridnour LA, Dimitry J, Frazier WA, Wink DA, and Roberts DD.** CD47 is necessary for inhibition of nitric oxide-stimulated vascular cell

responses by thrombospondin-1. *The Journal of biological chemistry* 281: 26069-26080, 2006.

108. **Isenberg JS, Romeo MJ, Yu C, Yu CK, Nghiem K, Monsale J, et al.**

Thrombospondin-1 stimulates platelet aggregation by blocking the antithrombotic activity of nitric oxide/cGMP signaling. *Blood* 111: 613-623, 2008.

109. **Isenberg JS, Shiva S, and Gladwin M.** Thrombospondin-1-CD47 blockade

and exogenous nitrite enhance ischemic tissue survival, blood flow and angiogenesis via coupled NO-cGMP pathway activation. *Nitric oxide : biology and chemistry / official journal of the Nitric Oxide Society* 21: 52-62, 2009.

110. **Jaiswal S, Jamieson CH, Pang WW, Park CY, Chao MP, Majeti R, et al.**

CD47 is upregulated on circulating hematopoietic stem cells and leukemia cells to avoid phagocytosis. *Cell* 138: 271-285, 2009.

111. **Janssen I, Katzmarzyk PT, and Ross R.** Waist circumference and not body mass index explains obesity-related health risk. *The American journal of clinical nutrition* 79: 379-384, 2004.

112. **Ji A, Wroblewski JM, Webb NR, and van der Westhuyzen DR.** Impact of

phospholipid transfer protein on nascent high-density lipoprotein formation and remodeling. *Arteriosclerosis, thrombosis, and vascular biology* 34: 1910-1916, 2014.

113. **Jimenez B, Volpert OV, Crawford SE, Febbraio M, Silverstein RL, and**

Bouck N. Signals leading to apoptosis-dependent inhibition of neovascularization by thrombospondin-1. *Nature medicine* 6: 41-48, 2000.

114. **Joshi-Barve S, Barve SS, Amancherla K, Gobejishvili L, Hill D, Cave M, et al.** Palmitic acid induces production of proinflammatory cytokine interleukin-8 from hepatocytes. *Hepatology (Baltimore, Md)* 46: 823-830, 2007.
115. **Jou J, Choi SS, and Diehl AM.** Mechanisms of disease progression in nonalcoholic fatty liver disease. *Seminars in liver disease* 28: 370-379, 2008.
116. **Kamei N, Tobe K, Suzuki R, Ohsugi M, Watanabe T, Kubota N, et al.** Overexpression of monocyte chemoattractant protein-1 in adipose tissues causes macrophage recruitment and insulin resistance. *The Journal of biological chemistry* 281: 26602-26614, 2006.
117. **Kanda H, Tateya S, Tamori Y, Kotani K, Hiasa K, Kitazawa R, et al.** MCP-1 contributes to macrophage infiltration into adipose tissue, insulin resistance, and hepatic steatosis in obesity. *The Journal of clinical investigation* 116: 1494-1505, 2006.
118. **Kaur S, Kuznetsova SA, Pendrak ML, Sipes JM, Romeo MJ, Li Z, et al.** Heparan sulfate modification of the transmembrane receptor CD47 is necessary for inhibition of T cell receptor signaling by thrombospondin-1. *The Journal of biological chemistry* 286: 14991-15002, 2011.
119. **Kaur S, Martin-Manso G, Pendrak ML, Garfield SH, Isenberg JS, and Roberts DD.** Thrombospondin-1 inhibits VEGF receptor-2 signaling by disrupting its association with CD47. *The Journal of biological chemistry* 285: 38923-38932, 2010.
120. **Kaur S, Soto-Pantoja DR, Stein EV, Liu C, Elkahloun AG, Pendrak ML, et al.** Thrombospondin-1 signaling through CD47 inhibits self-renewal by

regulating c-Myc and other stem cell transcription factors. *Scientific reports* 3: 1673, 2013.

121. **Kawano Y, and Cohen DE.** Mechanisms of hepatic triglyceride accumulation in non-alcoholic fatty liver disease. *Journal of gastroenterology* 48: 434-441, 2013.

122. **Keaney JF, Jr., Larson MG, Vasan RS, Wilson PW, Lipinska I, Corey D, et al.** Obesity and systemic oxidative stress: clinical correlates of oxidative stress in the Framingham Study. *Arteriosclerosis, thrombosis, and vascular biology* 23: 434-439, 2003.

123. **Kelly T, Yang W, Chen CS, Reynolds K, and He J.** Global burden of obesity in 2005 and projections to 2030. *International journal of obesity (2005)* 32: 1431-1437, 2008.

124. **Kim HJ, Miyazaki M, Man WC, and Ntambi JM.** Sterol regulatory element-binding proteins (SREBPs) as regulators of lipid metabolism: polyunsaturated fatty acids oppose cholesterol-mediated induction of SREBP-1 maturation. *Annals of the New York Academy of Sciences* 967: 34-42, 2002.

125. **Kim JK.** Fat uses a TOLL-road to connect inflammation and diabetes. *Cell metabolism* 4: 417-419, 2006.

126. **Koenigsknecht J, and Landreth G.** Microglial phagocytosis of fibrillar beta-amyloid through a beta1 integrin-dependent mechanism. *The Journal of neuroscience : the official journal of the Society for Neuroscience* 24: 9838-9846, 2004.

127. **Kojima Y, Volkmer JP, McKenna K, Civelek M, Lusic AJ, Miller CL, et al.** CD47-blocking antibodies restore phagocytosis and prevent atherosclerosis. *Nature* 536: 86-90, 2016.
128. **Kong P, Gonzalez-Quesada C, Li N, Cavalera M, Lee DW, and Frangogiannis NG.** Thrombospondin-1 regulates adiposity and metabolic dysfunction in diet-induced obesity enhancing adipose inflammation and stimulating adipocyte proliferation. *American journal of physiology Endocrinology and metabolism* 305: E439-450, 2013.
129. **Koonen DP, Jacobs RL, Febbraio M, Young ME, Soltys CL, Ong H, et al.** Increased hepatic CD36 expression contributes to dyslipidemia associated with diet-induced obesity. *Diabetes* 56: 2863-2871, 2007.
130. **Koppaka S, Kehlenbrink S, Carey M, Li W, Sanchez E, Lee DE, et al.** Reduced adipose tissue macrophage content is associated with improved insulin sensitivity in thiazolidinedione-treated diabetic humans. *Diabetes* 62: 1843-1854, 2013.
131. **Kupiec-Weglinski JW, and Busuttil RW.** Ischemia and reperfusion injury in liver transplantation. *Transplantation proceedings* 37: 1653-1656, 2005.
132. **Lafontan M, and Berlan M.** Fat cell adrenergic receptors and the control of white and brown fat cell function. *Journal of lipid research* 34: 1057-1091, 1993.
133. **Lafontan M, Moro C, Berlan M, Crampes F, Sengenès C, and Galitzky J.** Control of lipolysis by natriuretic peptides and cyclic GMP. *Trends in endocrinology and metabolism: TEM* 19: 130-137, 2008.

134. **Lakka HM, Lakka TA, Tuomilehto J, and Salonen JT.** Abdominal obesity is associated with increased risk of acute coronary events in men. *European heart journal* 23: 706-713, 2002.
135. **Lamy L, Foussat A, Brown EJ, Bornstein P, Ticchioni M, and Bernard A.** Interactions between CD47 and thrombospondin reduce inflammation. *Journal of immunology (Baltimore, Md : 1950)* 178: 5930-5939, 2007.
136. **Lamy L, Ticchioni M, Rouquette-Jazdanian AK, Samson M, Deckert M, Greenberg AH, et al.** CD47 and the 19 kDa interacting protein-3 (BNIP3) in T cell apoptosis. *The Journal of biological chemistry* 278: 23915-23921, 2003.
137. **Larter CZ, and Yeh MM.** Animal models of NASH: getting both pathology and metabolic context right. *Journal of gastroenterology and hepatology* 23: 1635-1648, 2008.
138. **Lawler J, Weinstein R, and Hynes RO.** Cell attachment to thrombospondin: the role of ARG-GLY-ASP, calcium, and integrin receptors. *The Journal of cell biology* 107: 2351-2361, 1988.
139. **Lee DH, Han DH, Nam KT, Park JS, Kim SH, Lee M, et al.** Ezetimibe, an NPC1L1 inhibitor, is a potent Nrf2 activator that protects mice from diet-induced nonalcoholic steatohepatitis. *Free radical biology & medicine* 99: 520-532, 2016.
140. **Lee MJ, Wu Y, and Fried SK.** Adipose tissue heterogeneity: implication of depot differences in adipose tissue for obesity complications. *Molecular aspects of medicine* 34: 1-11, 2013.

141. **Lee MJ, Wu Y, and Fried SK.** Adipose tissue remodeling in pathophysiology of obesity. *Current opinion in clinical nutrition and metabolic care* 13: 371-376, 2010.
142. **Lee P, Linderman JD, Smith S, Brychta RJ, Wang J, Idelson C, et al.** Irisin and FGF21 are cold-induced endocrine activators of brown fat function in humans. *Cell metabolism* 19: 302-309, 2014.
143. **Li F, Wang Y, Zeller KI, Potter JJ, Wonsey DR, O'Donnell KA, et al.** Myc stimulates nuclearly encoded mitochondrial genes and mitochondrial biogenesis. *Molecular and cellular biology* 25: 6225-6234, 2005.
144. **Li Y, Tong X, Rumala C, Clemons K, and Wang S.** Thrombospondin1 deficiency reduces obesity-associated inflammation and improves insulin sensitivity in a diet-induced obese mouse model. *PloS one* 6: e26656, 2011.
145. **Liao W, Hui TY, Young SG, and Davis RA.** Blocking microsomal triglyceride transfer protein interferes with apoB secretion without causing retention or stress in the ER. *Journal of lipid research* 44: 978-985, 2003.
146. **Lindberg FP, Gresham HD, Reinhold MI, and Brown EJ.** Integrin-associated protein immunoglobulin domain is necessary for efficient vitronectin bead binding. *The Journal of cell biology* 134: 1313-1322, 1996.
147. **Lindberg FP, Gresham HD, Schwarz E, and Brown EJ.** Molecular cloning of integrin-associated protein: an immunoglobulin family member with multiple membrane-spanning domains implicated in alpha v beta 3-dependent ligand binding. *The Journal of cell biology* 123: 485-496, 1993.

148. **Liu J, Wang L, Zhao F, Tseng S, Narayanan C, Shura L, et al.** Pre-Clinical Development of a Humanized Anti-CD47 Antibody with Anti-Cancer Therapeutic Potential. *PloS one* 10: e0137345, 2015.
149. **Liu Y, Merlin D, Burst SL, Pochet M, Madara JL, and Parkos CA.** The role of CD47 in neutrophil transmigration. Increased rate of migration correlates with increased cell surface expression of CD47. *The Journal of biological chemistry* 276: 40156-40166, 2001.
150. **Liu Z, Morgan S, Ren J, Wang Q, Annis DS, Mosher DF, et al.** Thrombospondin-1 (TSP1) contributes to the development of vascular inflammation by regulating monocytic cell motility in mouse models of abdominal aortic aneurysm. *Circulation research* 117: 129-141, 2015.
151. **Lo J, Lau EY, Ching RH, Cheng BY, Ma MK, Ng IO, et al.** Nuclear factor kappa B-mediated CD47 up-regulation promotes sorafenib resistance and its blockade synergizes the effect of sorafenib in hepatocellular carcinoma in mice. *Hepatology (Baltimore, Md)* 62: 534-545, 2015.
152. **Lopez-Dee Z, Pidcock K, and Gutierrez LS.** Thrombospondin-1: multiple paths to inflammation. *Mediators of inflammation* 2011: 296069, 2011.
153. **Lu YC, Yeh WC, and Ohashi PS.** LPS/TLR4 signal transduction pathway. *Cytokine* 42: 145-151, 2008.
154. **Maier KG, Han X, Sadowitz B, Gentile KL, Middleton FA, and Gahtan V.** Thrombospondin-1: a proatherosclerotic protein augmented by hyperglycemia. *Journal of vascular surgery* 51: 1238-1247, 2010.

155. **Maimaitiyiming H, Clemons K, Zhou Q, Norman H, and Wang S.** Thrombospondin1 deficiency attenuates obesity-associated microvascular complications in ApoE^{-/-} mice. *PLoS one* 10: e0121403, 2015.
156. **Maimaitiyiming H, Norman H, Zhou Q, and Wang S.** CD47 deficiency protects mice from diet-induced obesity and improves whole body glucose tolerance and insulin sensitivity. *Scientific reports* 5: 8846, 2015.
157. **Majeti R, Chao MP, Alizadeh AA, Pang WW, Jaiswal S, Gibbs KD, Jr., et al.** CD47 is an adverse prognostic factor and therapeutic antibody target on human acute myeloid leukemia stem cells. *Cell* 138: 286-299, 2009.
158. **Malhi H, and Gores GJ.** Molecular mechanisms of lipotoxicity in nonalcoholic fatty liver disease. *Seminars in liver disease* 28: 360-369, 2008.
159. **Martin S, and Parton RG.** Lipid droplets: a unified view of a dynamic organelle. *Nature reviews Molecular cell biology* 7: 373-378, 2006.
160. **Matozaki T, Murata Y, Okazawa H, and Ohnishi H.** Functions and molecular mechanisms of the CD47-SIRPalpha signalling pathway. *Trends in cell biology* 19: 72-80, 2009.
161. **Matsubara M, Maruoka S, and Katayose S.** Inverse relationship between plasma adiponectin and leptin concentrations in normal-weight and obese women. *European journal of endocrinology / European Federation of Endocrine Societies* 147: 173-180, 2002.
162. **Matsuo Y, Tanaka M, Yamakage H, Sasaki Y, Muranaka K, Hata H, et al.** Thrombospondin 1 as a novel biological marker of obesity and metabolic syndrome. *Metabolism: clinical and experimental* 64: 1490-1499, 2015.

163. **Matsuzawa-Nagata N, Takamura T, Ando H, Nakamura S, Kurita S, Misu H, et al.** Increased oxidative stress precedes the onset of high-fat diet-induced insulin resistance and obesity. *Metabolism: clinical and experimental* 57: 1071-1077, 2008.
164. **Mawby WJ, Holmes CH, Anstee DJ, Spring FA, and Tanner MJ.** Isolation and characterization of CD47 glycoprotein: a multispanning membrane protein which is the same as integrin-associated protein (IAP) and the ovarian tumour marker OA3. *The Biochemical journal* 304 (Pt 2): 525-530, 1994.
165. **Maxhimer JB, Shih HB, Isenberg JS, Miller TW, and Roberts DD.** Thrombospondin-1/CD47 blockade following ischemia-reperfusion injury is tissue protective. *Plastic and reconstructive surgery* 124: 1880-1889, 2009.
166. **Mei Y, and Thevananther S.** Endothelial nitric oxide synthase is a key mediator of hepatocyte proliferation in response to partial hepatectomy in mice. *Hepatology (Baltimore, Md)* 54: 1777-1789, 2011.
167. **Melichar VO, Behr-Roussel D, Zabel U, Uttenthal LO, Rodrigo J, Rupin A, et al.** Reduced cGMP signaling associated with neointimal proliferation and vascular dysfunction in late-stage atherosclerosis. *Proceedings of the National Academy of Sciences of the United States of America* 101: 16671-16676, 2004.
168. **Mendis S, Davis S, and Norrving B.** Organizational update: the world health organization global status report on noncommunicable diseases 2014; one more landmark step in the combat against stroke and vascular disease. *Stroke; a journal of cerebral circulation* 46: e121-122, 2015.

169. **Mikhailenko I, Krylov D, Argraves KM, Roberts DD, Liao G, and Strickland DK.** Cellular internalization and degradation of thrombospondin-1 is mediated by the amino-terminal heparin binding domain (HBD). High affinity interaction of dimeric HBD with the low density lipoprotein receptor-related protein. *The Journal of biological chemistry* 272: 6784-6791, 1997.
170. **Miller TW, Isenberg JS, Shih HB, Wang Y, and Roberts DD.** Amyloid-beta inhibits No-cGMP signaling in a CD36- and CD47-dependent manner. *PloS one* 5: e15686, 2010.
171. **Mitschke MM, Hoffmann LS, Gnad T, Scholz D, Kruthoff K, Mayer P, et al.** Increased cGMP promotes healthy expansion and browning of white adipose tissue. *FASEB journal : official publication of the Federation of American Societies for Experimental Biology* 27: 1621-1630, 2013.
172. **Miyashita K, Itoh H, Tsujimoto H, Tamura N, Fukunaga Y, Sone M, et al.** Natriuretic peptides/cGMP/cGMP-dependent protein kinase cascades promote muscle mitochondrial biogenesis and prevent obesity. *Diabetes* 58: 2880-2892, 2009.
173. **Miyashita M, Ohnishi H, Okazawa H, Tomonaga H, Hayashi A, Fujimoto TT, et al.** Promotion of neurite and filopodium formation by CD47: roles of integrins, Rac, and Cdc42. *Molecular biology of the cell* 15: 3950-3963, 2004.
174. **Morinaga H, Mayoral R, Heinrichsdorff J, Osborn O, Franck N, Hah N, et al.** Characterization of distinct subpopulations of hepatic macrophages in HFD/obese mice. *Diabetes* 64: 1120-1130, 2015.

175. **Muoio DM, Seefeld K, Witters LA, and Coleman RA.** AMP-activated kinase reciprocally regulates triacylglycerol synthesis and fatty acid oxidation in liver and muscle: evidence that sn-glycerol-3-phosphate acyltransferase is a novel target. *The Biochemical journal* 338 (Pt 3): 783-791, 1999.
176. **Murata Y, Kotani T, Ohnishi H, and Matozaki T.** The CD47-SIRPalpha signalling system: its physiological roles and therapeutic application. *Journal of biochemistry* 155: 335-344, 2014.
177. **Murphy-Ullrich JE, and Iozzo RV.** Thrombospondins in physiology and disease: new tricks for old dogs. *Matrix biology : journal of the International Society for Matrix Biology* 31: 152-154, 2012.
178. **Murphy-Ullrich JE, and Mosher DF.** Interactions of thrombospondin with endothelial cells: receptor-mediated binding and degradation. *The Journal of cell biology* 105: 1603-1611, 1987.
179. **Nadal-Casellas A, Amengual-Cladera E, Proenza AM, Llado I, and Gianotti M.** Long-term high-fat-diet feeding impairs mitochondrial biogenesis in liver of male and female rats. *Cellular physiology and biochemistry : international journal of experimental cellular physiology, biochemistry, and pharmacology* 26: 291-302, 2010.
180. **Nakamura S, Takamura T, Matsuzawa-Nagata N, Takayama H, Misu H, Noda H, et al.** Palmitate induces insulin resistance in H4IIEC3 hepatocytes through reactive oxygen species produced by mitochondria. *The Journal of biological chemistry* 284: 14809-14818, 2009.

181. **Nathan C, and Xie QW.** Nitric oxide synthases: roles, tolls, and controls. *Cell* 78: 915-918, 1994.
182. **Ng M, Fleming T, Robinson M, Thomson B, Graetz N, Margono C, et al.** Global, regional, and national prevalence of overweight and obesity in children and adults during 1980-2013: a systematic analysis for the Global Burden of Disease Study 2013. *Lancet (London, England)* 384: 766-781, 2014.
183. **Nguyen T, Nioi P, and Pickett CB.** The Nrf2-antioxidant response element signaling pathway and its activation by oxidative stress. *The Journal of biological chemistry* 284: 13291-13295, 2009.
184. **Nicholls DG, Bernson VS, and Heaton GM.** The identification of the component in the inner membrane of brown adipose tissue mitochondria responsible for regulating energy dissipation. *Experientia Supplementum* 32: 89-93, 1978.
185. **Nikolic DM, Li Y, Liu S, and Wang S.** Overexpression of constitutively active PKG-I protects female, but not male mice from diet-induced obesity. *Obesity (Silver Spring, Md)* 19: 784-791, 2011.
186. **Nishimura S, Manabe I, Nagasaki M, Eto K, Yamashita H, Ohsugi M, et al.** CD8⁺ effector T cells contribute to macrophage recruitment and adipose tissue inflammation in obesity. *Nature medicine* 15: 914-920, 2009.
187. **Nisoli E, Clementi E, Tonello C, Sciorati C, Briscini L, and Carruba MO.** Effects of nitric oxide on proliferation and differentiation of rat brown adipocytes in primary cultures. *British journal of pharmacology* 125: 888-894, 1998.

188. **Nisoli E, Falcone S, Tonello C, Cozzi V, Palomba L, Fiorani M, et al.** Mitochondrial biogenesis by NO yields functionally active mitochondria in mammals. *Proceedings of the National Academy of Sciences of the United States of America* 101: 16507-16512, 2004.
189. **Nozaki Y, Fujita K, Wada K, Yoneda M, Shinohara Y, Imajo K, et al.** Deficiency of eNOS exacerbates early-stage NAFLD pathogenesis by changing the fat distribution. *BMC gastroenterology* 15: 177, 2015.
190. **Ogden CL, Carroll MD, Kit BK, and Flegal KM.** Prevalence of childhood and adult obesity in the United States, 2011-2012. *Jama* 311: 806-814, 2014.
191. **Oh DY, Morinaga H, Talukdar S, Bae EJ, and Olefsky JM.** Increased macrophage migration into adipose tissue in obese mice. *Diabetes* 61: 346-354, 2012.
192. **Ohlson LO, Larsson B, Svardsudd K, Welin L, Eriksson H, Wilhelmsen L, et al.** The influence of body fat distribution on the incidence of diabetes mellitus. 13.5 years of follow-up of the participants in the study of men born in 1913. *Diabetes* 34: 1055-1058, 1985.
193. **Oldenborg PA.** CD47: A Cell Surface Glycoprotein Which Regulates Multiple Functions of Hematopoietic Cells in Health and Disease. *ISRN hematology* 2013: 614619, 2013.
194. **Oldenborg PA, Gresham HD, and Lindberg FP.** CD47-signal regulatory protein alpha (SIRPalpha) regulates Fcgamma and complement receptor-mediated phagocytosis. *The Journal of experimental medicine* 193: 855-862, 2001.

195. **Oldenborg PA, Zheleznyak A, Fang YF, Lagenaur CF, Gresham HD, and Lindberg FP.** Role of CD47 as a marker of self on red blood cells. *Science (New York, NY)* 288: 2051-2054, 2000.
196. **Oliver E, McGillicuddy F, Phillips C, Toomey S, and Roche HM.** The role of inflammation and macrophage accumulation in the development of obesity-induced type 2 diabetes mellitus and the possible therapeutic effects of long-chain n-3 PUFA. *The Proceedings of the Nutrition Society* 69: 232-243, 2010.
197. **Orava J, Nuutila P, Noponen T, Parkkola R, Viljanen T, Enerback S, et al.** Blunted metabolic responses to cold and insulin stimulation in brown adipose tissue of obese humans. *Obesity (Silver Spring, Md)* 21: 2279-2287, 2013.
198. **Orazizadeh M, Lee HS, Groenendijk B, Sadler SJ, Wright MO, Lindberg FP, et al.** CD47 associates with alpha 5 integrin and regulates responses of human articular chondrocytes to mechanical stimulation in an in vitro model. *Arthritis research & therapy* 10: R4, 2008.
199. **Palmieri VO, Grattagliano I, Portincasa P, and Palasciano G.** Systemic oxidative alterations are associated with visceral adiposity and liver steatosis in patients with metabolic syndrome. *The Journal of nutrition* 136: 3022-3026, 2006.
200. **Pan Y, Wang F, Liu Y, Jiang J, Yang YG, and Wang H.** Studying the mechanism of CD47-SIRPalpha interactions on red blood cells by single molecule force spectroscopy. *Nanoscale* 6: 9951-9954, 2014.

201. **Pelleymounter MA, Cullen MJ, Baker MB, Hecht R, Winters D, Boone T, et al.** Effects of the obese gene product on body weight regulation in ob/ob mice. *Science (New York, NY)* 269: 540-543, 1995.
202. **Pfeifer A, Kilic A, and Hoffmann LS.** Regulation of metabolism by cGMP. *Pharmacology & therapeutics* 140: 81-91, 2013.
203. **Poirier P, Giles TD, Bray GA, Hong Y, Stern JS, Pi-Sunyer FX, et al.** Obesity and cardiovascular disease: pathophysiology, evaluation, and effect of weight loss: an update of the 1997 American Heart Association Scientific Statement on Obesity and Heart Disease from the Obesity Committee of the Council on Nutrition, Physical Activity, and Metabolism. *Circulation* 113: 898-918, 2006.
204. **Qian SW, Tang Y, Li X, Liu Y, Zhang YY, Huang HY, et al.** BMP4-mediated brown fat-like changes in white adipose tissue alter glucose and energy homeostasis. *Proceedings of the National Academy of Sciences of the United States of America* 110: E798-807, 2013.
205. **Qu LL, Yu B, Li Z, Jiang WX, Jiang JD, and Kong WJ.** Gastrodin Ameliorates Oxidative Stress and Proinflammatory Response in Nonalcoholic Fatty Liver Disease through the AMPK/Nrf2 Pathway. *Phytotherapy research : PTR* 30: 402-411, 2016.
206. **Racanelli V, and Rehermann B.** The liver as an immunological organ. *Hepatology (Baltimore, Md)* 43: S54-62, 2006.
207. **Ramanathan S, Mazzalupo S, Boitano S, and Montfort WR.** Thrombospondin-1 and angiotensin II inhibit soluble guanylyl cyclase through an

increase in intracellular calcium concentration. *Biochemistry* 50: 7787-7799, 2011.

208. **Randle PJ, Garland PB, Hales CN, and Newsholme EA.** The glucose fatty-acid cycle. Its role in insulin sensitivity and the metabolic disturbances of diabetes mellitus. *Lancet (London, England)* 1: 785-789, 1963.

209. **Ratziu V, Bellentani S, Cortez-Pinto H, Day C, and Marchesini G.** A position statement on NAFLD/NASH based on the EASL 2009 special conference. *Journal of hepatology* 53: 372-384, 2010.

210. **Rebres RA, Vaz LE, Green JM, and Brown EJ.** Normal ligand binding and signaling by CD47 (integrin-associated protein) requires a long range disulfide bond between the extracellular and membrane-spanning domains. *The Journal of biological chemistry* 276: 34607-34616, 2001.

211. **Rector RS, Thyfault JP, Uptergrove GM, Morris EM, Naples SP, Borengasser SJ, et al.** Mitochondrial dysfunction precedes insulin resistance and hepatic steatosis and contributes to the natural history of non-alcoholic fatty liver disease in an obese rodent model. *Journal of hepatology* 52: 727-736, 2010.

212. **Reinhold MI, Lindberg FP, Plas D, Reynolds S, Peters MG, and Brown EJ.** In vivo expression of alternatively spliced forms of integrin-associated protein (CD47). *Journal of cell science* 108 (Pt 11): 3419-3425, 1995.

213. **Richard D, and Picard F.** Brown fat biology and thermogenesis. *Frontiers in bioscience (Landmark edition)* 16: 1233-1260, 2011.

214. **Rizzo NO, Maloney E, Pham M, Luttrell I, Wessells H, Tateya S, et al.** Reduced NO-cGMP signaling contributes to vascular inflammation and insulin

resistance induced by high-fat feeding. *Arteriosclerosis, thrombosis, and vascular biology* 30: 758-765, 2010.

215. **Roberts-Toler C, O'Neill BT, and Cypess AM.** Diet-induced obesity causes insulin resistance in mouse brown adipose tissue. *Obesity (Silver Spring, Md)* 23: 1765-1770, 2015.

216. **Roberts DD, Miller TW, Rogers NM, Yao M, and Isenberg JS.** The matricellular protein thrombospondin-1 globally regulates cardiovascular function and responses to stress via CD47. *Matrix biology : journal of the International Society for Matrix Biology* 31: 162-169, 2012.

217. **Rogers NM, Seeger F, Garcin ED, Roberts DD, and Isenberg JS.** Regulation of soluble guanylate cyclase by matricellular thrombospondins: implications for blood flow. *Frontiers in physiology* 5: 134, 2014.

218. **Rogers NM, Sharifi-Sanjani M, Csanyi G, Pagano PJ, and Isenberg JS.** Thrombospondin-1 and CD47 regulation of cardiac, pulmonary and vascular responses in health and disease. *Matrix biology : journal of the International Society for Matrix Biology* 37: 92-101, 2014.

219. **Rogers NM, Yao M, Novelli EM, Thomson AW, Roberts DD, and Isenberg JS.** Activated CD47 regulates multiple vascular and stress responses: implications for acute kidney injury and its management. *American journal of physiology Renal physiology* 303: F1117-1125, 2012.

220. **Rogers NM, Zhang ZJ, Wang JJ, Thomson AW, and Isenberg JS.** CD47 regulates renal tubular epithelial cell self-renewal and proliferation following renal ischemia reperfusion. *Kidney international* 90: 334-347, 2016.

221. **Rolo AP, Teodoro JS, and Palmeira CM.** Role of oxidative stress in the pathogenesis of nonalcoholic steatohepatitis. *Free radical biology & medicine* 52: 59-69, 2012.
222. **Rosen ED, and MacDougald OA.** Adipocyte differentiation from the inside out. *Nature reviews Molecular cell biology* 7: 885-896, 2006.
223. **Rosen ED, and Spiegelman BM.** What we talk about when we talk about fat. *Cell* 156: 20-44, 2014.
224. **Rothwell NJ, and Stock MJ.** A role for brown adipose tissue in diet-induced thermogenesis. *Nature* 281: 31-35, 1979.
225. **Ruan H, Miles PD, Ladd CM, Ross K, Golub TR, Olefsky JM, et al.** Profiling gene transcription in vivo reveals adipose tissue as an immediate target of tumor necrosis factor-alpha: implications for insulin resistance. *Diabetes* 51: 3176-3188, 2002.
226. **Saito M, Okamatsu-Ogura Y, Matsushita M, Watanabe K, Yoneshiro T, Nio-Kobayashi J, et al.** High incidence of metabolically active brown adipose tissue in healthy adult humans: effects of cold exposure and adiposity. *Diabetes* 58: 1526-1531, 2009.
227. **Saito M, Yoneshiro T, and Matsushita M.** Activation and recruitment of brown adipose tissue by cold exposure and food ingredients in humans. *Best practice & research Clinical endocrinology & metabolism* 30: 537-547, 2016.
228. **Samuel VT, Liu ZX, Qu X, Elder BD, Bilz S, Befroy D, et al.** Mechanism of hepatic insulin resistance in non-alcoholic fatty liver disease. *The Journal of biological chemistry* 279: 32345-32353, 2004.

229. **Santos VN, Leite-Mor MM, Kondo M, Martins JR, Nader H, Lanzoni VP, et al.** Serum laminin, type IV collagen and hyaluronan as fibrosis markers in non-alcoholic fatty liver disease. *Brazilian journal of medical and biological research = Revista brasileira de pesquisas medicas e biologicas / Sociedade Brasileira de Biofisica [et al]* 38: 747-753, 2005.
230. **Satapati S, Kucejova B, Duarte JA, Fletcher JA, Reynolds L, Sunny NE, et al.** Mitochondrial metabolism mediates oxidative stress and inflammation in fatty liver. *The Journal of clinical investigation* 126: 1605, 2016.
231. **Schattenberg JM, Wang Y, Singh R, Rigoli RM, and Czaja MJ.** Hepatocyte CYP2E1 overexpression and steatohepatitis lead to impaired hepatic insulin signaling. *The Journal of biological chemistry* 280: 9887-9894, 2005.
232. **Schonfeld P, and Wojtczak L.** Short- and medium-chain fatty acids in energy metabolism: the cellular perspective. *Journal of lipid research* 57: 943-954, 2016.
233. **Schreurs M, Kuipers F, and van der Leij FR.** Regulatory enzymes of mitochondrial beta-oxidation as targets for treatment of the metabolic syndrome. *Obesity reviews : an official journal of the International Association for the Study of Obesity* 11: 380-388, 2010.
234. **Seale P, Bjork B, Yang W, Kajimura S, Chin S, Kuang S, et al.** PRDM16 controls a brown fat/skeletal muscle switch. *Nature* 454: 961-967, 2008.
235. **Shen W, Hao J, Feng Z, Tian C, Chen W, Packer L, et al.** Lipoamide or lipoic acid stimulates mitochondrial biogenesis in 3T3-L1 adipocytes via the

endothelial NO synthase-cGMP-protein kinase G signalling pathway. *British journal of pharmacology* 162: 1213-1224, 2011.

236. **Shi H, Kokoeva MV, Inouye K, Tzamei I, Yin H, and Flier JS.** TLR4 links innate immunity and fatty acid-induced insulin resistance. *The Journal of clinical investigation* 116: 3015-3025, 2006.

237. **Shimizu I, Aprahamian T, Kikuchi R, Shimizu A, Papanicolaou KN, MacLauchlan S, et al.** Vascular rarefaction mediates whitening of brown fat in obesity. *The Journal of clinical investigation* 124: 2099-2112, 2014.

238. **Sick E, Jeanne A, Schneider C, Dedieu S, Takeda K, and Martiny L.** CD47 update: a multifaceted actor in the tumour microenvironment of potential therapeutic interest. *British journal of pharmacology* 167: 1415-1430, 2012.

239. **Smadja DM, d'Audigier C, Bieche I, Evrard S, Mauge L, Dias JV, et al.** Thrombospondin-1 is a plasmatic marker of peripheral arterial disease that modulates endothelial progenitor cell angiogenic properties. *Arteriosclerosis, thrombosis, and vascular biology* 31: 551-559, 2011.

240. **Song MJ, Kim KH, Yoon JM, and Kim JB.** Activation of Toll-like receptor 4 is associated with insulin resistance in adipocytes. *Biochemical and biophysical research communications* 346: 739-745, 2006.

241. **Soto-Pantoja DR, Isenberg JS, and Roberts DD.** Therapeutic Targeting of CD47 to Modulate Tissue Responses to Ischemia and Radiation. *Journal of genetic syndrome & gene therapy* 2: 2011.

242. **Soto-Pantoja DR, Kaur S, and Roberts DD.** CD47 signaling pathways controlling cellular differentiation and responses to stress. *Critical reviews in biochemistry and molecular biology* 50: 212-230, 2015.
243. **Spahis S, Delvin E, Borys JM, and Levy E.** Oxidative Stress as a Critical Factor in Nonalcoholic Fatty Liver Disease Pathogenesis. *Antioxidants & redox signaling* 2016.
244. **Stamler JS, and Meissner G.** Physiology of nitric oxide in skeletal muscle. *Physiological reviews* 81: 209-237, 2001.
245. **Stasch JP, and Hobbs AJ.** NO-independent, haem-dependent soluble guanylate cyclase stimulators. *Handbook of experimental pharmacology* 277-308, 2009.
246. **Stein EV, Miller TW, Ivins-O'Keefe K, Kaur S, and Roberts DD.** Secreted Thrombospondin-1 Regulates Macrophage Interleukin-1beta Production and Activation through CD47. *Scientific reports* 6: 19684, 2016.
247. **Stenina OI, Krukovets I, Wang K, Zhou Z, Forudi F, Penn MS, et al.** Increased expression of thrombospondin-1 in vessel wall of diabetic Zucker rat. *Circulation* 107: 3209-3215, 2003.
248. **Stephens JM, Lee J, and Pilch PF.** Tumor necrosis factor-alpha-induced insulin resistance in 3T3-L1 adipocytes is accompanied by a loss of insulin receptor substrate-1 and GLUT4 expression without a loss of insulin receptor-mediated signal transduction. *The Journal of biological chemistry* 272: 971-976, 1997.

249. **Strissel KJ, Stancheva Z, Miyoshi H, Perfield JW, 2nd, DeFuria J, Jick Z, et al.** Adipocyte death, adipose tissue remodeling, and obesity complications. *Diabetes* 56: 2910-2918, 2007.
250. **Subramanian S, Parthasarathy R, Sen S, Boder ET, and Discher DE.** Species- and cell type-specific interactions between CD47 and human SIRPalpha. *Blood* 107: 2548-2556, 2006.
251. **Suganami T, Mieda T, Itoh M, Shimoda Y, Kamei Y, and Ogawa Y.** Attenuation of obesity-induced adipose tissue inflammation in C3H/HeJ mice carrying a Toll-like receptor 4 mutation. *Biochemical and biophysical research communications* 354: 45-49, 2007.
252. **Suganami T, and Ogawa Y.** Adipose tissue macrophages: their role in adipose tissue remodeling. *Journal of leukocyte biology* 88: 33-39, 2010.
253. **Sullivan PG, Dube C, Dorenbos K, Steward O, and Baram TZ.** Mitochondrial uncoupling protein-2 protects the immature brain from excitotoxic neuronal death. *Annals of neurology* 53: 711-717, 2003.
254. **Sullivan PG, Geiger JD, Mattson MP, and Scheff SW.** Dietary supplement creatine protects against traumatic brain injury. *Annals of neurology* 48: 723-729, 2000.
255. **Sullivan PG, Rippey NA, Dorenbos K, Concepcion RC, Agarwal AK, and Rho JM.** The ketogenic diet increases mitochondrial uncoupling protein levels and activity. *Annals of neurology* 55: 576-580, 2004.

256. **Sullivan TJ, Miao Z, Zhao BN, Ertl LS, Wang Y, Krasinski A, et al.** Experimental evidence for the use of CCR2 antagonists in the treatment of type 2 diabetes. *Metabolism: clinical and experimental* 62: 1623-1632, 2013.
257. **Takahashi Y, Soejima Y, and Fukusato T.** Animal models of nonalcoholic fatty liver disease/nonalcoholic steatohepatitis. *World journal of gastroenterology* 18: 2300-2308, 2012.
258. **Taraboletti G, Roberts DD, and Liotta LA.** Thrombospondin-induced tumor cell migration: haptotaxis and chemotaxis are mediated by different molecular domains. *The Journal of cell biology* 105: 2409-2415, 1987.
259. **Targher G, and Byrne CD.** Clinical Review: Nonalcoholic fatty liver disease: a novel cardiometabolic risk factor for type 2 diabetes and its complications. *The Journal of clinical endocrinology and metabolism* 98: 483-495, 2013.
260. **Tateya S, Rizzo NO, Handa P, Cheng AM, Morgan-Stevenson V, Daum G, et al.** Endothelial NO/cGMP/VASP signaling attenuates Kupffer cell activation and hepatic insulin resistance induced by high-fat feeding. *Diabetes* 60: 2792-2801, 2011.
261. **Tchernof A, and Despres JP.** Pathophysiology of human visceral obesity: an update. *Physiological reviews* 93: 359-404, 2013.
262. **Thon M, Hosoi T, and Ozawa K.** Possible Integrative Actions of Leptin and Insulin Signaling in the Hypothalamus Targeting Energy Homeostasis. *Frontiers in endocrinology* 7: 138, 2016.

263. **Tilg H, and Moschen AR.** Evolution of inflammation in nonalcoholic fatty liver disease: the multiple parallel hits hypothesis. *Hepatology (Baltimore, Md)* 52: 1836-1846, 2010.
264. **Tseng D, Volkmer JP, Willingham SB, Contreras-Trujillo H, Fathman JW, Fernhoff NB, et al.** Anti-CD47 antibody-mediated phagocytosis of cancer by macrophages primes an effective antitumor T-cell response. *Proceedings of the National Academy of Sciences of the United States of America* 110: 11103-11108, 2013.
265. **Uysal KT, Wiesbrock SM, Marino MW, and Hotamisligil GS.** Protection from obesity-induced insulin resistance in mice lacking TNF-alpha function. *Nature* 389: 610-614, 1997.
266. **van Beek EM, Cochrane F, Barclay AN, and van den Berg TK.** Signal regulatory proteins in the immune system. *Journal of immunology (Baltimore, Md : 1950)* 175: 7781-7787, 2005.
267. **van Marken Lichtenbelt WD, Vanhommerig JW, Smulders NM, Drossaerts JM, Kemerink GJ, Bouvy ND, et al.** Cold-activated brown adipose tissue in healthy men. *The New England journal of medicine* 360: 1500-1508, 2009.
268. **Varma V, Yao-Borengasser A, Bodles AM, Rasouli N, Phanavanh B, Nolen GT, et al.** Thrombospondin-1 is an adipokine associated with obesity, adipose inflammation, and insulin resistance. *Diabetes* 57: 432-439, 2008.
269. **Verma S, Jensen D, Hart J, and Mohanty SR.** Predictive value of ALT levels for non-alcoholic steatohepatitis (NASH) and advanced fibrosis in non-

alcoholic fatty liver disease (NAFLD). *Liver international : official journal of the International Association for the Study of the Liver* 33: 1398-1405, 2013.

270. **Vernon G, Baranova A, and Younossi ZM.** Systematic review: the epidemiology and natural history of non-alcoholic fatty liver disease and non-alcoholic steatohepatitis in adults. *Alimentary pharmacology & therapeutics* 34: 274-285, 2011.

271. **Videla LA, Rodrigo R, Araya J, and Poniachik J.** Oxidative stress and depletion of hepatic long-chain polyunsaturated fatty acids may contribute to nonalcoholic fatty liver disease. *Free radical biology & medicine* 37: 1499-1507, 2004.

272. **Vincent HK, and Taylor AG.** Biomarkers and potential mechanisms of obesity-induced oxidant stress in humans. *International journal of obesity (2005)* 30: 400-418, 2006.

273. **Virtanen KA, van Marken Lichtenbelt WD, and Nuutila P.** Brown adipose tissue functions in humans. *Biochimica et biophysica acta* 1831: 1004-1008, 2013.

274. **Voros G, and Lijnen HR.** Deficiency of thrombospondin-1 in mice does not affect adipose tissue development. *Journal of thrombosis and haemostasis : JTH* 4: 277-278, 2006.

275. **Wajchenberg BL.** Subcutaneous and visceral adipose tissue: their relation to the metabolic syndrome. *Endocrine reviews* 21: 697-738, 2000.

276. **Wang S, Herndon ME, Ranganathan S, Godyna S, Lawler J, Argraves WS, et al.** Internalization but not binding of thrombospondin-1 to low density

lipoprotein receptor-related protein-1 requires heparan sulfate proteoglycans.

Journal of cellular biochemistry 91: 766-776, 2004.

277. **Wang S, Wu X, Lincoln TM, and Murphy-Ullrich JE.** Expression of constitutively active cGMP-dependent protein kinase prevents glucose stimulation of thrombospondin 1 expression and TGF-beta activity. *Diabetes* 52: 2144-2150, 2003.

278. **Wang XQ, and Frazier WA.** The thrombospondin receptor CD47 (IAP) modulates and associates with alpha2 beta1 integrin in vascular smooth muscle cells. *Molecular biology of the cell* 9: 865-874, 1998.

279. **Weigand K, Brost S, Steinebrunner N, Buchler M, Schemmer P, and Muller M.** Ischemia/Reperfusion injury in liver surgery and transplantation: pathophysiology. *HPB surgery : a world journal of hepatic, pancreatic and biliary surgery* 2012: 176723, 2012.

280. **Weisberg SP, Hunter D, Huber R, Lemieux J, Slaymaker S, Vaddi K, et al.** CCR2 modulates inflammatory and metabolic effects of high-fat feeding. *The Journal of clinical investigation* 116: 115-124, 2006.

281. **Weisberg SP, McCann D, Desai M, Rosenbaum M, Leibel RL, and Ferrante AW, Jr.** Obesity is associated with macrophage accumulation in adipose tissue. *The Journal of clinical investigation* 112: 1796-1808, 2003.

282. **Weyer C, Bogardus C, Mott DM, and Pratley RE.** The natural history of insulin secretory dysfunction and insulin resistance in the pathogenesis of type 2 diabetes mellitus. *The Journal of clinical investigation* 104: 787-794, 1999.

283. **Whitlock G, Lewington S, Sherliker P, Clarke R, Emberson J, Halsey J, et al.** Body-mass index and cause-specific mortality in 900 000 adults: collaborative analyses of 57 prospective studies. *Lancet (London, England)* 373: 1083-1096, 2009.
284. **Whittle AJ, Carobbio S, Martins L, Slawik M, Hondares E, Vazquez MJ, et al.** BMP8B increases brown adipose tissue thermogenesis through both central and peripheral actions. *Cell* 149: 871-885, 2012.
285. **Williamson JR, Kreisberg RA, and Felts PW.** Mechanism for the stimulation of gluconeogenesis by fatty acids in perfused rat liver. *Proceedings of the National Academy of Sciences of the United States of America* 56: 247-254, 1966.
286. **Willingham SB, Volkmer JP, Gentles AJ, Sahoo D, Dalerba P, Mitra SS, et al.** The CD47-signal regulatory protein alpha (SIRP α) interaction is a therapeutic target for human solid tumors. *Proceedings of the National Academy of Sciences of the United States of America* 109: 6662-6667, 2012.
287. **Wilson PW.** Diabetes mellitus and coronary heart disease. *American journal of kidney diseases : the official journal of the National Kidney Foundation* 32: S89-100, 1998.
288. **Wilson PW, D'Agostino RB, Levy D, Belanger AM, Silbershatz H, and Kannel WB.** Prediction of coronary heart disease using risk factor categories. *Circulation* 97: 1837-1847, 1998.

289. **Wobser H, Dorn C, Weiss TS, Amann T, Bollheimer C, Buttner R, et al.** Lipid accumulation in hepatocytes induces fibrogenic activation of hepatic stellate cells. *Cell research* 19: 996-1005, 2009.
290. **World Health Organization.** Obesity and overweight
<http://www.who.int/mediacentre/factsheets/fs311/en/>. 2016].
291. **Wu J, Bostrom P, Sparks LM, Ye L, Choi JH, Giang AH, et al.** Beige adipocytes are a distinct type of thermogenic fat cell in mouse and human. *Cell* 150: 366-376, 2012.
292. **Xiao Z, Banan B, Xu M, Jia J, Manning PT, Hiebsch RR, et al.** Attenuation of Ischemia-Reperfusion Injury and Improvement of Survival in Recipients of Steatotic Rat Livers Using CD47 Monoclonal Antibody. *Transplantation* 100: 1480-1489, 2016.
293. **Xiao ZY, Banan B, Jia J, Manning PT, Hiebsch RR, Gunasekaran M, et al.** CD47 blockade reduces ischemia/reperfusion injury and improves survival in a rat liver transplantation model. *Liver transplantation : official publication of the American Association for the Study of Liver Diseases and the International Liver Transplantation Society* 21: 468-477, 2015.
294. **Xu H, Barnes GT, Yang Q, Tan G, Yang D, Chou CJ, et al.** Chronic inflammation in fat plays a crucial role in the development of obesity-related insulin resistance. *The Journal of clinical investigation* 112: 1821-1830, 2003.
295. **Xu L, Kitade H, Ni Y, and Ota T.** Roles of Chemokines and Chemokine Receptors in Obesity-Associated Insulin Resistance and Nonalcoholic Fatty Liver Disease. *Biomolecules* 5: 1563-1579, 2015.

296. **Yamamoto T, Shimano H, Inoue N, Nakagawa Y, Matsuzaka T, Takahashi A, et al.** Protein kinase A suppresses sterol regulatory element-binding protein-1C expression via phosphorylation of liver X receptor in the liver. *The Journal of biological chemistry* 282: 11687-11695, 2007.
297. **Yao M, Roberts DD, and Isenberg JS.** Thrombospondin-1 inhibition of vascular smooth muscle cell responses occurs via modulation of both cAMP and cGMP. *Pharmacological research : the official journal of the Italian Pharmacological Society* 63: 13-22, 2011.
298. **Yao M, Rogers NM, Csanyi G, Rodriguez AI, Ross MA, St Croix C, et al.** Thrombospondin-1 activation of signal-regulatory protein- α stimulates reactive oxygen species production and promotes renal ischemia reperfusion injury. *Journal of the American Society of Nephrology : JASN* 25: 1171-1186, 2014.
299. **Yao ZM, and Vance DE.** Reduction in VLDL, but not HDL, in plasma of rats deficient in choline. *Biochemistry and cell biology = Biochimie et biologie cellulaire* 68: 552-558, 1990.
300. **Yoshida H, Tomiyama Y, Ishikawa J, Oritani K, Matsumura I, Shiraga M, et al.** Integrin-associated protein/CD47 regulates motile activity in human B-cell lines through CDC42. *Blood* 96: 234-241, 2000.
301. **Zechner R, Zimmermann R, Eichmann TO, Kohlwein SD, Haemmerle G, Lass A, et al.** FAT SIGNALS--lipases and lipolysis in lipid metabolism and signaling. *Cell metabolism* 15: 279-291, 2012.

302. **Zhang H, Gao P, Fukuda R, Kumar G, Krishnamachary B, Zeller KI, et al.** HIF-1 inhibits mitochondrial biogenesis and cellular respiration in VHL-deficient renal cell carcinoma by repression of C-MYC activity. *Cancer cell* 11: 407-420, 2007.
303. **Zhang H, Lu H, Xiang L, Bullen JW, Zhang C, Samanta D, et al.** HIF-1 regulates CD47 expression in breast cancer cells to promote evasion of phagocytosis and maintenance of cancer stem cells. *Proceedings of the National Academy of Sciences of the United States of America* 112: E6215-6223, 2015.
304. **Zhang X, Ji J, Yan G, Wu J, Sun X, Shen J, et al.** Sildenafil promotes adipogenesis through a PKG pathway. *Biochemical and biophysical research communications* 396: 1054-1059, 2010.
305. **Zhang Y, Proenca R, Maffei M, Barone M, Leopold L, and Friedman JM.** Positional cloning of the mouse obese gene and its human homologue. *Nature* 372: 425-432, 1994.
306. **Zhou Y, Poczatek MH, Berecek KH, and Murphy-Ullrich JE.** Thrombospondin 1 mediates angiotensin II induction of TGF-beta activation by cardiac and renal cells under both high and low glucose conditions. *Biochemical and biophysical research communications* 339: 633-641, 2006.
307. **Zraika S, Dunlop M, Proietto J, and Andrikopoulos S.** Effects of free fatty acids on insulin secretion in obesity. *Obesity reviews : an official journal of the International Association for the Study of Obesity* 3: 103-112, 2002.

VITA

Name: Heather Layne Norman-Burgdolf

Place of birth: Madisonville, Kentucky

Educational History

August 2012 – Present	PhD Candidate University of Kentucky, Lexington, Kentucky Dept. of Pharmacology & Nutritional Sciences College of Medicine
May 2011	Bachelor of Science Georgetown College, Georgetown, Kentucky Major: Biological Sciences Minor: Chemistry

Research Experience

January 2013 – Present	University of Kentucky, Lexington, Kentucky Novel Role of CD47 in Obesity-Associated Metabolic Dysfunctions Mentor: Shuxia Wang, MD, PhD Dept. of Pharmacology & Nutritional Sciences
May – July 2010	Georgetown College, Georgetown, Kentucky

Investigation of the early stages of staurosporine-induced apoptosis in multiple cancer cell lines

Mentor: Tracy Livingston, PhD

Dept. of Biological Sciences

Teaching Experience

March 2016-Sept 2016

Guest Lecture Opportunities

March 3, 2016; Glutamine, Arginine, and Nitric Oxide;

NS602 – Integrated Nutritional Sciences II

March 10, 2016; Effective Informational Interviews;

GS600 – Preparing Future Professionals

September 1, 2016; Proteins: Second Largest Energy Store in the Body; NS601 – Integrated Nutritional Sciences I

September 6, 2016; Protein Function and How It's Regulated; NS601 – Integrated Nutritional Sciences I

January – May 2016

College Teaching Practicum

Advisor: Alison Gustafson, PhD

College Teaching & Learning Certificate

University of Kentucky, Lexington, Kentucky

May – October 2011

Internship, Office of Academic Enhancement

Georgetown College, Georgetown, Kentucky

August 2010 – May 2011 Biology Tutor

Georgetown College, Georgetown, Kentucky

Honors and Awards

2016 First place poster presentation at University of Kentucky Society of Postdoctoral Scholars Research Symposium

2016 Third place poster presentation at Barnstable Brown Obesity and Diabetes Research Day

2015 Dept. of Pharmacology and Nutritional Sciences Doctoral Student of the Year Award Recipient

2015 Third place poster presentation at Barnstable Brown Obesity and Diabetes Research Day

2011 Georgetown College Outstanding Biology Student Award Recipient

2011 Georgetown College Outstanding Student Leader Award

2011 Georgetown College Norman and Martha Yocum Lytle Graduating Senior Award

2010 Howard Hughes Medical Institute Research Program Grant Recipient (GCPALS)

Research Support

2013 – 2015 Predoctoral financial support from Training Grant in Oxidative Stress and Nutrition, National Institutes of Health T32 DK007778-14

Publications

Norman-Burgdolf H, Vanderford NL. Preparing Future Professionals: A Career Development Course Focused on Enhancing Workforce Readiness. *Nat. Biotechnol.* 2016 Jan; 34:111-113

Cui W, Maimaitiyiming H, Zhou Q, **Norman H**, Zhou C, Wang S. Interaction of thrombospondin1 and CD36 contributes to obesity-associated podocytopathy. *Biochim Biophys Acta.* 2015 Jul; 1852(7):1323-1333

Maimaitiyiming H, Clemons K, Zhou Q, **Norman H**, Wang S. Thrombospondin1 deficiency attenuates obesity-associated microvascular complications in ApoE^{-/-} mice. *PLoS One.* 2015 Mar; 10(3):e0121403

Maimaitiyiming H*, **Norman H***, Zhou Q, Wang S. CD47 deficiency protects mice from diet-induced obesity and improves whole body glucose tolerance and insulin sensitivity. *Sci Rep.* 2015 Mar; 5:8846 * Co-first authors

Cui W, Maimaitiyiming H, Qi X, **Norman H**, Zhou Q, Wang X, Fu J, Wang S. Increasing cGMP-dependent cGMP-dependent protein kinase activity attenuates unilateral ureteral obstruction-induced renal fibrosis. *Am J Physiol Renal Physiol.* 2014 May;306(9):F996-F1007

Cui W, Maimaitiyiming H, Qi X, **Norman H**, Wang S. Thrombospondin 1 mediates renal dysfunction in a mouse model of high fat diet-induced obesity. *Am J Physiol Renal Physiol*. 2013 Sep;305(6): F871-80; 2013

Maimaitiyiming H, Li Y, Cui W, Tong X, **Norman H**, Qi X, Wang S. Increasing cGMP-dependent protein kinase I activity attenuates cisplatin-induced kidney injury through protection of mitochondria function. *Am J Physiol Renal Physiol*. 2013 Sep;305(6):F881-90.

Abstracts

“Adipocyte Differentiation is Inhibited in Primary Brown Adipocytes Lacking CD47 Through a cMyc-dependent Mechanism,” Gill Heart Cardiovascular Research Day, University of Kentucky, Lexington, Kentucky, November 4, 2016

“CD47 Deficiency Protects Against Diet-Induced Fatty Liver Through Suppression of ROS Generation and Increased eNOS Activation,” Society of Postdoctoral Scholars Research Symposium, University of Kentucky, Lexington, Kentucky, June 3, 2016

“CD47 Plays a Novel Role in Adipocyte Function,” Gill Heart Cardiovascular Research Day, University of Kentucky, Lexington, Kentucky, October 2, 2015

“CD47 Plays a Novel Role in Regulating Adipocyte Lipolysis,” American Diabetes Association 75th Annual Scientific Sessions, Boston, MA, June 5-9, 2015

“CD47 Plays a Novel Role in Regulating Adipocyte Lipolysis,” Barnstable Brown Diabetes Obesity Center Research Day, University of Kentucky, Lexington, KY, May 20, 2015

“CD47 Deficiency Preserves Brown Adipose Tissue Phenotype in High-Fat Diet-Induced Obesity Mouse Model,” Gill Heart Cardiovascular Research Day, University of Kentucky, Lexington, KY, October 17, 2014

“CD47 Deficiency Reduces Adipose Tissue MCP1/CCR2-Dependent Macrophage Infiltration in a Diet-Induced Obesity Model,” American Diabetes Association 74th Annual Scientific Sessions, San Francisco, CA, June 12-17, 2014

“CD47 Deficiency Protects Mice from High-Fat Diet-induced Obesity and Inflammation,” Barnstable Brown Diabetes Obesity Center Research Day, University of Kentucky, Lexington, KY, May 20, 2014

Oral Presentations

“CD47 plays a novel role in adipocyte function,” Gill Heart Cardiovascular Research Day, University of Kentucky, Lexington, Kentucky, October 2, 2015

“CD47 deficiency protects mice from diet-induced obesity and improves whole body glucose tolerance and insulin sensitivity,” Barnstable Brown Diabetes Obesity Center Research Day 2015, University of Kentucky, Lexington, KY, May 20, 2015

“Novel role of CD47 in brown adipocyte function,” Departmental Seminar, Department of Pharmacology and Nutritional Sciences, College of Medicine, University of Kentucky, Lexington, KY, March 26, 2015

“Role of CD47 in Metabolic Syndrome,” Departmental Seminar, Graduate Center for Nutritional Sciences, College of Medicine, University of Kentucky, Lexington, KY, January 16, 2014